

NOISE ANALYSIS APPLIED TO
A LIQUID-SOLID FLUIDIZED BED

by

DARROL HOLT TIMMONS

B. S., Kansas State University, 1963

A MASTER'S THESIS

submitted in partial fulfillment of the
requirements for the degree

MASTER OF SCIENCE

Department of Nuclear Engineering

KANSAS STATE UNIVERSITY

Manhattan, Kansas

1966

Approved by:

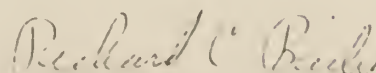

Major Professor

TABLE OF CONTENTS

1.0	INTRODUCTION.....	1
2.0	THEORETICAL DEVELOPMENT.....	4
3.0	ANALYSIS OF FINITE AMOUNTS OF DATA.....	13
4.0	DIGITAL ANALYSIS.....	21
5.0	EXPERIMENTAL.....	25
5.1	Apparatus.....	25
5.2	Particles.....	29
5.3	Procedure.....	30
6.0	DISCUSSION AND RESULTS.....	32
7.0	CONCLUSIONS.....	73
8.0	SUGGESTIONS FOR FURTHER STUDY.....	74
9.0	ACKNOWLEDGEMENT.....	75
10.0	LITERATURE CITED.....	76
11.0	APPENDICES.....	78
	APPENDIX A: Statistical Analysis of Continuous Random Functions.....	79
	APPENDIX B: Input-Output Relationship of the Power Spectrum.....	83
	APPENDIX C: Description and explanation of the IBM-1410 Computer Program Used for Calculation of the Autocorrelation Function and Power Spectrum.....	87

APPENDIX D: Description and Explanation of the IBM-1410 Computer Program Used for Calculation of the Break Frequency and Damping Factor.....	93
APPENDIX E: Results of Autocorrelation Function and Power Spectrum Calculations.....	101
APPENDIX F: Results of Least Squares Fit to the Power Spectrum.....	119

LIST OF TABLES

I. Properties of the bed particles.....	30
II. List of runs and the values of the parameters.....	34
III. Standard deviation of the autocorrelation function.....	45
IV. Break frequency and damping factor of the experimental data with the corresponding squared error.....	54
V. Results of the analysis for prewhitened data.....	55
VI. List of runs used in the statistical analysis.....	57
VII. List of step input response runs.....	64
C-1. Input data and variables required for the IBM-1410 autocorrelation function and power spectrum computer program.....	88
D-1. Input data and variables required for the IBM-1410 break frequency and damping factor computer program.....	96

LIST OF FIGURES

1. Plot of the spectral windows.....	17
2. Photograph of the experimental assembly.....	26
3. Positioning of the camera and lighting fixture.....	27
4. Schematic diagram of the experimental apparatus.....	28
5. Excerpts from the photographic data.....	36
6. Frequency distribution of Run A-10.....	37
7. Frequency distribution of Run B-1.....	38
8. Frequency distribution of Run C-2.....	39
9. Autocorrelation function of Run A-10.....	41
10. Autocorrelation function of Run B-1.....	42
11. Autocorrelation function of Run C-2.....	43
12. Power spectrum of Run A-10.....	46
13. Power spectrum of Run B-1.....	47
14. Power spectrum of Run C-2.....	48
15. Confidence limits on the power spectrum.....	50
16. Break frequency as a function of bed expansion ratio.....	60
17. Damping factor as a function of bed expansion ratio.....	61
18. Break frequency and damping factor as a function of packed bed height.....	62
19. Step input response, Run S-7-On.....	65
20. Step input response, Run S-6-On.....	66
21. Step input response, Run S-5-On.....	67
22. Step input response, Run S-7-Off.....	68
23. Step input response, Run S-6-Off.....	69

24. Step input response, Run S-5-Off.....	70
25. Logic diagram for autocorrelation function and power spectrum computer program.....	90
26. Logic diagram for break frequency and damping factor computer program.....	98

NOMENCLATURE

A	Least-squares constant
b	General lag window
b_1	Lag window corresponding to no modification of the power spectrum
b_2	Hanning lag window
B	Least-squares constant
B	General spectral window
B_1	Spectral window corresponding to b_1
B_2	Spectral window corresponding to b_2
D	Column diameter
D_p	Particle diameter
E	Expectation value
f	Frequency
f_N	Nyquist folding frequency
$F_{i,j}$	Variance ratio with i and j degrees of freedom
h	Fluidized bed height
h_o	Packed bed height
k	Equivalent degrees of freedom of a chi-square distribution
K	Magnitude of the power spectrum of white noise input
M	Maximum number of time lags
N	Total number of data points
O	General output function
p	Power spectrum of filtered data
P	Modified power spectrum
P_1	Power spectrum by B_1

P_2	Power spectrum modified by B_2
S	Sum of the squared errors
t	Time
T	Sample duration
w_1	Weighting factor
x	General continuous random variable
x_1	Sample bed height
\bar{x}	Average bed height (time average)
X	Fourier transform of x
y	Digital filtered variable
Y	Fourier transform of y
Z	Transfer function of the system

Greek Symbols

α	Break frequency
β	Damping factor
γ	Prewhitening filter coefficient
Γ	Transfer function of the digital filter
δ	Dirac delta function
η	Integration variable
ϕ	Autocorrelation function
ϕ_b	Autocorrelation function of band limited white noise
Φ	Power spectrum
ϕ_b	Power spectrum of band limited white noise
ϕ_o	Power spectrum of the output of the system
ϕ_w	Power spectrum of white noise

ρ	Particle density
σ	Standard deviation of the bed height
σ_c	Standard deviation of the autocorrelation function
τ	Time displacement variable
τ_c	Correlation time constant
τ_m	Maximum time lag
ω	Angular frequency

INTRODUCTION

One of the basic interests of the nuclear engineer is the design and development of improved reactor types. In the pursuit of this goal many advanced concepts are proposed and experimentally tested. One such advanced concept which has drawn considerable attention is the fluidized bed nuclear reactor (FBR), (17). The primary reasons for the interest in this concept are the advantages that it has over the fixed fuel nuclear reactors. Some of the important advantages are (14,17):

1. Small temperature gradient
2. Even fuel burn-up rates
3. Low fuel fabrication costs
4. Easy fuel replacement.

Previous experience with fixed fuel nuclear reactors has shown that not all these properties are attainable in a single reactor. The FBR concept appears to combine all the properties in a relatively simple core configuration.

Two of the questionable properties of the FBR concept are:

1. Erosion and corrosion of the fuel elements
2. Nuclear safety of a moving fuel nuclear reactor.

Erosion of the fuel is due to the friction caused when the pellets collide with one another and with the vessel walls. The powder resulting is carried in the fluid stream and can cause damage as an abrasive and as a result of the radioactivity it carries. This problem has been studied by Martin Nuclear Company through a contract with the United States Atomic Energy Commission. Their experience with a prototype nuclear reactor, the Organic Moderated Fluidized Bed Reactor (OMFBR), indicated that fuel erosion is a major problem

of the FBR concept.

The nuclear safety of a system depends upon its dynamic behavior. Nuclear dynamics (kinetics) has been studied extensively for a number of years. As a result one can predict the behavior of a fixed fuel reactor with reasonable accuracy. The problem, however, is compounded in a moving fuel reactor because the core size may be changing as a function of time. One must know the dynamic behavior of the core before he can use the existing knowledge of kinetics. Since little is known about time behavior of fluidized beds, the FBR systems proposed to date have been restricted to those which have very stable expansion behavior and a minimum of inhomogeneous characteristics. This is a very large restriction which might be removed if more were known about the dynamic behavior of fluidized beds.

Various methods have been devised to experimentally determine the dynamic behavior of the traditional "black box". They are particularly useful in the analysis of systems whose complexity is such that mathematical formulation is prohibitive. The more important of these methods relate the output response to particular input functions, namely, sinusoidal, step, or impulse. The sinusoidal response method has been applied successfully to fluidized beds in the measurement of significant time constants of the system (9).

Noise analysis, another important method employed in the study of dynamic response, was developed and is used extensively in the field of electronics. Its purpose is to extract meaningful information from a signal in which noise obscures the desired signal. The concepts of noise analysis, however, can be applied to any physical system in which the output response to a given input has an inherent noisy characteristic (10,12,16,19).

The purpose of the work reported here was to study the applicability of noise analysis techniques to fluidized beds. No such application has been reported in the literature to date. The study is a preliminary investigation to determine whether or not further work is feasible. A complete and thorough study of fluidized bed dynamics is not intended.

2.0 THEORETICAL DEVELOPMENT

A complete development of the statistical analysis of random functions is beyond the scope of this thesis. Several good references which describe the application of statistical theory to noise analysis are available (3,5,7,8,12). Chapter 12 of (5) is recommended as an easily readable review of the treatment of random functions, whereas (3,7,8,12) present a more detailed analysis. The development which follows is limited to the more important concepts of noise analysis.

The output of the system considered is assumed to be a typical random function from an ergodic stationary random process. The details of this assumption are discussed in Appendix A. An important expression employed in the statistical analysis of random functions is the autocorrelation function defined as

$$\phi(\tau) = \overline{x(t) x(t + \tau)} \quad (1)$$

where $x(t)$ is a continuous stationary random variable. $x(t + \tau)$ is the value of the same random variable sampled at a future time determined by the time displacement variable τ . The bar denotes an average. The special case of $\tau = 0$ defines the mean square value of $x(t)$. If $x(t)$ has a zero mean, $\phi(0)$ defines the variance of $x(t)$. For $\tau \neq 0$ the autocorrelation function represents the degree of correlation between the value of x at the instant (t) and the value at some future time $(t + \tau)$.

The statistical average of a random function is generally defined as an ensemble average. However, since $x(t)$ is assumed to be ergodic, Eq. (1) can be expressed as

$$\phi(\tau) = \lim_{T \rightarrow \infty} \frac{1}{T} \int_{-\frac{T}{2}}^{\frac{T}{2}} x(t) x(t + \tau) dt \quad (2)$$

where T is the duration of the sample. Equation (2) is the defining expression for the autocorrelation function as computed using time averages. One of the important properties of $\phi(\tau)$, the fact that it is always less than or equal to the variance, can be exhibited by considering the inequality

$$0 \leq \{x(t) \pm x(t + \tau)\}^2 = x^2(t) + x^2(t + \tau) \pm 2x(t) x(t + \tau). \quad (3)$$

Transposing the last term of Eq. (3) and averaging yields

$$\overline{\pm 2x(t) x(t + \tau)} \leq \overline{x^2(t)} + \overline{x^2(t + \tau)}. \quad (4)$$

Averages computed for stationary processes are independent of time displacement, thus

$$\overline{x^2(t + \tau)} = \overline{x^2(t)} = \phi(0). \quad (5)$$

Substituting Eqs. (5) and (1) into Eq. (4) yields

$$\begin{aligned} \pm 2\phi(\tau) &\leq 2\phi(0) \\ \text{or, } |\phi(\tau)| &= \phi(0). \end{aligned} \quad (6)$$

The inequality in Eq. (6) becomes an equality only when $x(t)$ contains a periodic component. If the period of the periodic component is $2a$, then

$$|\phi(na)| = \phi(0), \quad n = 0, 1, 2, \dots$$

The autocorrelation function of a sine wave is thus seen to be a series of alternately positive and negative spikes of height $|\phi(0)|$ spaced at intervals of $\tau = na$. If $x(t)$ is truly random, $x(t)$ and $x(t + \tau)$ become uncorrelated for large values of τ , i.e.,

$$\lim_{\tau \rightarrow \infty} \phi(\tau) = 0.$$

The autocorrelation function can therefore be regarded as a measure of the randomness of a function.

Another useful property of the autocorrelation function is its symmetry. This can be demonstrated by considering

$$\phi(-\tau) = \lim_{T \rightarrow \infty} \frac{1}{T} \int_{-\frac{T}{2}}^{\frac{T}{2}} x(t) x(t - \tau) dt.$$

Changing the variable to $\eta = t - \tau$ yields

$$\phi(-\tau) = \lim_{T \rightarrow \infty} \frac{1}{T} \int_{-\frac{T}{2} - \tau}^{\frac{T}{2} - \tau} x(\eta + \tau) x(\eta) d\eta. \quad (7)$$

The interval of integration continues to be $2T$. Translation of the time axis does not alter the statistical properties of a stationary process, therefore Eq. (7) is equivalent to Eq. (2), and

$$\phi(-\tau) = \phi(\tau). \quad (8)$$

It is often convenient to express the behavior of a function in the frequency rather than in the time domain. The transformation from time to frequency is typically performed by the Fourier transform defined as

$$X(f) = \int_{-\infty}^{\infty} x(t) e^{-i\omega t} dt \quad (9)$$

where $\omega = 2\pi f$

$X(f)$ is called the spectral density function of the variable $x(t)$. A necessary condition for the existence of $X(f)$ is the requirement that

$$\int_{-\infty}^{\infty} |x(t)| dt = K \quad (10)$$

where K is finite. If $X(f)$ exists, then the inverse Fourier transform is given as

$$x(t) = \int_{-\infty}^{\infty} X(f) e^{1\omega t} df. \quad (11)$$

Equations (9) and (11) are commonly called the Fourier transform pair.

If $x(t)$ is a stationary random function known for all time, the integral in Equation (10) will in general be infinite and $X(f)$ will not exist. Therefore, in order to study the frequency characteristics of such a function, one may consider a finite segment of the random function defined by

$$x_T(t) = \begin{cases} x(t), & -\frac{T}{2} \leq t \leq \frac{T}{2} \\ 0, & |t| > \frac{T}{2} \end{cases}. \quad (12)$$

As long as $x(t)$ is bounded, the Fourier transform of $x_T(t)$ is guaranteed to exist.

$$X_T(f) = \int_{-\infty}^{\infty} x_T(t) e^{-1\omega t} dt \quad (13)$$

An equivalent expression for the autocorrelation function in terms of the variable defined in Eq. (12) is

$$\phi(\tau) = \lim_{T \rightarrow \infty} \frac{1}{T} \int_{-\frac{T}{2}}^{\frac{T}{2}} x_T(t) x_T(t + \tau) dt. \quad (14)$$

Due to the definition of $x_T(t)$, $\phi(\tau)$ contains no contribution for $|t| > \frac{T}{2}$, thus Eq. (14) can be written as

$$\phi(\tau) = \lim_{T \rightarrow \infty} \frac{1}{T} \int_{-\infty}^{\infty} x_T(t) x_T(t + \tau) dt. \quad (15)$$

Applying the Fourier transform, Eq. (9), to Eq. (15) yields

$$\begin{aligned}
\phi(f) &= \int_{-\infty}^{\infty} \phi(\tau) e^{-i\omega\tau} d\tau \\
&= \int_{-\infty}^{\infty} \left\{ \lim_{T \rightarrow \infty} \frac{1}{T} \int_{-\infty}^{\infty} x_T(t) x_T(t + \tau) dt \right\} e^{-i\omega\tau} d\tau
\end{aligned} \tag{16}$$

where $\phi(f)$ is the spectral density function of $\phi(\tau)$. If the variable of integration is changed to $\tau = \eta - t$ and if the order of integrating and taking the limit is interchanged, Eq. (16) becomes

$$\begin{aligned}
\phi(f) &= \lim_{T \rightarrow \infty} \frac{1}{T} \int_{-\infty}^{\infty} x_T(t) e^{i\omega t} dt \int_{-\infty}^{\infty} x_T(\eta) e^{-i\omega\eta} d\eta \\
&= \lim_{T \rightarrow \infty} \frac{1}{T} X_T^*(f) X_T(f)
\end{aligned} \tag{17}$$

where $X_T^*(f)$ denotes the complex conjugate of $X_T(f)$.

Equation (17) is the defining expression for the function $\phi(f)$, the power density spectrum of $x_T(t)$. It describes the square of the frequency distribution of the random function $x_T(t)$. The name, power density spectrum, arises from the original applications in electronics where $x_T(t)$ was normally a current or voltage. The function $x_T^2(t)$ describes the power output of a system when a resistance of one ohm is assumed.

An equivalent expression can be found for the Fourier transform, Eq. (9), by substituting the polar form of the imaginary exponential,

$$e^{-i\omega t} = \cos \omega t - i \sin \omega t.$$

The resulting relation is

$$X(f) = \int_{-\infty}^{\infty} x(t) \cos \omega t dt - i \int_{-\infty}^{\infty} x(t) \sin \omega t dt. \tag{18}$$

Substituting $\phi(\tau)$ for $x(t)$ in Eq. (18) gives $\Phi(f)$ according to Eq. (16).

It was previously shown that $\phi(\tau)$ is an even function, hence $\phi(\tau) \sin \omega\tau$ is odd and integrates to zero over symmetrical limits. The result is

$$\Phi(f) = \int_{-\infty}^{\infty} \phi(\tau) \cos \omega\tau \, d\tau. \quad (19)$$

It follows directly from Fourier analysis that the inverse of Eq. (19) is

$$\phi(\tau) = \int_{-\infty}^{\infty} \Phi(f) \cos \omega\tau \, df. \quad (20)$$

The relation between the power density spectrum and the autocorrelation function exhibited in Eqs. (19) and (20) is a statement of the Wiener theorem for autocorrelation. Wiener was the first to establish the validity of the relationship for stationary random processes. A rigorous proof of the theorem is given by Lee (12).

The utility of the power spectrum of a random function comes from its relationship to the transfer function, $Z(f)$. It is convenient to distinguish between the amplitude and phase of $Z(f)$ by the expression

$$Z(f) = |Z(f)| e^{j\theta} \quad (21)$$

where $|Z(f)|$ is the magnitude and θ is the phase of the transfer function.

It is shown in Appendix B that for a given system

$$\Phi_o(f) = \Phi_i(f) |Z(f)|^2 \quad (22)$$

where Φ_o and Φ_i are the power spectra of the system output and input, respectively. The transfer function enters Eq. (22) as the square of the magnitude, therefore, according to Eq. (21) no phase information is available. This is

a consequence of noise analysis based on the autocorrelation function. An analogous technique called crosscorrelation may be employed to determine the transfer function, complete with phase information (12). The significant time constants, however, can be determined from the magnitude of the transfer function.

Equation (22) may be used to determine $|Z(f)|$ if both ϕ_o and ϕ_1 are known. The power spectra can be found by measuring the input and output of the system and applying Eqs. (15) and (19). The analysis is greatly simplified, however, if the input is assumed to be white Gaussian noise. Noise is said to be white if it has a constant power spectrum, i.e., if

$$\phi_w(f) = K$$

where K is a constant and the subscript w denotes white noise. Rice (20) has shown that white noise may be regarded as a superposition of an infinite number of simple harmonic oscillators having the following properties:

1. Distribution continuous in frequency
2. All amplitudes the same at all frequencies
3. Phases independent and random.

If the input to a system is white noise, then the input-output relation, Eq. (22), becomes

$$\phi_o(f) = K |Z(f)|^2. \quad (23)$$

Thus, for white noise input, only the power spectrum of the output is necessary to determine $|Z(f)|$. The input to the system may be arbitrary so long as it is white noise.

Rice has also shown that a stationary Gaussian random process may be regarded as the result of passing white Gaussian noise through a linear system.

Hence, if the system is assumed to be linear and if the output of the system has a normal distribution in steady state operation, the input may be considered as white noise.

It should be noted that ideal white noise is physically unrealizable because its mean square value is infinite. This can be demonstrated by considering the autocorrelation function of white noise. Noting that the Fourier transform of a constant is the Dirac delta function, $\delta(t)$, it follows from Eq. (20) that $\phi_w(\tau)$ is given by

$$\phi_w(\tau) = K \delta(\tau).$$

Since $\delta(0)$ is infinite, the mean square value of white noise, $\phi_w(0)$, is also seen to be infinite.

An approximation called band-limited white noise is physically realizable. This concept refers to a random signal whose power spectrum is flat over a certain finite frequency range and zero elsewhere.

$$\phi_b(f) = \begin{cases} K, & \omega_1 \leq |\omega| \leq \omega_2 \\ 0, & |\omega| < \omega_1 \text{ and } |\omega| > \omega_2 \end{cases}$$

where ω_1 and ω_2 are the band limits of the white noise. The mean square value of $x(t)$ is finite for band-limited white noise. This can be exhibited by performing the Fourier transformation of ϕ_b to obtain the autocorrelation function.

$$\begin{aligned} \phi_b(\tau) &= \int_{-\infty}^{\infty} \phi_b(f) \cos \omega \tau \, df \\ &= 2 \int_{+\omega_1}^{+\omega_2} K \cos \omega \tau \, df \\ &= \frac{K}{\pi} \frac{\sin \omega_2 \tau - \sin \omega_1 \tau}{\tau} \end{aligned} \tag{24}$$

The mean square value is found by evaluating Eq. (24) for $\tau = 0$. Applying l' Hospital's rule once gives

$$\phi_b(0) = \frac{K}{\pi} (\omega_2 - \omega_1)$$

which is finite. For practical applications noise may be considered as white if ϕ_b is constant over the band width of interest.

3.0 ANALYSIS OF FINITE AMOUNTS OF DATA

The power spectrum of the output of a system can be calculated from either Eq. (17) or Eq. (19). These two expressions were shown to be equivalent in the theoretical development. Methods of analysis based on both expressions have been developed and applied successfully to the determination of power spectra (1,4,19). The more popular method of estimating $\phi(f)$ is based on the Wiener theorem, Eq. (19). Since this method depends on knowledge of the autocorrelation function, it is commonly called the autocorrelation method. This method is thoroughly treated by Blackman and Tukey (4) with the applications to both the continuous and discrete analysis of electrical signals. Thie (19) considers the method in its application to nuclear reactor noise analysis. Both authors treat the resolution and stability of the calculations and develop relationships that enable one to obtain predetermined statistical accuracy from experimental data.

The direct Fourier analysis method, Eq. (17), is treated by Akcasu (1). His expressed intention is to supplement the material presented by Blackman and Tukey (4). He compared the resolution and stability of the two methods and reached the conclusion that in general neither is superior to the other. Although the autocorrelation technique is indirect, the required computation time is no more than the direct method. An advantage offered by the autocorrelation method is the additional information contained in the autocorrelation function. One quantity of importance which is obtained from $\phi(\tau)$ is the correlation time constant τ_c . This time constant can be used to estimate the statistical reliability of the power spectrum calculation. For this reason

the autocorrelation method was chosen for the analysis of the data in this thesis. Details of the method are discussed below.

The Wiener theorem states that the power spectrum of a stationary random process is related to the autocorrelation function of the process by the expression

$$\phi(f) = \int_{-\infty}^{\infty} \phi(\tau) \cos \omega \tau \, d\tau \quad (19)$$

$$\text{where } \phi(\tau) = \lim_{T \rightarrow \infty} \frac{1}{T} \int_{-\frac{T}{2}}^{\frac{T}{2}} x_T(t) x_T(t + \tau) \, dt. \quad (15)$$

In the limit as the sample duration, T , approaches infinity, $\phi(\tau)$ is defined for all τ . Under these circumstances $\phi(f)$ can be calculated directly from Eq. (19). In practical applications, however, one deals with samples of finite duration. The result is a truncation of $\phi(\tau)$ at some maximum, $\tau_m \leq \frac{T}{2}$. Equation (19) must therefore be modified to include the effect of this truncation. It is convenient to introduce a new function, the lag window, defined by

$$\begin{aligned} b(\tau) &\leq 1, \quad |\tau| \leq \tau_m \\ b(\tau) &= 0, \quad |\tau| > \tau_m. \end{aligned} \quad (25)$$

The product $b(\tau) \cdot \phi(\tau)$ can be used to represent the truncated autocorrelation function. Insertion of $b(\tau)$ into Eq. (19) modifies the expression as required by truncation while retaining the identity of $\phi(\tau)$. Denoting the truncated power spectrum by $P(f)$, Eq. (16) becomes

$$P(f) = \int_{-\infty}^{\infty} b(\tau) \phi(\tau) e^{-i\omega \tau} \, d\tau. \quad (26)$$

The exponential form of the Fourier integral is used in Eq. (26) since, in general, $b(\tau)$ need not be symmetrical. If $b(\tau)$ is defined as an even function, then Eq. (26) reduces to the cosine transform of Eq. (19).

The relationship between $P(f)$ and $\phi(f)$ is found by substituting the Fourier integral representation of $\phi(\tau)$ into Eq. (26).

$$P(f) = \int_{-\infty}^{\infty} b(\tau) e^{-i\omega\tau} \int_{-\infty}^{\infty} \phi(f') e^{i\omega'\tau} df' d\tau.$$

Rearranging the order of integration yields

$$P(f) = \int_{-\infty}^{\infty} \left\{ \int_{-\infty}^{\infty} b(\tau) e^{-i(\omega - \omega')\tau} d\tau \right\} \phi(f') df'.$$

The quantity in brackets is recognized as the Fourier transform of $b(\tau)$. Defining this transform as $B(f)$ gives

$$P(f) = \int_{-\infty}^{\infty} B(f - f') \phi(f') df'. \quad (27)$$

Equation (27) is a convolution integral in the frequency domain. The weighting function, $B(f)$, is known as the spectral window corresponding to the lag window, $b(\tau)$. The power spectrum computed from data of finite duration is thus seen to be a weighted average of the true power spectrum. The accurate estimation of $\phi(f)$ depends to a large extent upon the frequency dependence of the spectral window.

A spectral window is analogous to an electrical filter which attenuates all frequencies except those within a certain band, Δf . The more narrow the band width of a filter, the sharper the resolution. The same conditions apply to the spectral window. The perfect spectral window is the zero band-width

window described by the Dirac delta function.

$$B(f - f') = \delta(f - f')$$

Substituting this spectral window into Eq. (27) yields

$$P(f) = \int_{-\infty}^{\infty} \delta(f - f') \phi(f') df' = \phi(f), \quad (28)$$

i.e., perfect estimation.

Since the delta function filter is physically unrealistic, the idealized band-pass filter has been introduced. This filter has unity transmission throughout the band width and zero transmission elsewhere. The frequency characteristics of the ideal band-pass filter are shown in Fig. 1. This idealized model is a reference by which actual filters can be evaluated.

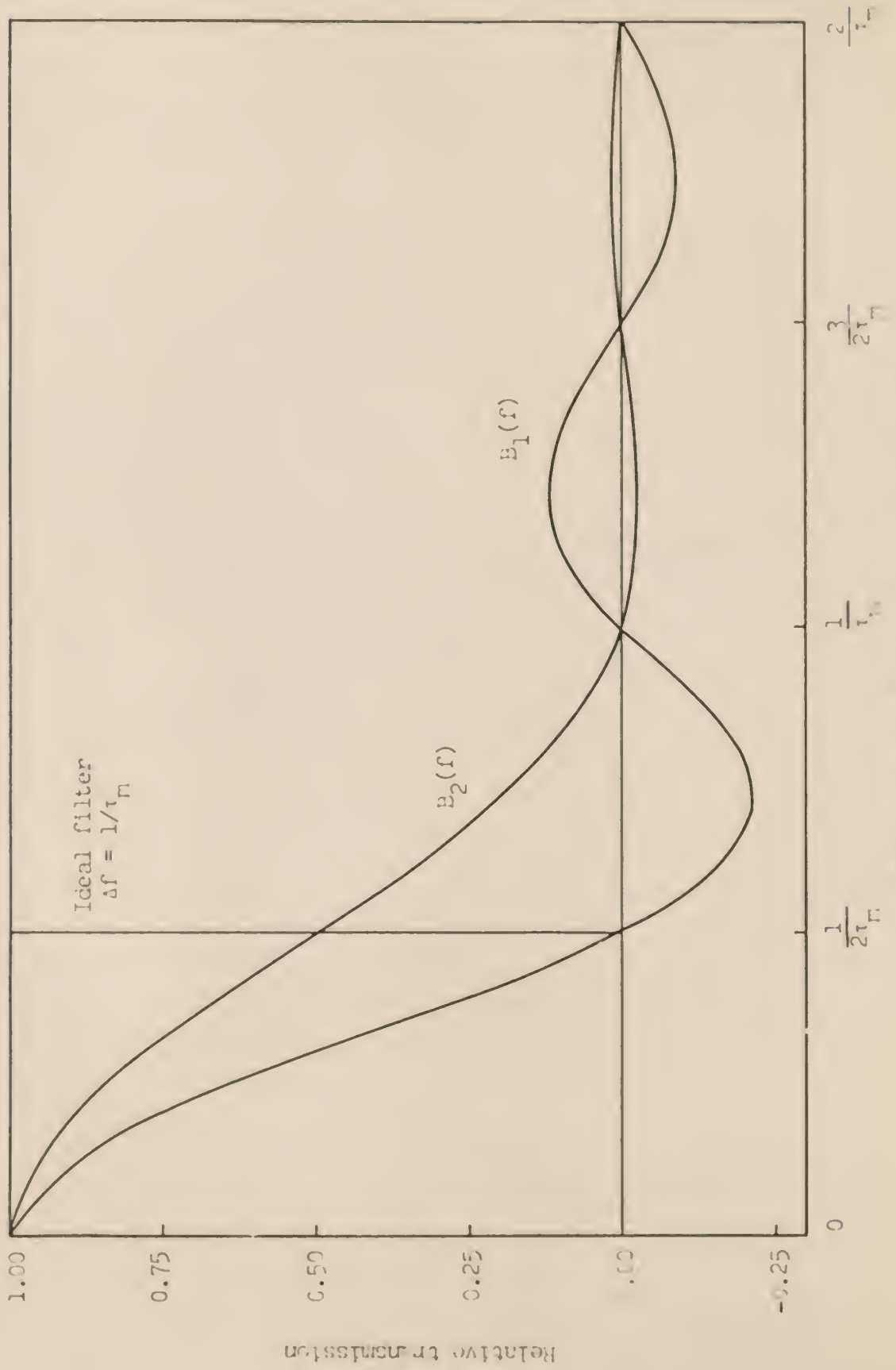
The simplest lag window is defined as

$$b_1(\tau) = \begin{cases} 1, & |\tau| \leq \tau_m \\ 0, & |\tau| > \tau_m. \end{cases}$$

This lag window corresponds to direct Fourier transformation of the truncated autocorrelation function. The spectral window which $b_1(\tau)$ introduces is found by Fourier transformation.

$$\begin{aligned} B_1(f) &= \int_{-\infty}^{\infty} b_1(\tau) \cos \omega \tau d\tau \\ &= \int_{-\tau_m}^{\tau_m} (1) \cos \omega \tau d\tau = \frac{\sin 2\pi f \tau_m}{\pi f} \end{aligned} \quad (29)$$

The spectral estimate obtained using $B_1(f)$ is found by substituting Eq. (29) into Eq. (27).



Frequency deviation from center of band
Figure 1. Plot of the spectral windows

$$P_1(f) = \int_{-\infty}^{\infty} \frac{\sin \{2\pi(f - f')\tau_m\}}{\pi(f - f')} \phi(f') df'. \quad (30)$$

$P_1(f)$ is known as the raw spectral estimate since it is found from the unmodified autocorrelation function.

Figure 1 shows the frequency dependence of $B_1(f)$ normalized to a bandwidth of $\frac{1}{2\tau_m}$. It is only a fair approximation to the ideal band-pass filter. The magnitude of the first minor lobe is approximately 20% of the major lobe. This means that the transmitted power spectrum will contain significant contributions from frequencies outside the band. The first minor lobe contribution will be negative. Under these conditions $P_1(f)$ will be a poor approximation to $\phi(f)$, especially if $\phi(f)$ is of significant magnitude in the vicinity of the first minor lobe.

A more suitable lag window, the hanning window, is defined by

$$b_2(\tau) = \begin{cases} \frac{1}{2} (1 + \cos \frac{\pi\tau}{\tau_m}), & |\tau| \leq \tau_m \\ 0, & |\tau| > \tau_m \end{cases}$$

The corresponding spectral window is found by Fourier transformation of $b_2(\tau)$.

$$\begin{aligned} B_2(f) &= \int_{-\infty}^{\infty} b_2(\tau) \cos \omega\tau d\tau \\ &= \int_{-\tau_m}^{\tau_m} \frac{1}{2} (1 + \cos \frac{\pi\tau}{\tau_m}) \cos \omega\tau d\tau. \end{aligned} \quad (31)$$

Introducing the identity

$$\cos A \cos B = \frac{1}{2} \cos (A + B) + \frac{1}{2} \cos (A - B)$$

gives

$$B_2(f) = \frac{1}{2} \int_{-\tau_m}^{\tau_m} \cos \omega \tau \, d\tau + \frac{1}{4} \int_{-\tau_m}^{\tau_m} \cos 2\pi(f + \frac{1}{2\tau_m})\tau \, d\tau \\ + \frac{1}{4} \int_{-\tau_m}^{\tau_m} \cos 2\pi(f - \frac{1}{2\tau_m})\tau \, d\tau. \quad (32)$$

Substituting Eq. (29) into Eq. (32) gives

$$B_2(f) = \frac{1}{4} B_1(f - \frac{1}{2\tau_m}) + \frac{1}{2} B_1(f) + \frac{1}{4} B_1(f + \frac{1}{2\tau_m}). \quad (33)$$

The spectral estimate, $P_2(f)$, corresponding to the spectral window, $B_2(f)$, is thus

$$P_2(f) = \frac{1}{4} P_1(f - \frac{1}{2\tau_m}) + \frac{1}{2} P_1(f) + \frac{1}{4} P_1(f + \frac{1}{2\tau_m}) \quad (34)$$

where $P_1(f)$ is the raw spectral estimate defined by Eq. (30). $P_2(f)$ depends on the raw spectral estimates spaced $\frac{1}{2\tau_m}$ on either side of the center of the band. A logical choice for spacing between adjacent spectral estimates is also $\frac{1}{2\tau_m}$.

The frequency characteristics of $B_2(f)$ are compared to $B_1(f)$ in Fig. (1). The magnitude of the first minor lobe of $B_2(f)$ is less than 3.0% of the major lobe. The transmission properties of $B_2(f)$, therefore, are better than those of $B_1(f)$. The resolution obtained with $B_2(f)$, however, is less than with $B_1(f)$. The equivalent band-width of $B_2(f)$, i.e., the frequency band included in the major lobe of the spectral window, is twice the band-width of $B_1(f)$. Hence, spectral estimates spaced by $\frac{1}{2\tau_m}$ will have considerably overlapping spectral windows and adjacent estimates will not be entirely independent.

Alternate estimates that are separated by $\frac{1}{\tau_m}$ have less overlap of spectral windows, hence these estimates are more nearly independent.

Equations (26) and (27) indicate two different ways of employing the lag window, $b_2(\tau)$, to improve the estimation of the power spectrum. After obtaining the truncated autocorrelation function one may either

1. Modify $\phi(\tau)$ by multiplying $b_2(\tau)$ and then
Fourier transform the product, or
2. Fourier transform $\phi(\tau)$ to obtain $P_1(f)$, and then
convolve the product $P_1(f) B_2(f)$.

The two methods are mathematically equivalent, however, the latter is easier to apply. Equation (34) shows that convolution of $P_1(f) B_2(f)$ is accomplished by smoothing the raw spectral estimates spaced at intervals of $\frac{1}{2\tau_m}$ with weights of $\frac{1}{4}$, $\frac{1}{2}$, and $\frac{1}{4}$.

4.0 DIGITAL ANALYSIS

The theory developed thus far in this thesis applies directly to the analysis of continuous samples of a random function. If the experimental data are available only as discrete points spaced at equal time intervals, the analysis must be modified to some extent. Where integration is indicated in the continuous case, summation or quadrature must be substituted in the discrete case. These modifications are straightforward and will not be discussed further here. Some consequences of digital analysis, however, are more involved. These factors along with methods of compensating for them are discussed below.

An important consequence of digital analysis of equally spaced data is the phenomenon known as aliasing. This effect results from the confusion of high and low frequency content of the sample function. The Nyquist sampling theorem (4) states that a band-limited function can be reconstructed from equally spaced data if the function is sampled at two or more points per cycle of the highest frequency. As a consequence, any frequency higher than $\frac{1}{2\Delta t}$ will not be resolvable from data sampled at intervals of time, Δt . The frequency

$$f_N = \frac{1}{2\Delta t}$$

is known as the Nyquist, or folding, frequency. High frequency information is effectively folded back over the low frequency spectrum, i.e., all information resulting from frequencies higher than f_N is detected within the band $0 \leq f \leq f_N$. This result can be shown by considering the function

$$g(t) = \sin 2\pi f t.$$

If $g(t)$ is sampled at equally spaced intervals, $\Delta t = \frac{1}{2f_N}$, it effectively becomes

$$g(k\Delta t) = \sin 2\pi f(k\Delta t), \quad k = 0, 1, 2, \dots$$

For multiples of the folding frequency, $f = nf_N$,

$$\begin{aligned} g(k\Delta t) &= \sin \left\{ 2\pi(nf_N) \left(\frac{k}{2f_N} \right) \right\} \\ &= \sin nk\pi = 0 \end{aligned}$$

for all n and k . The actual frequencies in the data which are multiples of f_N cannot be distinguished from f_N . Every frequency greater than f_N will appear within the frequency band $0 \leq f \leq f_N$ under an assumed name, or alias. The result is an erroneous estimate of the power spectrum. One method of avoiding aliasing effects is to make certain that the sampling interval, Δt , is chosen sufficiently small so that the folding frequency is higher than the highest frequency of interest in the power spectrum.

A second method of reducing the possibility of error due to aliasing is by filtering the data. Filtering attenuates the frequencies outside the range of interest and prevents their interference with the analysis. An additional motive for filtering the data is to smooth the spectrum so as to make it more nearly white. This latter use of filtering is known as prewhitening and is used primarily to compensate for the non-ideal nature of the spectral windows. Prewhitening reduces the effect of the contributions of the minor lobes by flattening out the spectrum. Filtering is typically carried out by incorporating an electrical filter in the sampling circuit. The filtering procedure can also be introduced digitally after the data has been digitalized.

Digital filters are based on a linear combination of the digitalized data. A simple filter is introduced by defining a new variable,

$$y_j = x_j + \gamma x_{j-1} \quad (35)$$

where γ is a constant and the x_j are the digital samples of the original function $x(t)$. Fourier analysis of the y_j results in a power spectrum $p(f)$. This power spectrum is related to the power spectrum of the original sample $P(f)$, through the transfer function of the filter.

In order to obtain the relationship it is convenient to express Eq. (35) in an equivalent form

$$y(t) = x(t) + \gamma x(t - \Delta t).$$

Treating $y(t)$ as the new input function replacing $x(t)$, it is seen by Eq. (17) that the new power spectrum, $p(f)$, is given by

$$p(f) = \lim_{T \rightarrow \infty} \frac{1}{T} \left| Y(f) \right|^2.$$

Substituting the Fourier integral representation for $Y(f)$ gives

$$\begin{aligned} p(f) &= \lim_{T \rightarrow \infty} \frac{1}{T} \left| \int_{-\infty}^{\infty} y(t) e^{-i\omega t} dt \right|^2 \\ &= \lim_{T \rightarrow \infty} \frac{1}{T} \left| \int_{-\infty}^{\infty} \{x(t) + \gamma x(t - \Delta t)\} e^{-i\omega t} dt \right|^2. \end{aligned} \quad (36)$$

Separating the integral into a sum of two integrals and substituting $\tau = t - \Delta t$ in the second term gives

$$\begin{aligned} p(f) &= \lim_{T \rightarrow \infty} \frac{1}{T} \left| \int_{-\infty}^{\infty} x(t) e^{-i\omega t} dt + \gamma e^{-i\omega \Delta t} \int_{-\infty}^{\infty} x(\tau) e^{-i\omega \tau} d\tau \right|^2 \\ &= \lim_{T \rightarrow \infty} \frac{1}{T} \left| X(f) + \gamma e^{-i\omega \Delta t} X(f) \right|^2 \\ &= P(f) \left| 1 + \gamma e^{-i\omega \Delta t} \right|^2 = P(f) r(f). \end{aligned} \quad (37)$$

Thus, filtering by means of a linear combination defined in Eq. (35) results in multiplying the power spectrum by the transfer function of the filter, $\Gamma(f)$. Expanding $\Gamma(f)$ gives

$$\begin{aligned}\Gamma(f) &= \left| 1 + \gamma \cos \omega \Delta t - i \gamma \sin \omega \Delta t \right|^2 \\ &= 1 + \gamma^2 + 2\gamma \cos \omega \Delta t.\end{aligned}\tag{38}$$

The desired function, $P(f)$, is found from the expression

$$P(f) = \frac{p(f)}{\Gamma(f)} = \frac{p(f)}{1 + \gamma^2 + 2\gamma \cos \omega \Delta t}.\tag{39}$$

More complicated filters may be introduced by including more terms in the linear combination, Eq. (35). The choice of coefficients and number of terms depends entirely upon the spectrum being treated. In general, the more peaks there are in the spectrum, the more terms will be necessary to prewhiten.

5.0 EXPERIMENTAL

5.1 Apparatus

A photograph of the experimental fluidized bed is shown in Fig. 2. The positioning of the movie camera and the lighting fixture relative to the bed section is shown in Fig. 3. A schematic diagram of the entire assembly is also presented in Fig. 4.

A 30-inch-high, 2-inch-diameter Pyrex column was used for the experimental bed section. This section was preceded by a 24-inch-high, 2-inch-diameter calming section filled with 1/4-inch-diameter ceramic tower packing spheres. The calming section provided a tortuous path for the liquid to follow in order to produce a roughly flat velocity profile at the inlet to the bed section. A fine mesh screen was used to support the bed and also to act as a final flow distributor. The screen was held in place by rubber gaskets with the same I.D. as the column so as to offer no restriction to the liquid flow.

For steady state operation the water stream was pumped by a 1/2 horse-power Allis-Chalmers centrifugal pump, Type SSR. The pump produced flow rates up to 10 gallons per minute with the by-pass valve closed. The flow to the column was regulated by a 3/4-inch globe valve and was measured with a Brooks rotameter, size R-10M-25-3. A fifty-five gallon drum was used for the reservoir.

An auxiliary step input stream was also included in the system. The source of water for this section was tap water. The flow rate was measured with a Brooks rotameter, size R-9M-25-2. Step inputs were produced using two 1/2-inch Gould solenoid valves. One solenoid valve, Type QR (normally open),

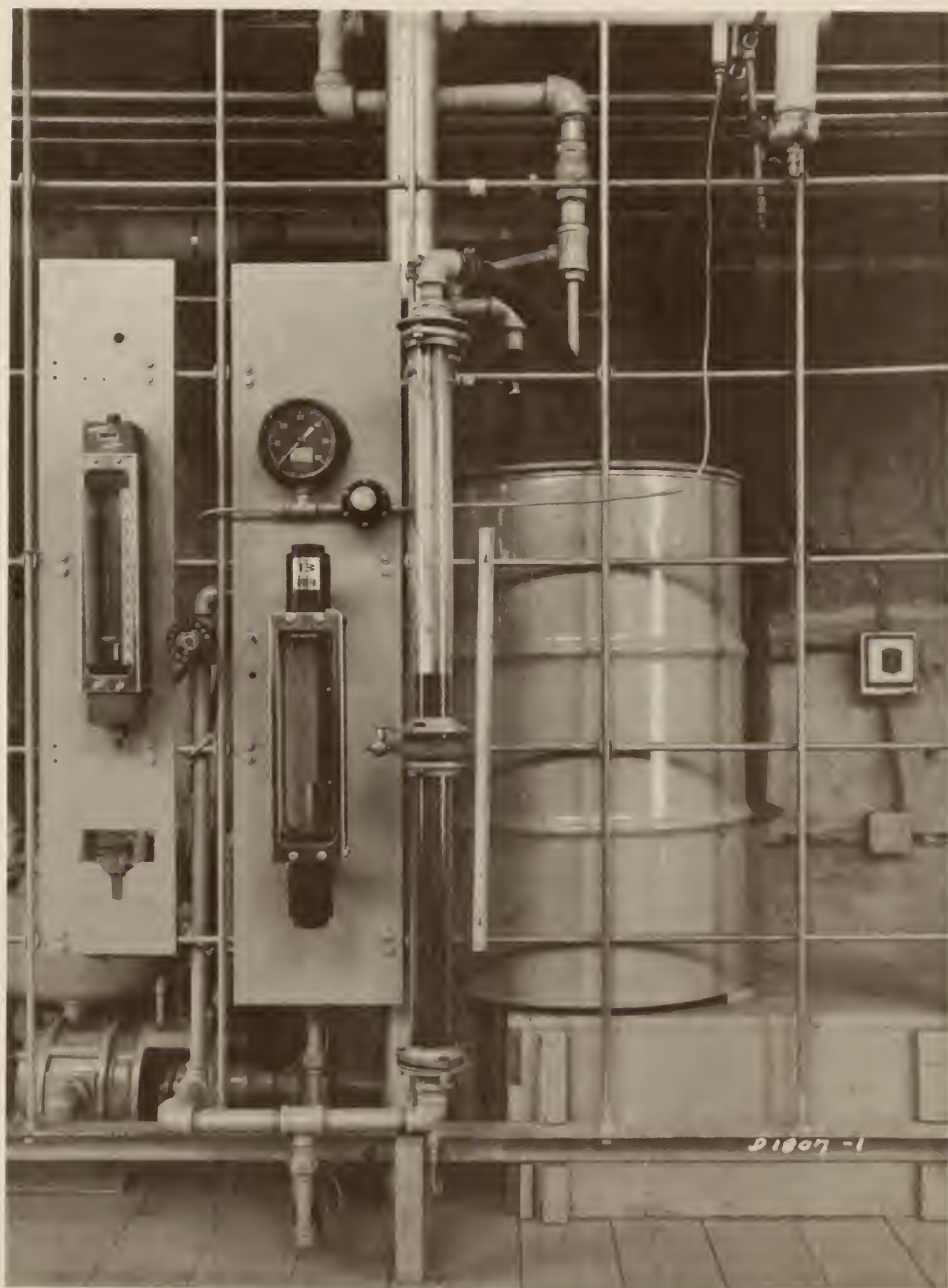


Figure 2. Photograph of the experimental assembly

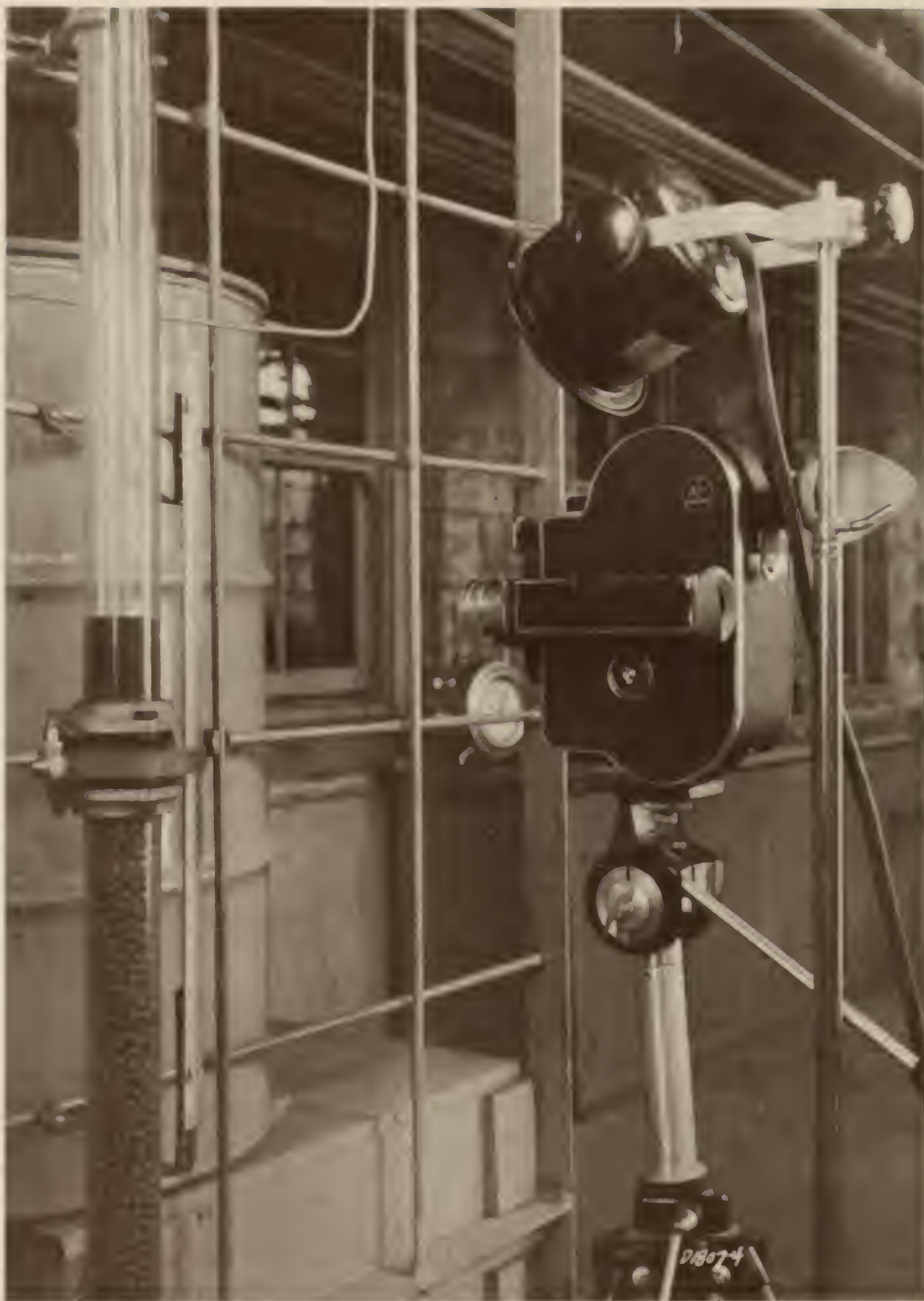


Figure 3. Positioning of the camera and lighting fixture

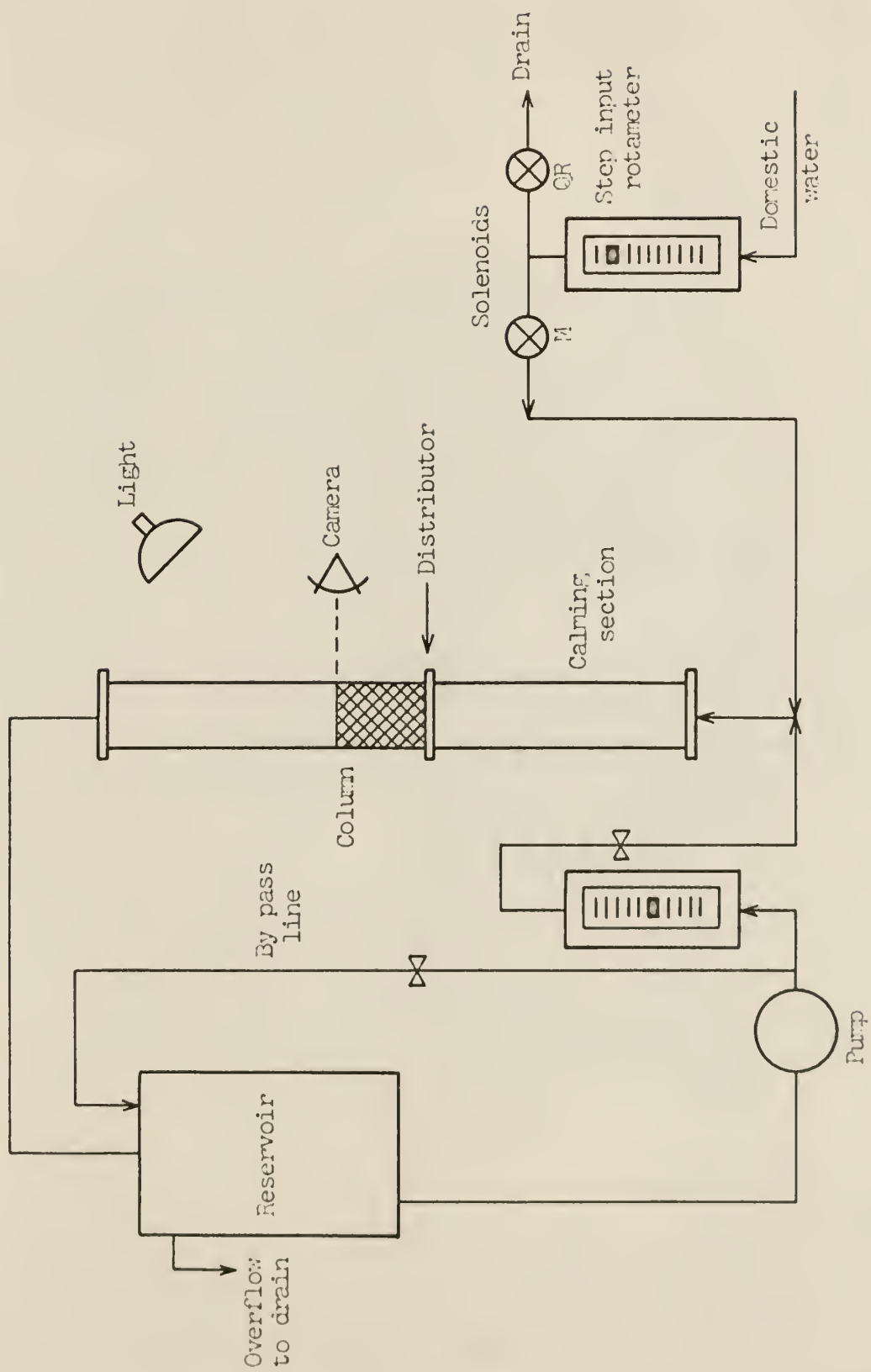


Figure 4. Schematic diagram of experimental apparatus

was in the by-pass line. The other valve, 'Type M (normally closed), was in the line which led to the column. Both valves were connected to the same electrical switch so that they could be actuated simultaneously. Upon closing the circuit, the auxiliary stream was introduced into the bed section as a step input.

The 16 mm. motion picture camera used to obtain the data was a Bolex H-16 Rex with a SOM Berthiot Lytar lens. The focal length of the lens was 25 mm. and the maximum lens opening was $f/1.8$. A Quartz-King Duo-Light 650 provided the light source. A white cardboard background was positioned behind the experimental bed section to give added contrast between the bed and the surroundings. A scale graduated in tenths of inches was included within the field of vision of the camera. A Weston Master IV exposure meter was used to measure the exposure settings. The Invercone attachment was employed to measure the incident light. Eastman Tri-X Reversal Safety Film, Type 7278, was used. The ASA rating of this film is 160.

5.2 Particles

The particles used in the fluidized bed were copper particles obtained from Indiana Copper Corporation (type S-650). The particles were obtained in bulk form which contained various sizes and shapes. Initial separation into size groups was accomplished by hand shaking of Taylor Standard sieves. After sufficient particles were obtained in each size group desired, the final grading was carried out on a shake table. The shaking operation was continued for one hour for each batch. The particles were then graded for shape. This was accomplished by scattering a few particles on an inclined smooth glass

surface and rejecting all those which did not roll down the plane. This procedure eliminated the majority of the ill-shaped particles and left only those which were essentially spherical. The density of the remaining particles was then measured by a liquid displacement technique. The sizes of the particles used in this thesis along with their respective densities and average diameters are listed in Table I. The average diameters are based on the geometric average of the seive openings.

Table I. Properties of the bed particles

Bed Index	Mesh Cut	Density (lb/ft ³)	Average Diameter (inches)
A	20-24	530.6	0.0305
B	12-14	527.5	0.0610
C	16-18	518.2	0.0433

5.3 Procedure

The particles were loaded into the column and a water flow rate was chosen to produce the desired bed expansion ratio, h/h_0 . Three expansion ratios were chosen for the experiment. These ratios were approximately duplicated for each particle size in order to keep h/h_0 as a parameter of the study. Camera settings were made and motion pictures were taken of the upper bed interface. The camera was equipped with a spring driven motor with a capacity of approximately 660 frames per winding. During collection of data, sub-runs of 500 frames each were used. The number 500 was chosen

to allow 8 full sub-runs per 100-foot roll of film and to insure that the film speed would not vary significantly at the end of the sub-run.

A Recordak Model C microfilm reader was used to obtain the bed height from the developed films. The reader projected an image on the back of a translucent glass screen. A straight edge was placed on the face of the screen and the data points were read visually from the scale in the photograph. The purpose of the experiment was to follow one point on the bed interface as a function of time. Due to the circular cross section of the experimental section, it was necessary to read the data at the side of the bed image in the photograph. An attempt was made to read the data points at the center of the bed, however, it was found that one could not differentiate between the motion of the near and far portions of the bed interface. Reading at the side of the bed avoided these undesirable two dimensional effects. Some of the runs were read from both sides of the bed in order to check the assumption that the data were representative of the entire bed interface. All data points were punched on IBM computer cards for analysis on the IBM-1410 digital computer.

Step input data were obtained for several runs for which steady state data had already been collected. Step sizes were chosen to introduce small, medium, and large perturbations into the inlet stream in order to study the effects of the non-linearities of the system. Readings were recorded first for a step increase in flow rate, then for a step decrease in flow rate. The flow rates of the main and auxiliary streams were left the same so that the positive and negative steps were of the same size.

6.0 DISCUSSION AND RESULTS

It is generally accepted that fluidized beds have two primary regimes of flow:

- 1) homogeneous
- 2) slugging or bubbling.

The first of these is characterized by uniform bed density and roughly constant interparticle spacing. The upper fluid-bed interface is well defined and remains quite stationary. Homogeneous fluidized beds generally result when both the particle mass to fluid mass ratio, ρ_p/ρ_f , and the particle diameter to bed diameter ratio, D_p/D , are relatively low.

The slugging condition exists in most fluidized beds using gas as the fluidizing medium. In these systems the mass ratio is quite high. Systems in which the diameter ratio is high also tend to operate in the slugging regime. The slugging fluidized bed has the appearance of a boiling fluid with voids forming at the bottom of the bed and rising to the top of the bed nominally intact. Under these conditions the upper fluid-bed interface fluctuates rapidly.

Many fluidized beds are neither purely homogeneous nor purely slugging but have some characteristics of both types. The copper-water system studied for this thesis is such a system. The mass ratio of the copper-water system is relatively high causing a fluctuating tendency. The diameter ratio, however, was kept small so that the true slugging flow was not experienced. The condition achieved was a relatively homogeneous bed with a fluctuating fluid-bed interface. Homogeneity was desired in order to remain within the class

of fluidized beds suitable for nuclear reactor applications. The fluctuation was necessary in order to apply the concept of noise analysis to obtain the time constants of the system.

There are several important parameters to be considered in the study of a fluidized bed. They are:

- 1) particle size
- 2) expansion ratio
- 3) packed bed depth
- 4) bed diameter
- 5) fluidizing medium
- 6) particle density.

Any or all of these parameters could have an effect on the dynamic behavior of the system. Of these six parameters only the first three were varied during the course of this work. The latter three were kept as constants of the system. The density of the particles did vary somewhat as shown in Table I, however, this variation should not have affected the overall results. The film speed of the camera was also varied. The film speed is directly related to the statistical analysis of the data so discussion of this effect will be postponed until later in this section.

Table II is a list of the experimental steady state runs and the values of the parameters in each case. Three particle sizes were used with at least three different values of h/h_0 for each particle size. The last three runs are replications of A-10, B-1, and C-2, respectively. The data for these runs were read from the opposite side of the bed in order to determine if the results were representative of the entire bed interface. Runs C-1, D-1, and

Table II. List of runs and the values of the parameters.

Run Number	Particle Size (mesh cut)	h_0 (inches)	h/h_0	Camera Speed (fps)
A-7	20-24	3.8	1.67	24
A-8	20-24	3.8	1.68	32
A-10	20-24	3.8	1.73	48
A-11	20-24	3.8	1.44	48
A-12	20-24	3.8	2.04	48
B-1	12-14	3.8	1.78	48
B-2	12-14	3.8	2.08	48
B-3	12-14	3.8	2.39	48
B-4	12-14	3.8	1.47	48
B-5	12-14	3.8	1.65	32
C-1	16-18	3.8	1.49	48
C-2	16-18	3.8	1.73	48
C-3	16-18	3.8	1.93	48
D-1	16-18	5.7	1.44	48
E-1	16-18	7.6	1.44	48
A-10-R	20-24	3.8	1.70	48
B-1-R	12-14	3.8	1.78	48
C-2-R	16-18	3.8	1.74	48

E-1 vary h_0 for constant particle size and constant h/h_0 .

Figure 5 shows enlarged sections of the photographic film from which the data were read. These sections of film were taken from runs A-10, B-1, and C-2. These runs were chosen for display since their h/h_0 values were approximately the same. In general it was observed that the magnitude of the fluctuation of the upper fluid-bed interface was roughly proportional to the size of the particles, the smaller particles fluctuating more than the larger particles. The variance of the experimental data which represents a measure of the fluctuation was computed for each run. The results of these calculations are included in Appendix E. It was found that the variance increased with increasing h/h_0 for a given particle size, i.e., the upper fluid-bed interface became more unstable with increasing bed expansion.

One of the basic requirements for application of noise analysis concepts to a system is that it be a Gaussian random process. The frequency distribution of the experimental data for each run was found in order to check the validity of this assumption. The frequency distribution was obtained by counting the number of times a particular bed height was observed in a run. The frequency of occurrence was then plotted versus bed height. Figures 6, 7 and 8 show representative curves obtained from the data. The curves plotted in these figures were calculated by substituting the experimental mean and variance into the equation for the Gaussian distribution,

$$f(x) = \frac{1}{\sqrt{2\pi} \sigma} \exp \left\{ -\frac{(x - \bar{x})^2}{2\sigma^2} \right\}$$

where \bar{x} is the mean and σ^2 is the variance. The fit of the experimental data suggests that the system approaches a Gaussian random process.

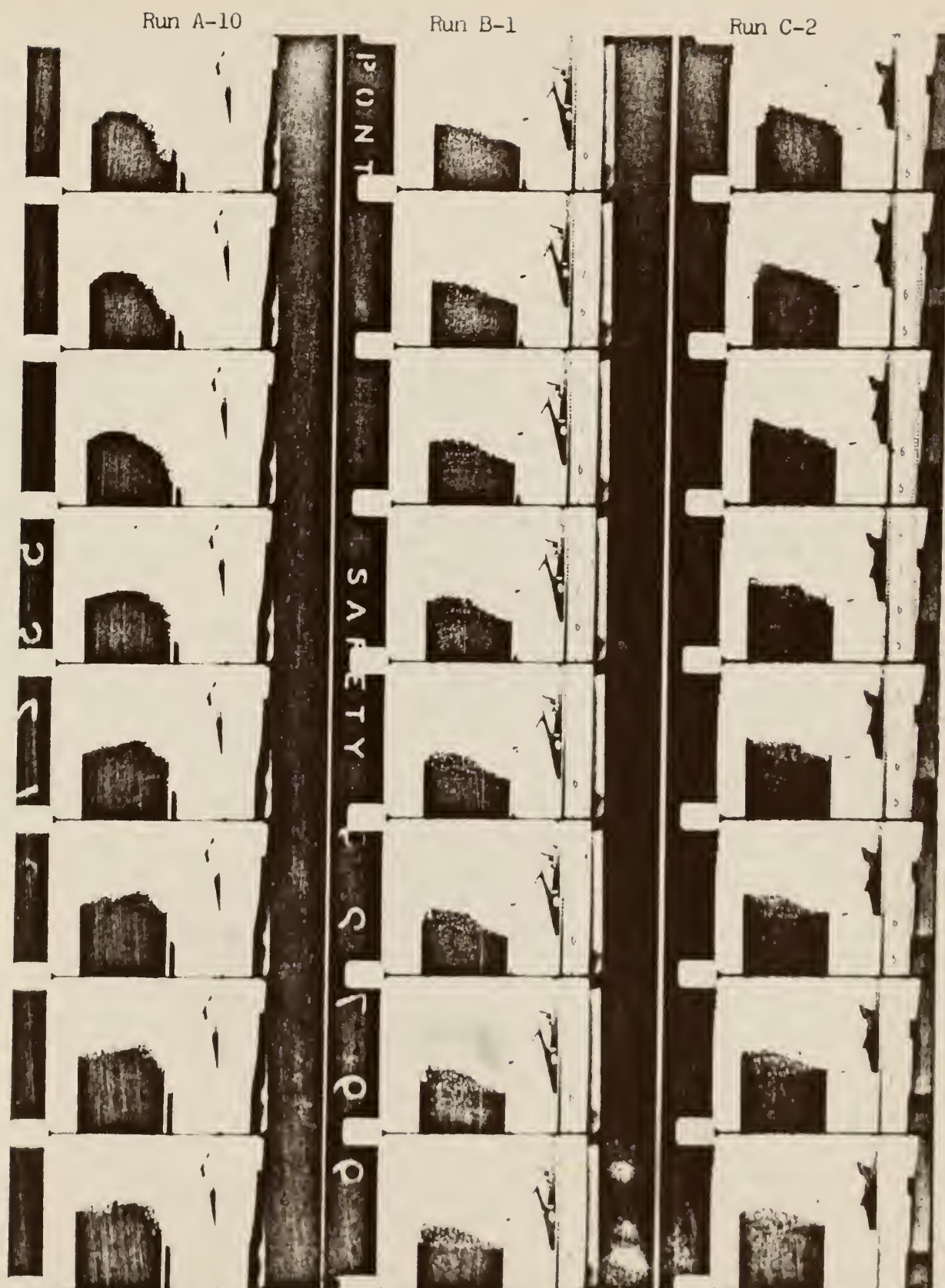


Figure 5. Excerpts from the photographic data

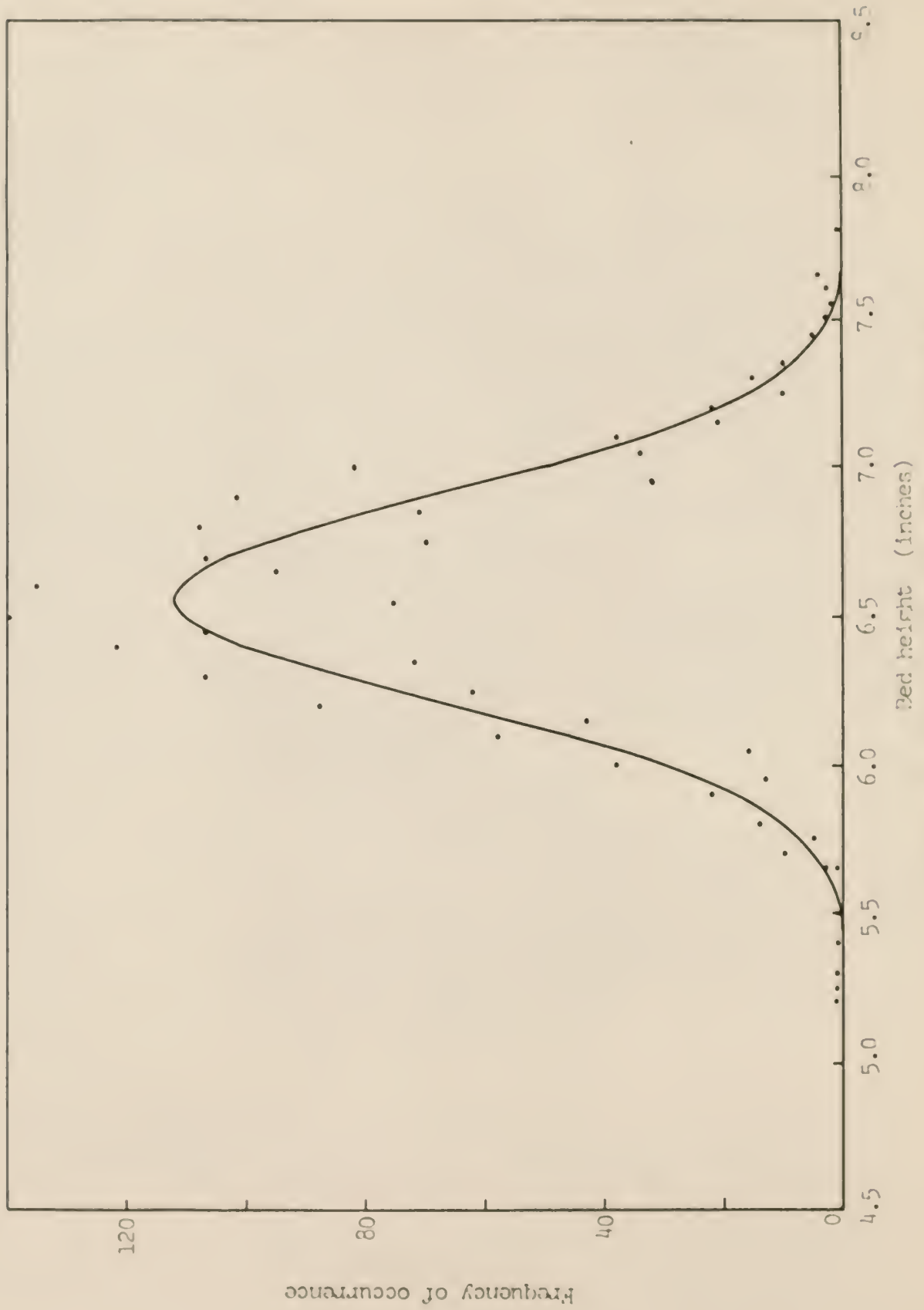


Figure 6. Frequency distribution of Red height (inches)

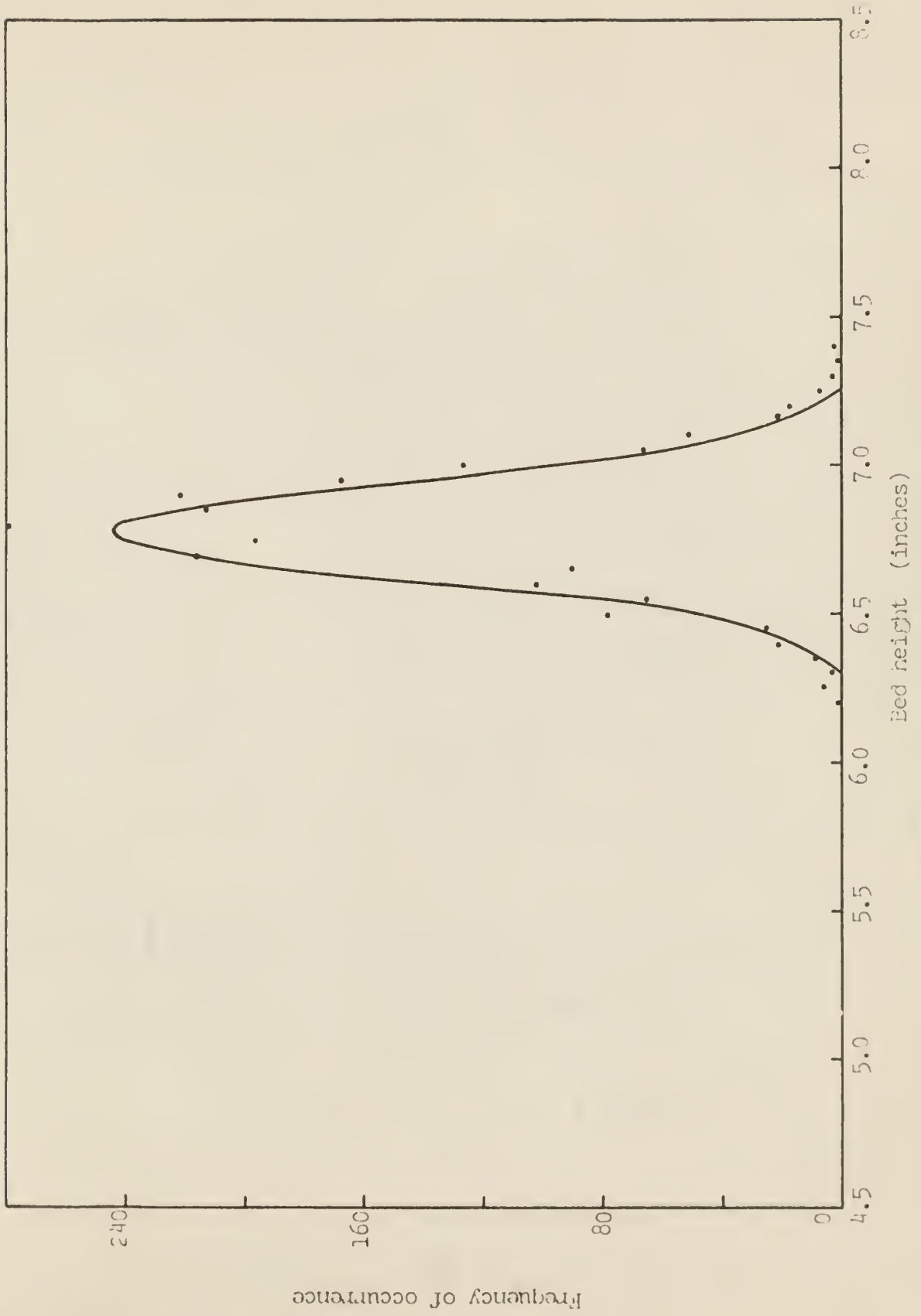


Figure 7. Frequency distribution of Fun B-1

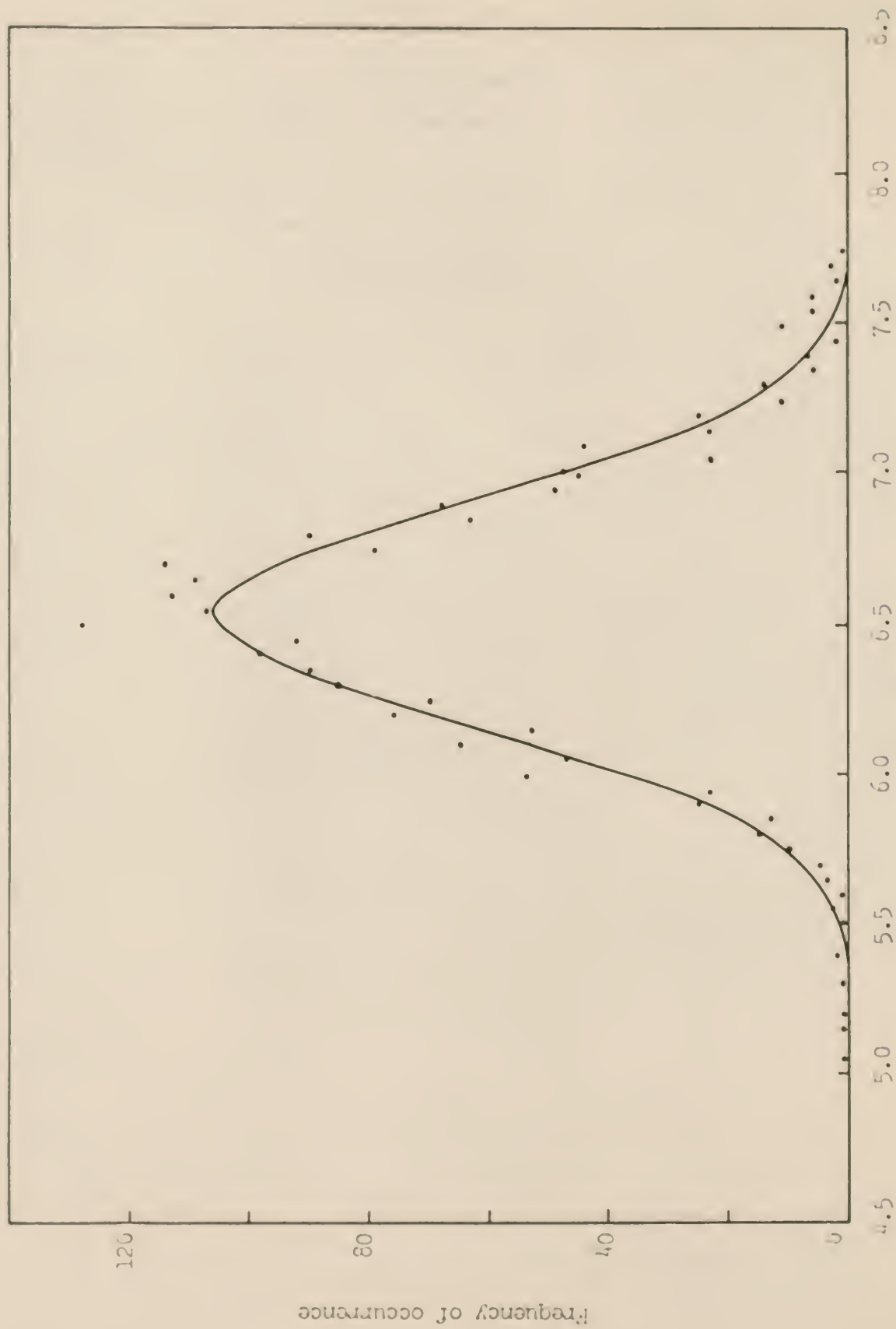


Figure 6. Frequency distribution of Plan C-2

The autocorrelation function and power spectrum were calculated using the IBM-1410 digital computer code described in Appendix C. Since the data were taken in digital form at equally spaced intervals of time, it was necessary to use digital approximations to obtain these functions. The autocorrelation function, Eq. (14), was approximated by a normalized sum of lagged products,

$$\phi(\tau_n) = \frac{\frac{1}{N-n} \sum_{i=1}^{N-n} x_i x_{i+n}}{\frac{1}{N} \sum_{i=1}^N x_i x_i}, \quad n = 0, 1, 2, \dots, M \quad (40)$$

where N is the total number of data points per run and M is the maximum number of time lags, $M = \tau_m / \Delta t$. Adjacent data points were used so that $\Delta \tau = \Delta t$. Figures 9, 10, and 11 show the normalized autocorrelation function for the three frequency distributions in Figs. 6, 7, and 8, respectively. The results of the computer calculations for all the runs are listed in Appendix E.

The autocorrelation function was estimated for each sub-run. The corresponding sub-run estimates were then averaged to obtain $\phi(\tau)$ for the entire run. M was chosen to give a final power spectrum resolution of one radian per second. The Nyquist sampling theorem requires two samples per cycle for resolution, therefore M was equal to one-half of the film speed, or $M = 1/2\Delta t$.

The statistical accuracy of the autocorrelation function has been estimated by Thie (19). He assumed that $\phi(\tau)$ could be approximated by

$$\phi(\tau) = \exp \{-\tau/\tau_c\} \quad (41)$$

where τ_c is the correlation time constant, i.e., the time at which the autocorrelation function is down by a factor of e . Equation (41) is exact only for a Markov process (5), however, it is sufficient for purposes of error

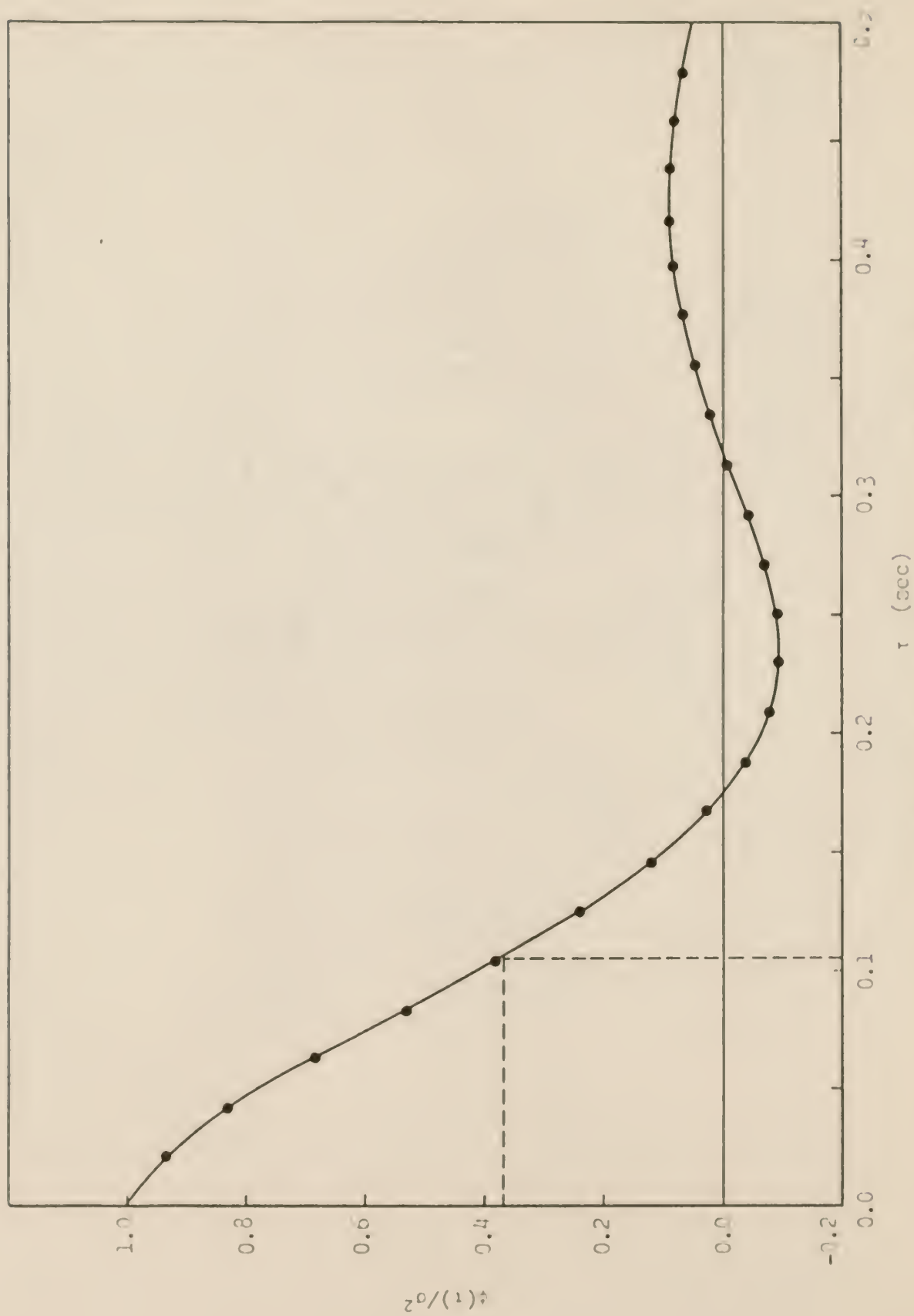


Figure 9. Autocorrelation function of Run A-10

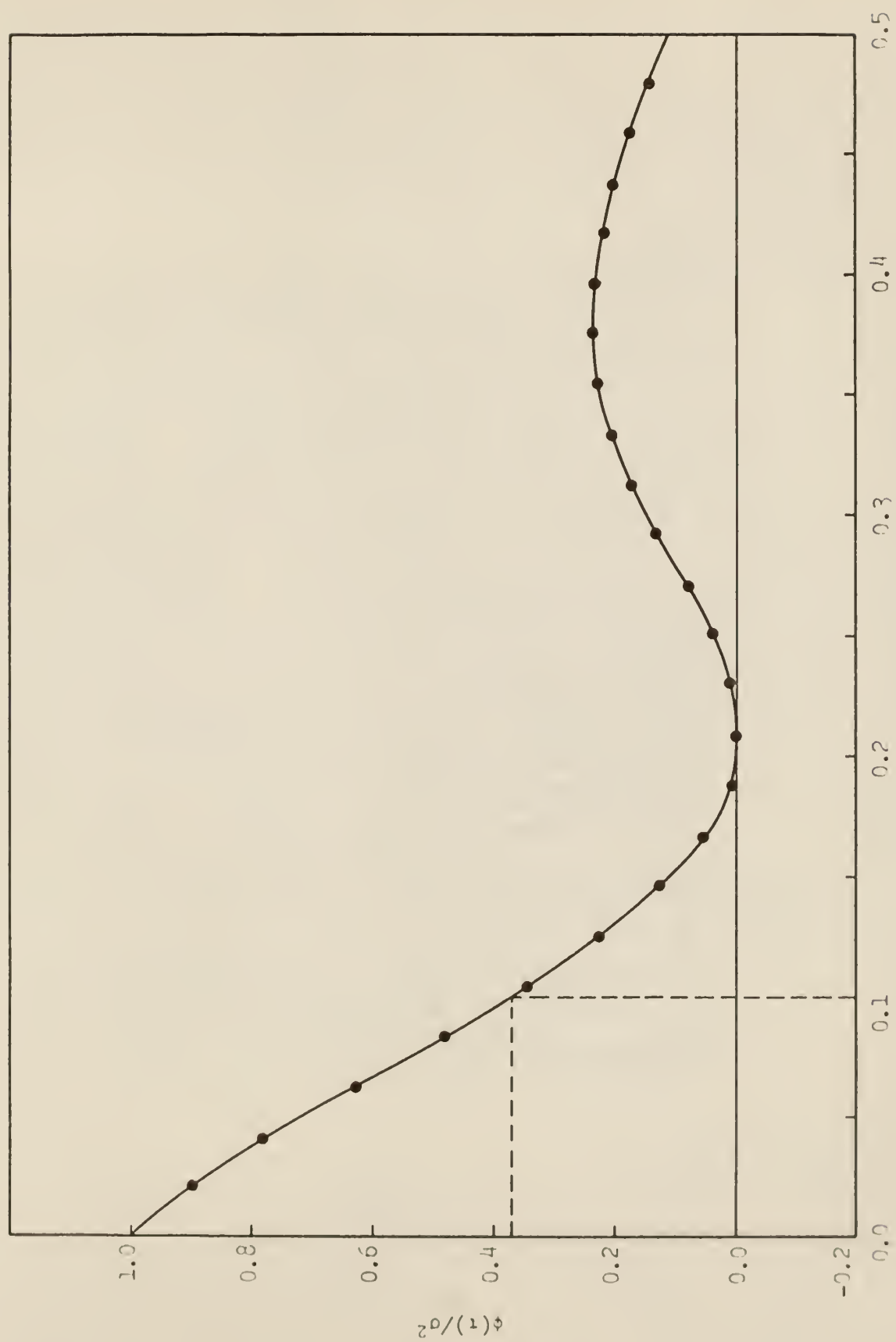


Figure 10. Autocorrelation function of Fun B-1

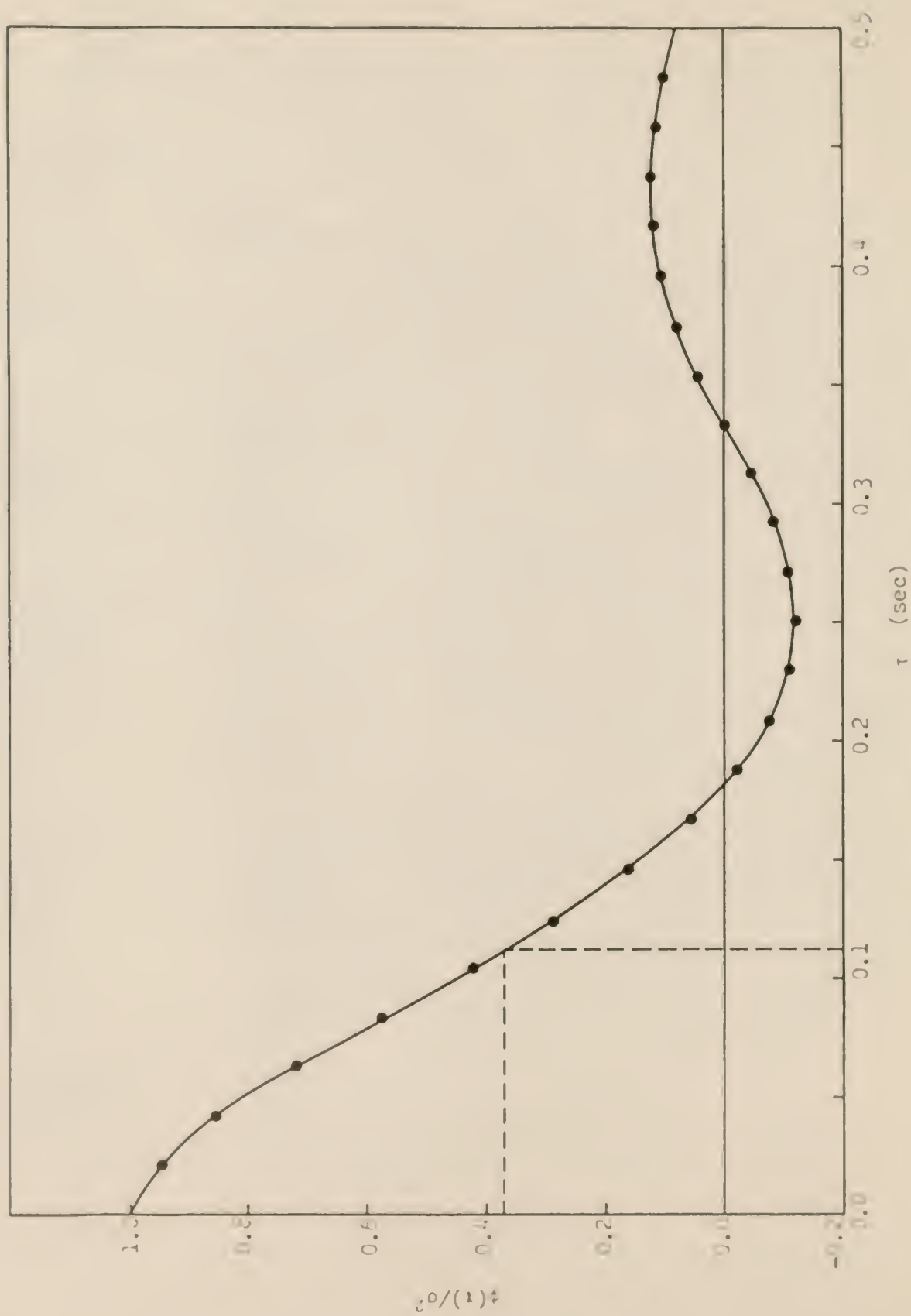


Figure 11. Autocorrelation function of Rm C-2

estimation for most Gaussian random processes. The expression for the standard deviation which Thie exhibits is

$$\sigma_c \leq \frac{1}{\sqrt{T/\tau_c}}$$

where T is the total time duration of the sample. Table III lists the various values of T , τ_c , and σ_c for the experimental data.

Figures 12, 13, and 14 show the power spectra corresponding to the autocorrelation functions shown in Figs. 9, 10, and 11. These power spectra were obtained by Fourier transforming the autocorrelation function as indicated by Eq. (19). The integration was approximated by trapezoidal quadrature which resulted in raw spectral estimates spaced at $\omega_1 = \frac{1}{2\tau_m}$. The resulting expression for the power spectrum was

$$\begin{aligned} \Phi(\omega_n) = \Delta\tau \left\{ \phi(0) + 2 \sum_{i=1}^{M-1} \phi(\tau_i) \cos \omega_n \tau_i \right. \\ \left. + \phi(\tau_m) \cos \omega_n \tau_m \right\}. \end{aligned} \quad (42)$$

For $\tau_m = M\Delta t$ and $M = \frac{1}{2\Delta t}$ the resolution becomes

$$\Delta\omega = \frac{2\Delta t}{2\Delta t} = 1.0 \text{ radian/sec.}$$

The calculated power spectra are listed in Appendix E.

Blackman and Tukey (4) show that estimates of ϕ for a Gaussian random process scatter about the true value according to the chi-square distribution. For spectra that are relatively flat, i.e., those containing no narrow peaks, the reliability of the measured values of the power spectra depend only on the sample length and on the number of separate estimates of the spectrum. The reliability of each estimate may be expressed in terms of k , the equiva-

Table III. Standard deviation of the autocorrelation function

Run Number	T (sec)	τ_c (sec)	σ_c
A-7	82.8	0.160	0.044
A-8	63.1	0.082	0.036
A-10	41.5	0.106	0.051
A-11	41.8	0.090	0.046
A-12	41.6	0.138	0.058
B-1	41.5	0.101	0.049
B-2	41.3	0.146	0.059
B-3	41.3	0.122	0.054
B-4	41.0	0.081	0.044
B-5	63.3	0.131	0.046
C-1	41.2	0.098	0.049
C-2	41.3	0.113	0.052
C-3	41.1	0.147	0.060
D-1	43.2	0.117	0.052
E-1	41.4	0.141	0.058
A-10-R	41.4	0.121	0.054
B-1-R	41.4	0.091	0.047
C-2-R	41.5	0.110	0.051

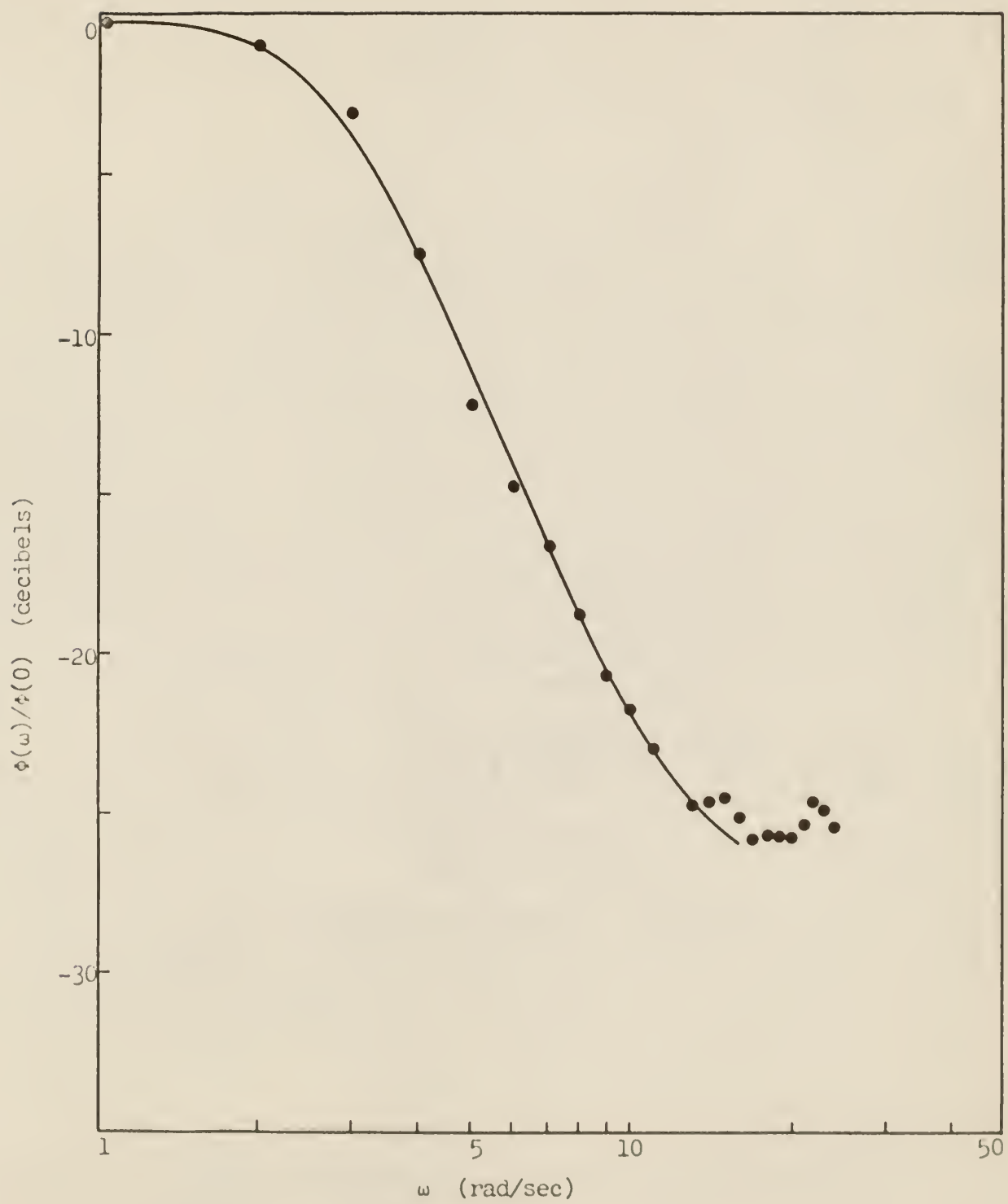


Figure 12. Power spectrum of Run A-10

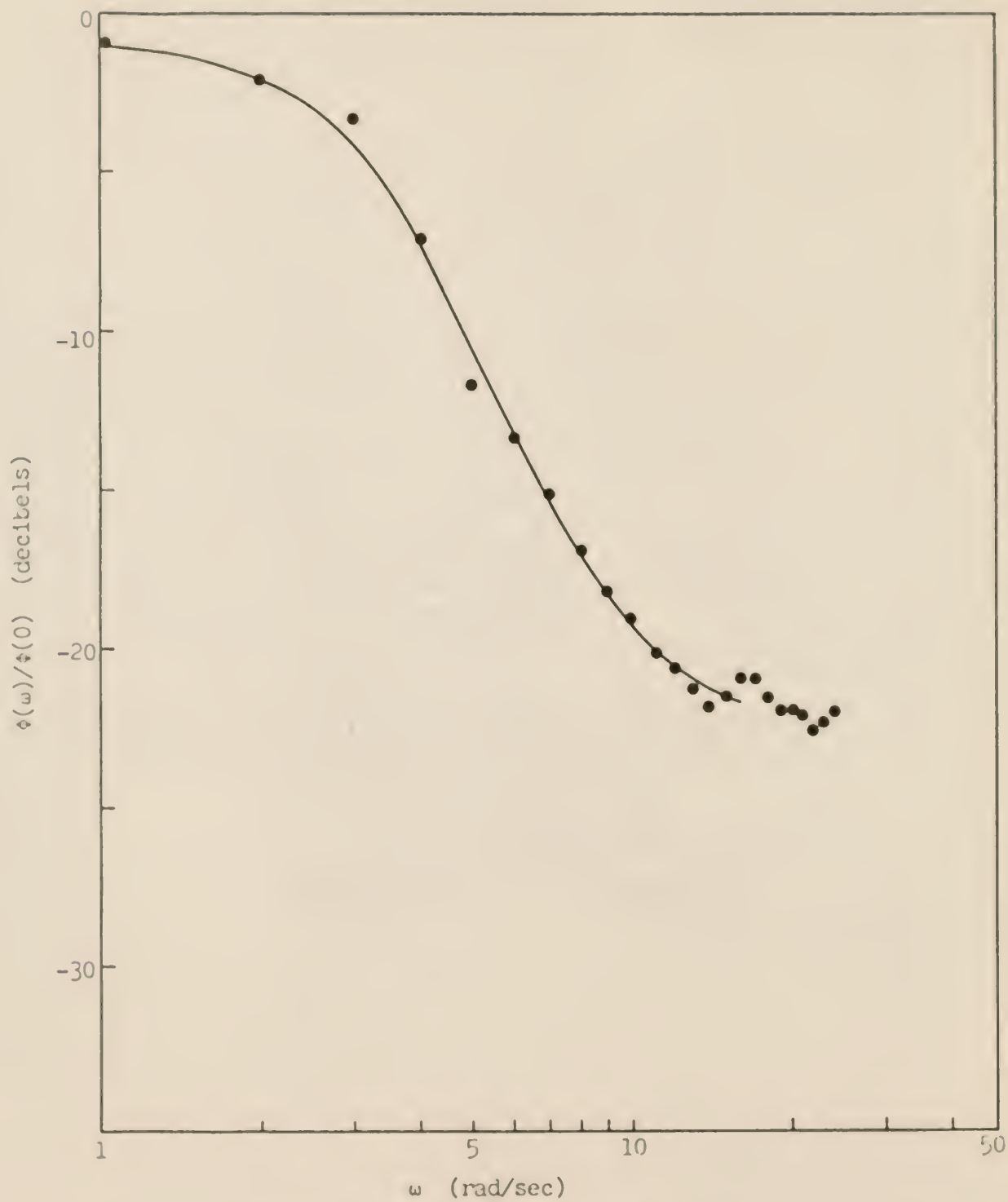


Figure 13. Power spectrum of Run B-1

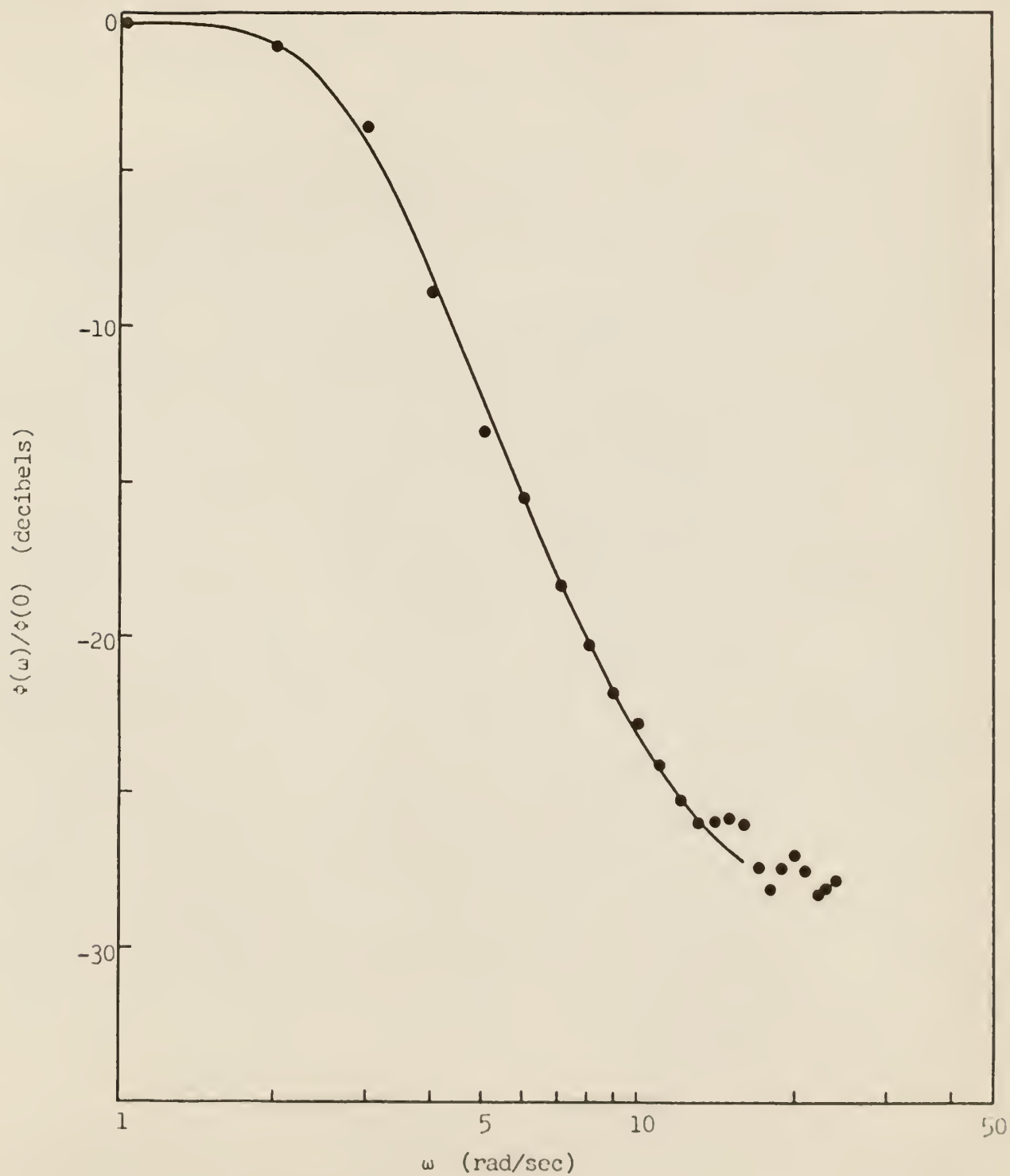


Figure 14. Power spectrum of Run C-2

lent degrees of freedom of the chi-square distribution. The quantity k may be approximated by the expression

$$k = (N - \frac{N}{5}) (\frac{2}{M}). \quad (43)$$

Figure 15 gives the 80% confidence limits for a chi-square distribution as a function of k . The limits marked by the dotted lines show the average statistical spread of the experimental power spectra using a resolution of one radian per second. Since the error analysis was only approximate, the limits

$$0.84 \phi_{\text{ave}} \leq \phi_{\text{meas}} \leq 1.16 \phi_{\text{ave}}$$

were assumed to be representative of the statistical reliability for all of the runs.

The curves drawn in Figs. 12, 13, and 14 are the least squares fit of a second order transfer function to the experimental power spectrum. The equation relating the power spectrum to the transfer function of a system is

$$\phi_o(f) = K |Z(f)|^2. \quad (23)$$

A second order transfer function is represented by the expression

$$Z(f) = \frac{1}{\alpha^2 + 2\alpha\beta(j\omega) + (j\omega)^2} \quad (44)$$

where α is the break frequency and β is the damping factor. Substituting Eq. (44) into Eq. (23) gives

$$\phi_o(f) = K \frac{1}{\alpha^4 + 2\alpha^2 \omega^2(2\beta^2 - 1) + \omega^4}. \quad (45)$$

The experimental power spectrum was observed to tail-off at the high frequency end of the spectrum. This behavior was also reported by Cohn (6) in the power spectrum of a nuclear reactor. He attributed the behavior to

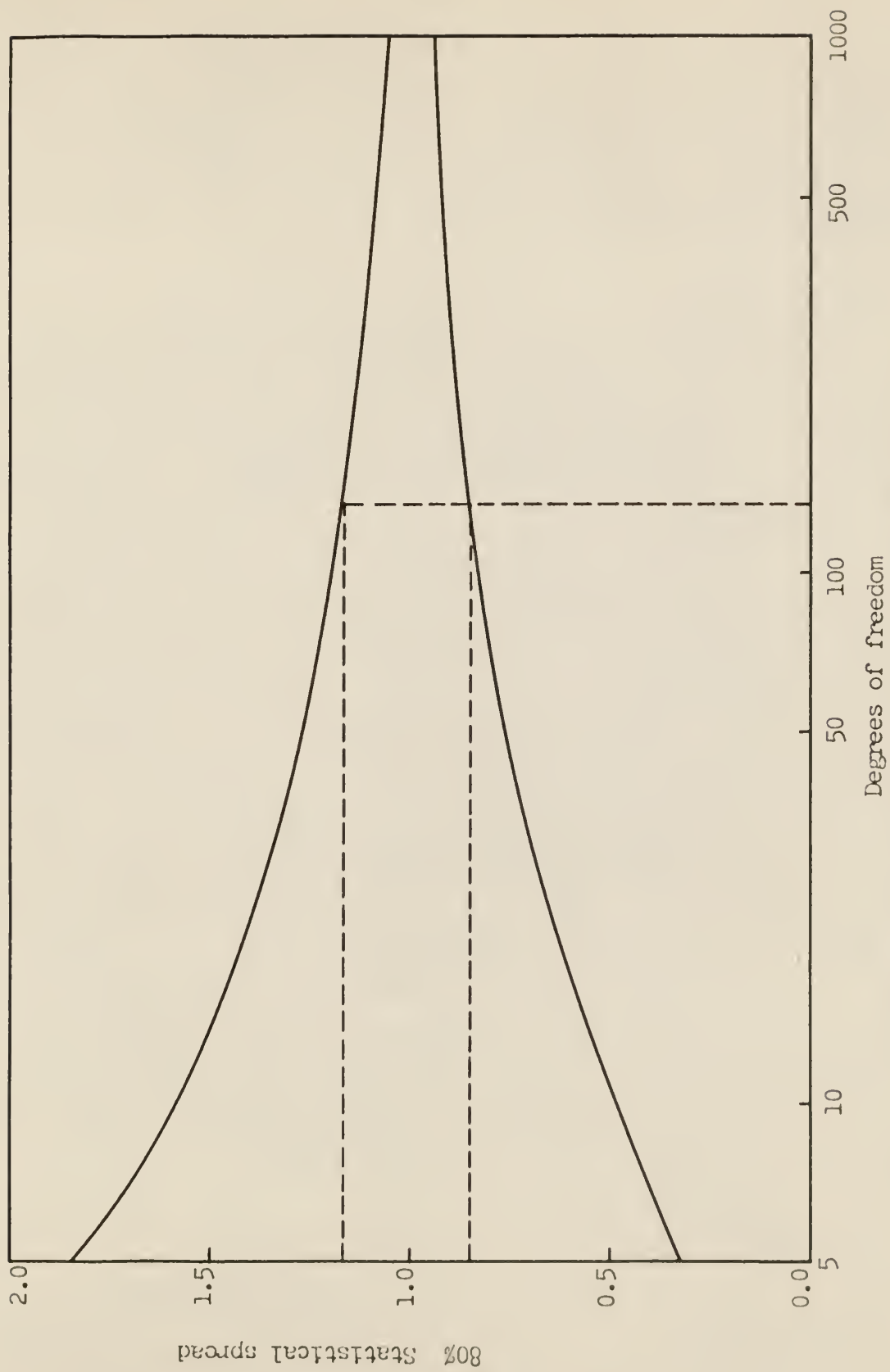


Figure 15. Confidence limits on the power spectrum

an uncorrelated white noise component of the spectrum. This uncorrelated component was constant throughout the spectrum so that its presence could be compensated for by adding an arbitrary constant to Eq. (45). Thus, the equation used in fitting the data was

$$\phi_o(f) = \frac{A}{\alpha^4 + 2\alpha^2\omega^2(2\beta^2 - 1) + \omega^4} + B. \quad (46)$$

Equation (46) has four unknown constants (α , β , A , and B) which were to be found by fitting the equation to the experimental data. The method of least squares was chosen as the criterion for the best fit. The sum of the squared errors is given by

$$S = \sum_{i=1}^M \left\{ \phi_{o1} - \frac{A}{F_1} - B \right\}^2$$

where

$$F_1 = \alpha^4 + 2\alpha^2\omega_1^2(2\beta^2 - 1) + \omega_1^4.$$

Differentiating S with respect to A , B , α , and β , respectively, gave the following four normal equations to be solved

$$\frac{\partial S}{\partial A} = 0 = 2 \sum_1 \left\{ \phi_{o1} - \frac{A}{F_1} - B \right\} \left(-\frac{1}{F_1} \right) \quad (47)$$

$$\frac{\partial S}{\partial B} = 0 = 2 \sum_1 \left\{ \phi_{o1} - \frac{A}{F_1} - B \right\} (-1) \quad (48)$$

$$\frac{\partial S}{\partial \alpha} = 0 = 2 \sum_1 \left\{ \phi_{o1} - \frac{A}{F_1} - B \right\} \left\{ \frac{4\alpha^3 + 4\alpha\omega_1^2(2\beta^2 - 1)}{F_1^2} \right\} \quad (49)$$

$$\frac{\partial S}{\partial \beta} = 0 = 2 \sum_1 \left\{ \phi_{o1} - \frac{A}{F_1} - B \right\} \left\{ \frac{8\alpha^2\omega_1^2\beta}{F_1^2} \right\} \quad (50)$$

The first two normal equations, Eqs. (47) and (48), are linear in A and

B and were solved directly for A and B in terms of α and β . Weighting factors given by

$$w_1 = 1/\phi_{o_1}$$

were used in the least squares determination of A and B. The weighting factors were necessary in order to get a reasonable fit to the high frequency end of the power spectrum. Initial calculations without the weighting factors gave unsatisfactory results with deviations of the order of 500% at the high frequencies. In some instances the least squares fit gave negative values at high frequencies. This is unreasonable since the power spectrum, which is the square of the magnitude of the transfer function, can never be negative. Introduction of the weighting factors caused the weighted error at the high frequency end to be of the same magnitude as the error at the low frequency end of the spectrum. The result was a reasonable fit to the experimental data. The use of the weighting factors did not significantly alter the values obtained for α and β .

The last two normal equations, Eqs. (49) and (50), are non-linear, therefore they could not be solved directly for α and β . An iterative technique based on the Newton-Raphson method was used to solve for these two variables. The details of this method are outlined in Appendix D so they will not be discussed here. No weighting factors were included in the least squares determination of α and β .

The steps employed in the iterative method were:

- 1) Guess α and β from the experimental spectrum.
- 2) Calculate A and B from Eqs. (47) and (48).

- 3) Calculate Δa and ΔB by the Newton-Raphson method using Eqs. (49) and (50).
- 4) Correct a and B .
- 5) Recalculate A and B and continue to iterate until the corrections were less than some predetermined ϵ .

Table IV gives the results of these calculations. The computer output for these calculations is also listed in Appendix F.

Only the first portion of the experimental power spectrum was used in the least squares fitting procedure. The last few points of the power spectrum were erratic. This behavior was attributed to inaccuracies in reading the data. Since the data were obtained with an accuracy of ± 0.05 inches, the high frequency resolution would be expected to be rather poor. For this reason the least squares fit was carried out over the first two-thirds of the spectrum only.

The results discussed up to this point have been for the special case of no prewhitening filter and a resolution of one radian per second in the power spectrum calculations. Additional calculations were made using a digital filter and a different resolution in order to ascertain the effects of these quantities on the final results of the calculations. The results of these calculations are discussed below.

All of the runs were analyzed with a prewhitening filter with a value of 0.5 for the prewhitening coefficient. The results of these calculations are listed in Table V. The use of the filter resulted in quite different autocorrelation functions, however, when $\phi(\tau)$ was Fourier transformed and corrected by the transfer function of the filter, the results were nearly the same

Table IV. Break frequency and damping factor of the experimental data with the corresponding squared error

Run Number	Break Frequency	Damping Factor	Squared Error
A-7	1.968	0.6232	0.0000217
A-8	3.235	0.5184	0.0003144
A-10	2.666	0.6284	0.0001161
A-11	3.005	0.6084	0.0000792
A-12	2.139	0.6374	0.0001591
B-1	2.928	0.6925	0.0002638
B-2	2.824	1.0197	0.0001631
B-3	2.552	0.7748	0.0001201
B-4	3.353	0.6466	0.0000220
B-5	2.550	0.8265	0.0000294
C-1	2.759	0.5643	0.0001628
C-2	2.491	0.6101	0.0001452
C-3	2.286	0.8044	0.0000626
D-1	2.745	0.7818	0.0001641
E-1	2.397	0.8198	0.0003907
A-10-R	2.552	0.7370	0.0000722
B-1-R	2.905	0.5432	0.0001154
C-2-R	2.607	0.6375	0.0001611

Table V. Results of the analysis for prewhitened data

Run Number	Break Frequency	Damping Factor	Squared Error
A-7	1.877	0.6430	0.0000416
A-8	3.142	0.5286	0.0012512
A-10	2.609	0.6332	0.0009379
A-11	2.693	0.6235	0.0005258
A-12	2.097	0.6356	0.0013386
B-1	2.866	0.7176	0.0015297
B-2	2.766	1.0433	0.0011172
B-3	2.510	0.7770	0.0007068
B-4	3.280	0.6602	0.0001532
B-5	2.459	0.8340	0.0001103
C-1	2.660	0.5672	0.0016677
C-2	2.438	0.6191	0.0011011
C-3	2.228	0.8027	0.0005112
D-1	2.692	0.7805	0.0013054
E-1	2.351	0.8030	0.0034571
A-10-R	2.504	0.7397	0.0005616
B-1-R	2.846	0.5496	0.0007626
C-2-R	2.553	0.6432	0.0013065

as for the non-filtered case. All of the runs taken at 48 frames per second gave break frequencies and damping factors which differed from the non-filtered values by less than 3%. These deviations were considered insignificant since the statistical reliability of the power spectrum calculations was of the order of 15%. However, the small deviation of α and β from the filtered to the non-filtered cases indicated that very little if any aliasing had occurred in the analysis. The squared error listed in Table V is larger than that in Table IV because the magnitude of the power spectrum calculated from the pre-whitened data was greater.

The three runs taken at slower film speeds, A-7, A-8, and B-5, showed more deviation when the prewhitening filter was applied. This indicated that aliasing could have occurred in the analysis and that the power spectra calculated from these runs were of dubious validity. Consequently these runs were rejected from further consideration.

The remaining runs were analyzed using a resolution of two radians per second. The resolution resulted in $k = 266$ equivalent degrees of freedom, which, according to Fig. 15, yielded a statistical spread of

$$.90 \phi_{ave} \leq \phi_{meas} \leq 1.10 \phi_{ave}.$$

The statistical reliability of these calculations is somewhat better, however, the resolution was found to be unsatisfactory for further analysis. Attempts to utilize this data in the least squares analysis to find the break frequency and damping factor resulted in an unstable condition which would not converge.

Table VI lists the nine experimental runs for which the parameter h/h_0 was duplicated for each particle size. There were three particle sizes and

Table VI: List of runs used in the statistical analysis

Particle Size	Bed Expansion Ratio		
	1.47	1.74	2.04
0.0305	A-11	A-10	A-12
0.0433	C-1	C-2	C-3
0.0610	B-4	B-1	B-2

three values of bed expansion ratio for which this was true. These runs were statistically analyzed to ascertain if D_p and h/h_o had a significant effect on the calculated values of α and β . The statistical analysis was carried out under the direction of Krause (11) and consisted of an analysis of the variance of the calculated data.

The first statistical analysis was the univariate analysis of variance which treated α and β as independent variables. Table 11-3 of Snedecor (18) is a flow sheet for this analysis and outlines the method of determining the mean squares associated with the two-way table of values. The variance ratio, F , which is defined as

$$F = \frac{\text{mean square for treatments}}{\text{mean square for discrepancy}}$$

was used for the significance test.

Treating α as an independent variable gave the following values of F .

$$F_{2,4} (h/h_o) = 17.5548$$

$$F_{2,4} (D_p) = 14.0812.$$

A standard table of the F distribution shows that both D_p and h/h_o were significant in the observed values of α at the 2.5% level, i.e., there is a 97.5% probability that both D_p and h/h_o had an effect on the observed values of the break frequency.

Treating β as an independent variable gave the following values of F.

$$F_{2,4} (h/h_o) = 4.2161$$

$$F_{2,4} (D_p) = 2.3284.$$

The table of F shows that D_p and h/h_o were significant in the observed values of β at the 25% level. This indicates that there is only a 75% probability that D_p and h/h_o were responsible for the variation observed in β , and that there is a 25% probability that the observations came from a random sample.

Since α and β were actually determined from the same experimental curve, Krause suggested the use of a multivariate analysis of variance. This analysis treated α and β as a coupled pair of observations and gave a value of F for the pair. Section 8.9 of Anderson (2) outlines the steps involved in the multivariate analysis of variance. The results of this treatment were the following values of F.

$$F_{4,6} (h/h_o) = 13.682$$

$$F_{4,6} (D_p) = 5.683$$

These results show that D_p was significant in the observed values of α and β at the 5% level, while h/h_o was significant at the 0.5% level. Thus h/h_o was still the more important parameter over the range covered by the experimental work, however, the effect of D_p was significant.

The calculated values of α and β using the prewhitening coefficient value of 0.5 were also statistically analyzed by the same tests. In every case the significance level was higher for the non-filtered case than for the filtered case.

Figure 16 is a plot of the calculated break frequencies as a function of the bed expansion ratio, h/h_0 . The values plotted are those corresponding to the A, B, and C runs taken at 48 frames per second and calculated without a prewhitening filter. The lines drawn in Fig. 16 merely show the trends of the data and are not intended to be a correlation of the data.

It is apparent that from Fig. 16 the break frequency decreases as the bed expansion ratio increases. The time constant of a system is inversely proportional to the break frequency, therefore, the system time constant increases as h/h_0 increases. This behavior was observed for all three particle sizes. The trends of the data in Fig. 16 also indicated that the break frequency changes more rapidly for small particles than for large particles.

Figure 17 shows the variation of the damping factor as a function of bed expansion ratio. Although the data are quite erratic, a general trend of increasing bed expansion ratio is apparent. This would indicate that the form of the transfer function changes as a function of bed expansion. Since $\beta < 1.0$ represents an underdamped system, one would expect more overshoot for step input responses when the bed expansion ratio is small than when it is large.

Figure 18 shows the effect that changing the packed bed height has on the break frequency and damping factor. The particle size and expansion ratio were kept constant so that the variation would be due to packed bed height

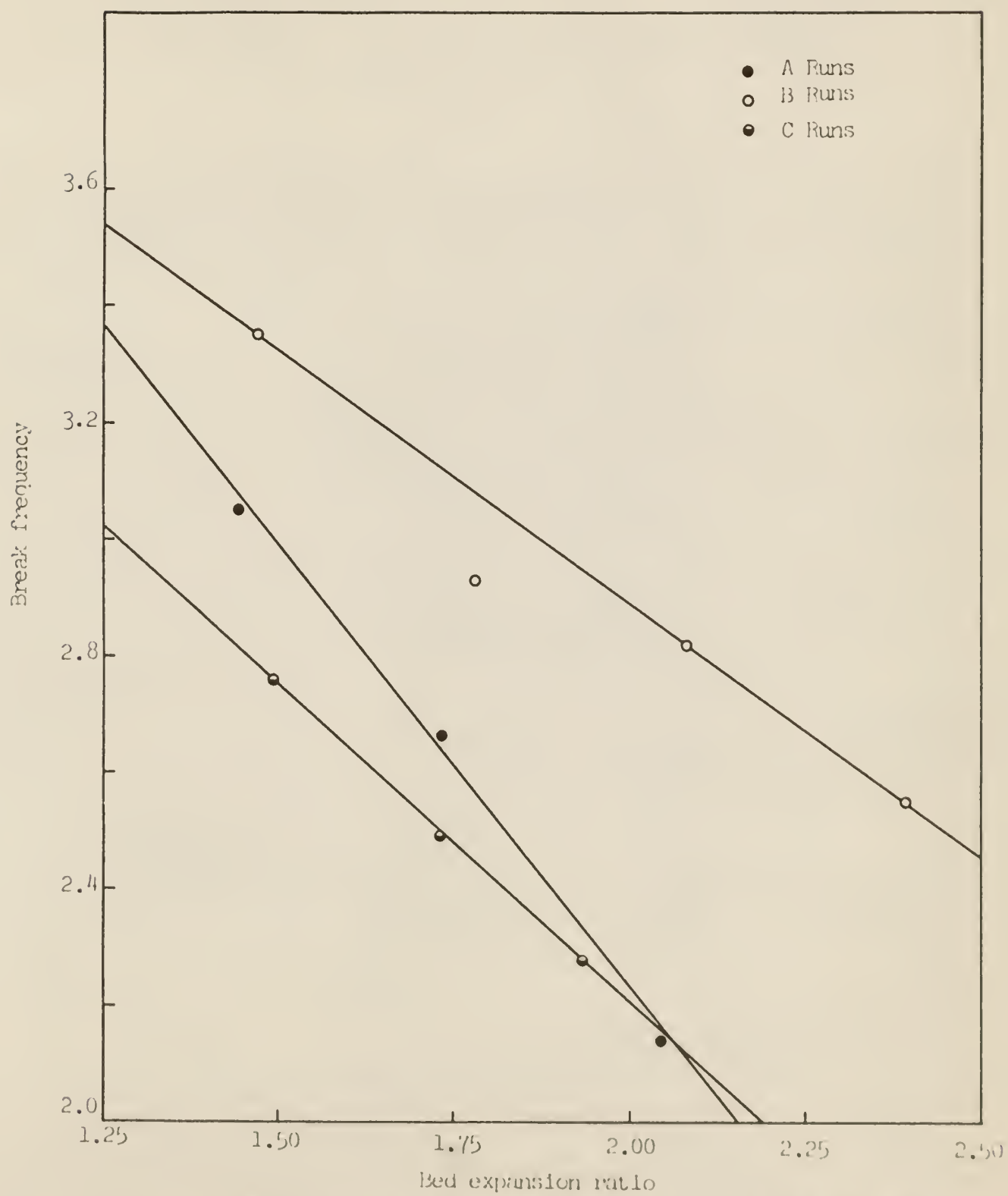


Figure 16. Break frequency as a function of bed expansion ratio

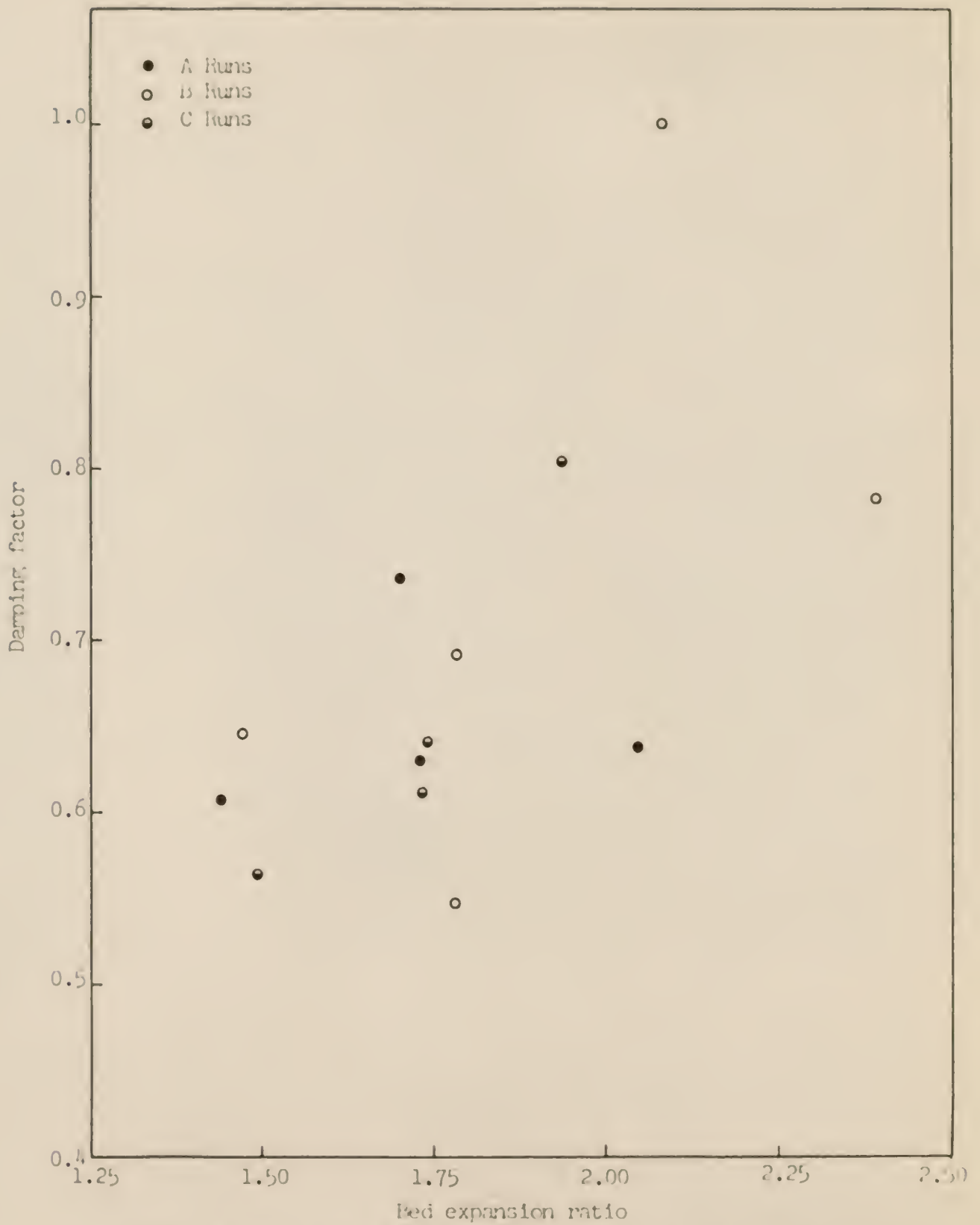


Figure 17. Damping factor as a function of bed expansion ratio

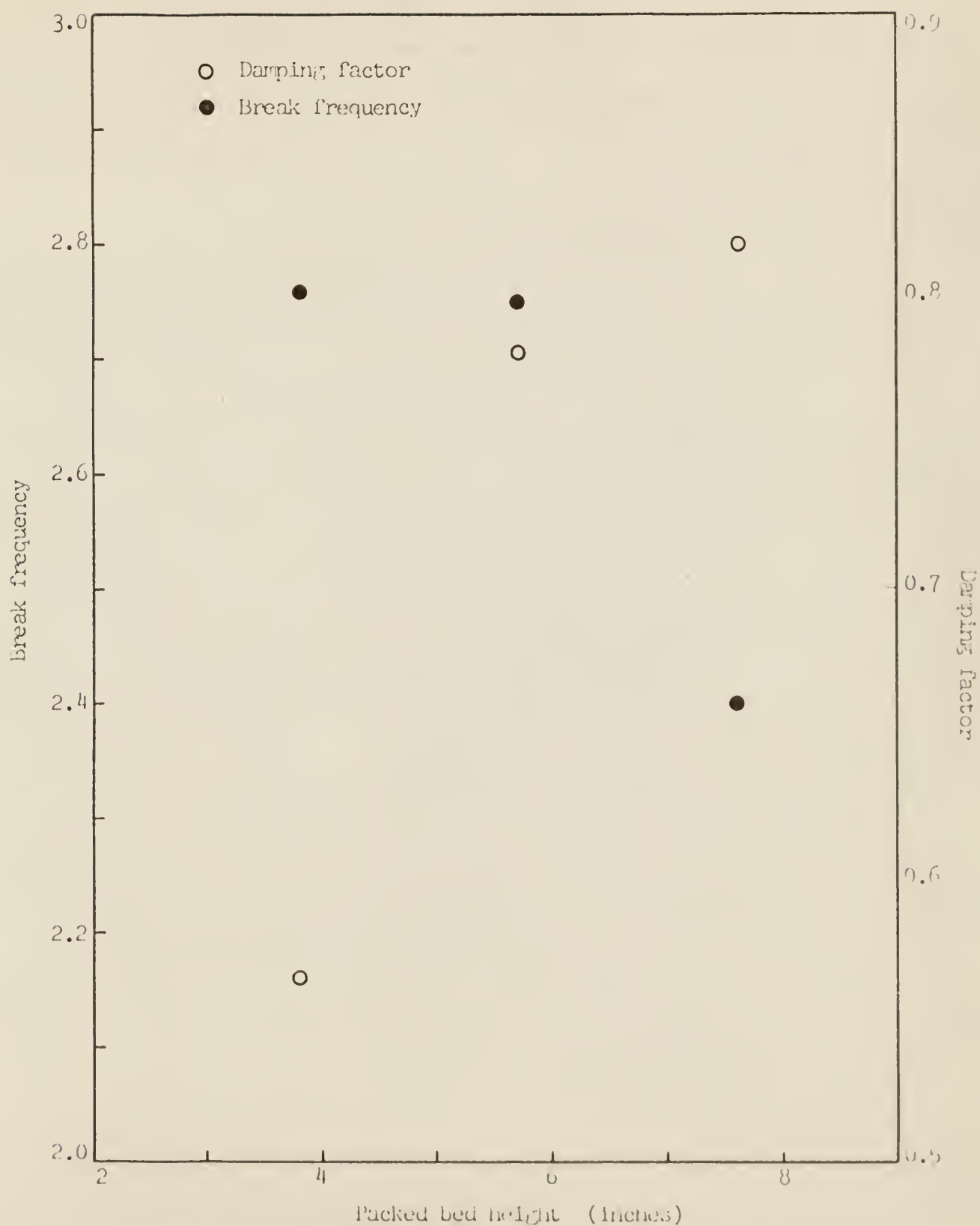


Figure 18. Break frequency and damping factor as a function of packed bed height

alone. The trend of these data show that the break frequency decreases with increasing packed bed height while the damping factor increases with increasing bed height.

The analysis of the steady state data indicated that the dynamic behavior of the fluidized bed could be described in terms of the second order transfer function, Eq. (44). In order to check these results, a series of step input responses were recorded and analyzed. Table VII lists the conditions of the step input response runs. One sequence of step response curves is shown in Figs. 19 through 24. The positive step responses began at conditions corresponding to steady state run B-1 while the negative step responses ended at the B-1 conditions. The curves included in the figures are the theoretical step responses calculated from the step size and from the least squares values of α and β for run B-1. Similar results were observed for other particle sizes and flow conditions.

The theoretical step input response for a second order system with a damping factor less than unity is given in reference (5) as

$$O(t) = 1 - \frac{e^{-\beta \alpha t}}{\sqrt{1 - \beta^2}} \cos(\alpha_r t - \theta) \quad (51)$$

where $\theta = \cos^{-1} \beta$

and $\alpha_r = \alpha \sin \theta$.

The relationship between the variables in Eq. (51) is readily seen in the Argand diagram, shown in Figure 24a. In this sketch α represents the magnitude of the break frequency and $\alpha\beta$ represents the real part of α . The real part of the break frequency determines the rise time of the response while the imagin-

Table VII. List of step input response runs

Run Number	Corresponding Steady State Run	$\Delta(h/h_o)$
S-2-ON	A-10	0.55
S-2-Off	A-10	0.54
S-3-On	A-10	0.34
S-5-On	B-1	0.38
S-5-Off	B-1	0.45
S-6-On	B-1	0.30
S-6-Off	B-1	0.30
S-7-On	B-1	0.15
S-7-Off	B-1	0.19
S-8-On	B-4	0.23
S-8-Off	B-4	0.18
S-9-On	B-1	0.25
S-9-Off	B-1	0.27
S-10-On	C-2	0.30
S-10-Off	C-2	0.21
S-11-On	C-2	0.10
S-11-Off	C-2	0.12
S-12-On	C-2	0.11
S-12-Off	C-2	0.08
S-13-On	C-2	0.24

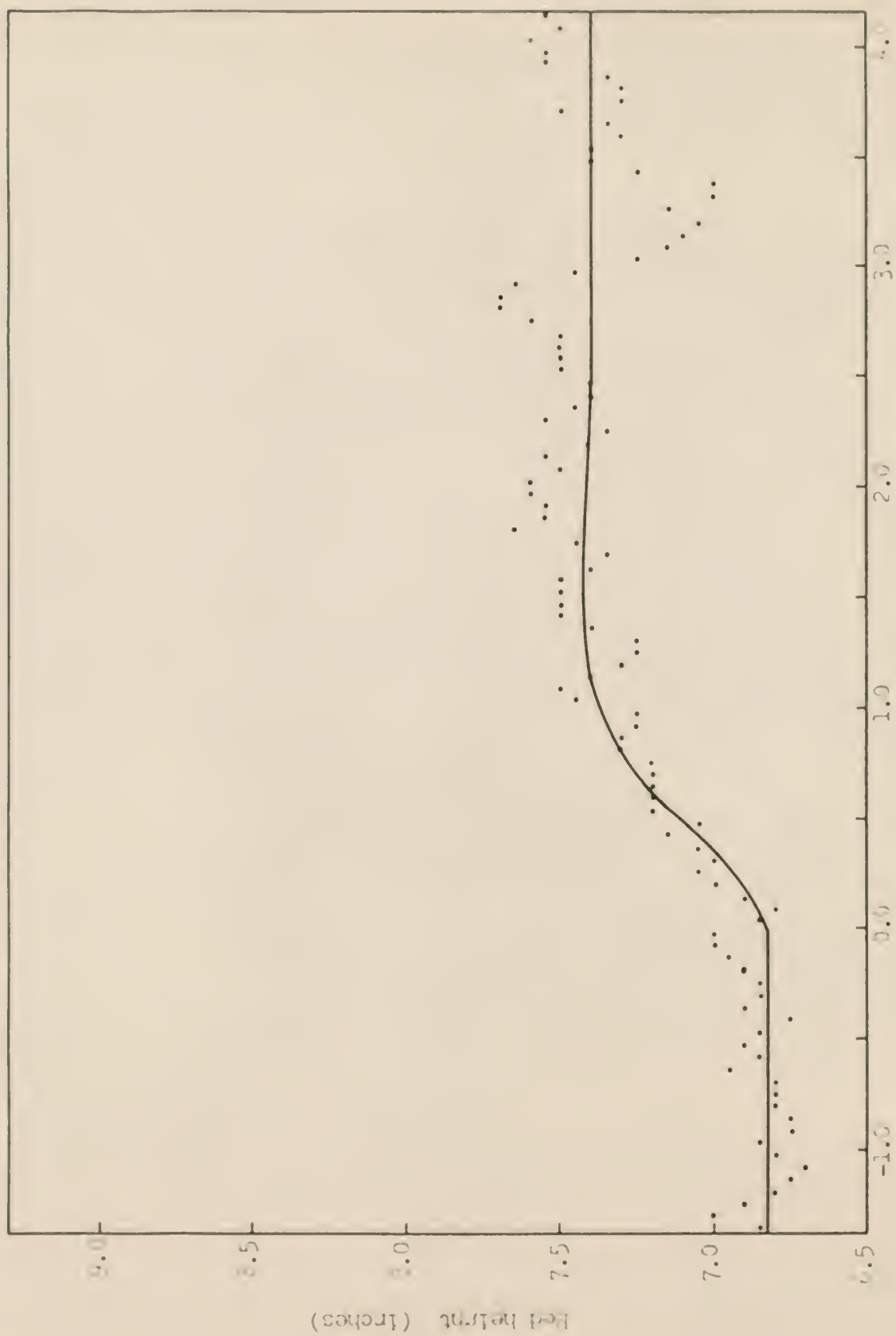


Figure 10. Step input response, Run 6-7-3n

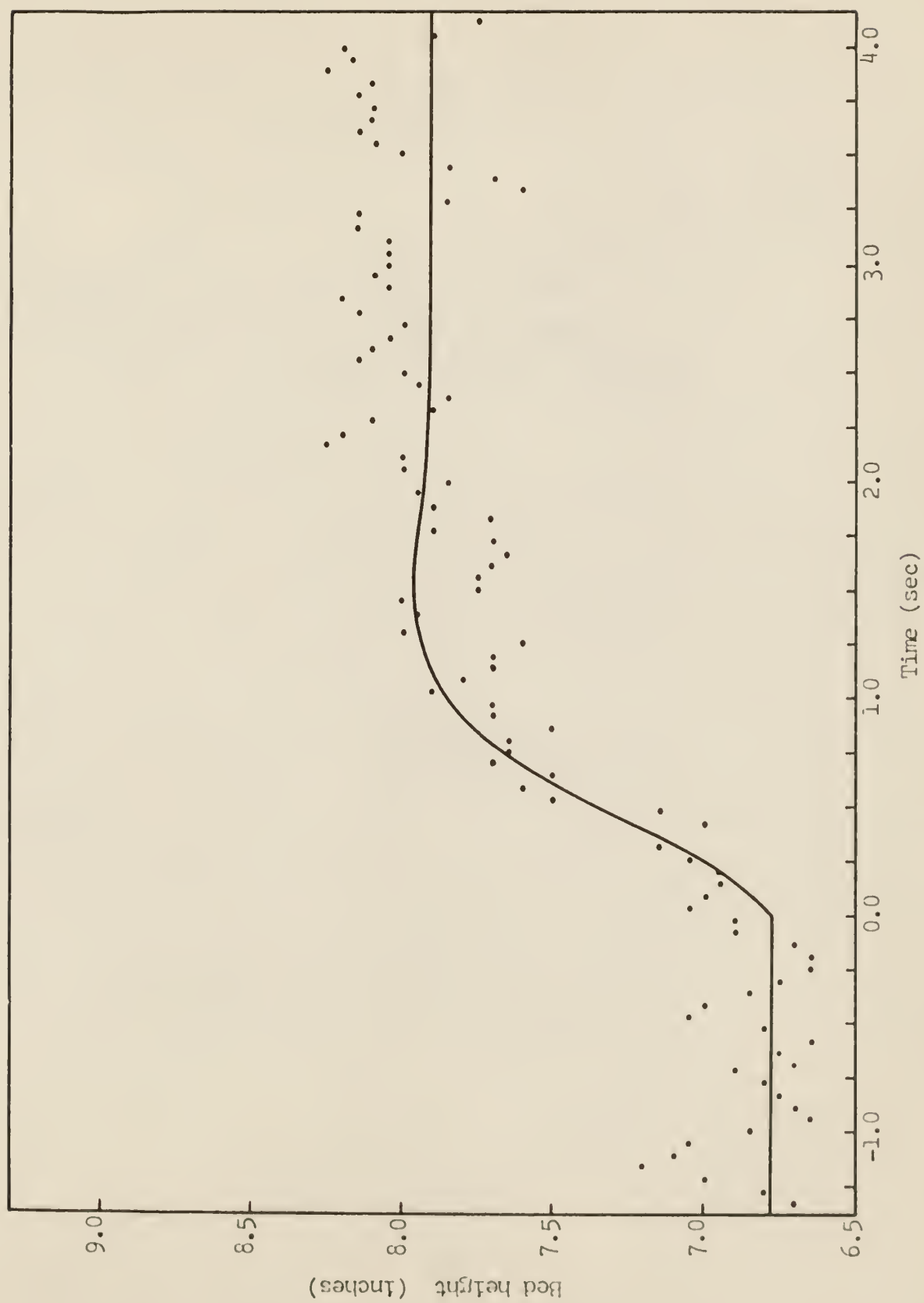


Figure 20. Step input response, Run S-6-On



Figure 21. Step input response, Run S-5-On



Figure 22. Step input response, Run S-7-Off



Figure 23. Step input response, Run 5-6-Off

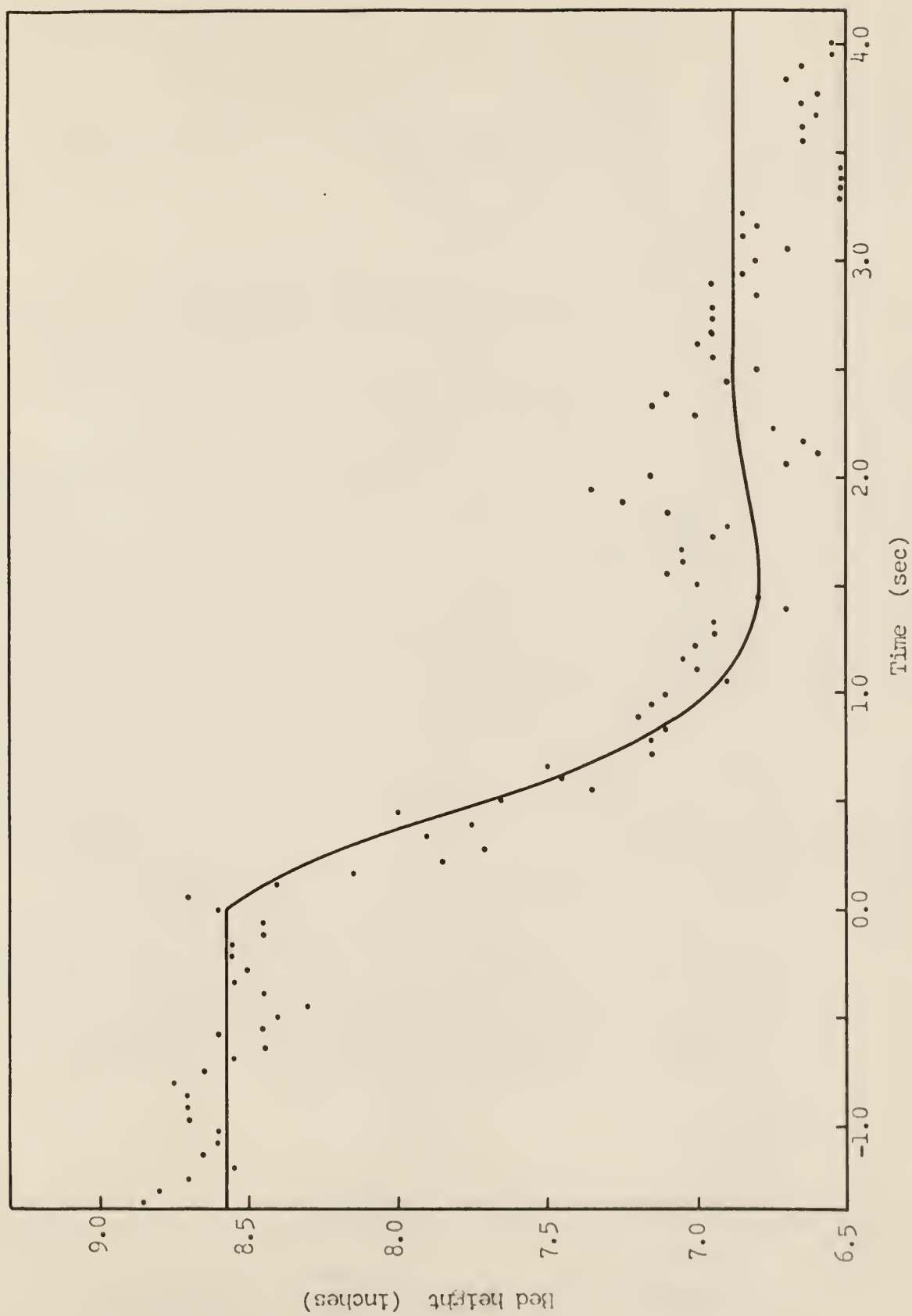


Figure 24. Step input response, Run S-5-Off

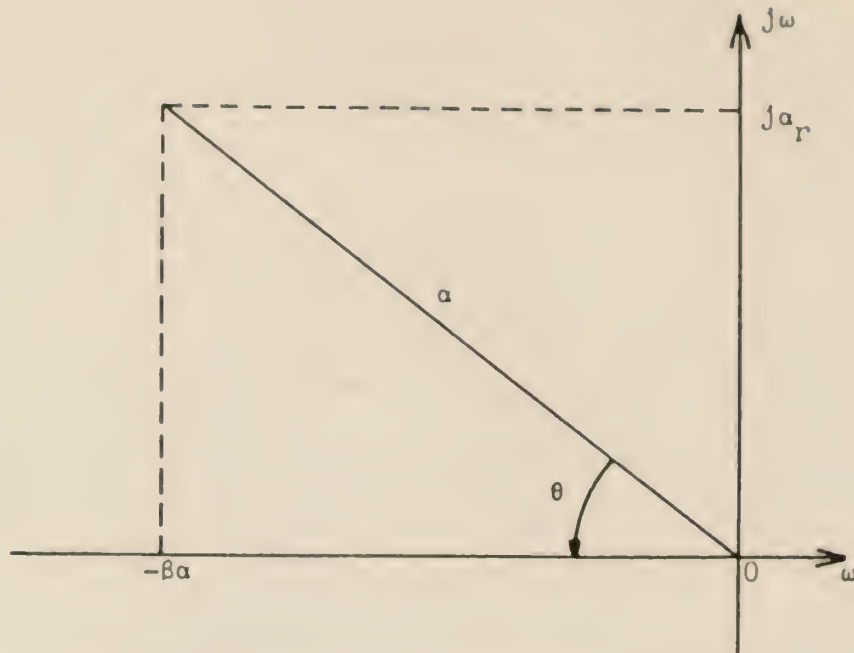


Figure 24a. Relationship of variables in Eq. (51)

ary part determines the overshoot. The value of $\beta = 1$ represents the critically damped condition.

The plots comparing the experimental and analytical step input responses show that the response can be predicted quite well for small step changes (for $\Delta(h/h_0)$ on the order of 0.15). As the step size increased, the average behavior of the bed interface deviated more and more from the predicted behavior. These results can be explained as being due to the change of the damping factor as a function of bed expansion ration. As bed expansion increases, the damping factor also increases, thus the overshoot of the step response decreases. Consequently, step responses calculated from the initial conditions of the bed as done here predict more overshoot than would be expected experimentally.

It was observed that the negative step responses agreed better, in general, with the analytical function than the positive step responses. These calculations were based on the final state of the bed, thus one would expect the agreement to be better, especially with regard to the amount of overshoot in the step response. Calculations based on α and β for an intermediate value of h/h_0 would probably give better results. Calculations of this type were not attempted since the data were too erratic to formulate an adequate correlation between α , β , and h/h_0 . The results of the step responses, however, were sufficiently close to indicate that the application of noise theory to the study of the dynamic behavior of fluidized beds is valid, at least for approximate results.

7.0 CONCLUSIONS

The results of these investigations have led to the conclusion that noise analysis is a valid method for determining the break frequency and damping factor of a copper-water fluidized bed system. This conclusion was based on the observations enumerated below.

1. The fluctuation of the upper fluid-bed interface had a Gaussian distribution about the mean, therefore it could be considered as a Gaussian random process to which noise theory is applicable.
2. Multivariate analysis of the variance indicated that the two experimental parameters were significant in their effect on the final results.
3. The copper-water fluidized bed system was described in terms of a second order transfer function with a break frequency and damping factor which varied as a function of bed expansion ratio.
4. The break frequencies and damping factors determined by least squares analysis of the power spectrum adequately described the step input response of the system.
5. The break frequency of the system decreased as a function of bed expansion ratio for constant particle size.
6. The damping factor of the system increased as a function of bed expansion ratio for constant particle size.
7. The break frequency decreased with packed bed height for constant particle size and constant bed expansion ratio.
8. The damping factor increased with packed bed height for constant particle size and constant bed expansion ratio.

8.0 SUGGESTIONS FOR FURTHER STUDY

This investigation was intended to establish the validity of the application of noise theory to fluidized beds. For this purpose only a few values of bed expansion were chosen for each particle size. An obvious extension of this study would be to include more particles sizes and more bed expansions ratios along with particles of different densities.

The results of this study tended to be erratic indicating that more data were needed to give more reliable results. The method of data acquisition was tedious since it depended upon visual reading of each data point. Development of a method to obtain the data either as an electrical signal or as a strip chart recording would greatly facilitate the analysis. The electrical signal would allow continuous analog computer analysis while the strip chart recording would allow more accurate reading of the digital data. Both methods have been applied to other systems with good results.

The transfer function of a system complete with phase information is available from cross-correlation analysis. This application necessitates a random input function whose time behavior is known so that the input power spectrum can be determined. An input of randomly spaced step inputs of random duration would appear to offer some promise. This type of input could be generated by using the output of a pulse radiation detector counting a radioactive source to trigger a solenoid system such as that used in this investigation.

9.0 ACKNOWLEDGMENT

This author wishes to express his gratitude to Dr. R. C. Baillie under whose direction this study was accomplished. Special thanks must also go to Dr. L. T. Fan whose original thinking prompted the study. Sincere appreciation is also extended to Dr. W. R. Kimel, Head of the Kansas State University Department of Nuclear Engineering, for his encouragement, and to the United States Atomic Energy Commission and the Kansas State University Experiment Station for their financial support.

10.0 LITERATURE CITED

1. Ackasu, A. Z.
Measurement of Noise Power Spectra by Fourier Analysis. J. Appl. Phys., 32, No. 4, pp. 565-8 (1961).
2. Anderson, T. W.
An Introduction to Multivariate Statistical Analysis. John Wiley and Sons, Inc., New York (1958).
3. Bendat, J. S.
Principles and Applications of Random Noise Theory. John Wiley and Sons, Inc., New York (1958).
4. Blackman, R. B. and Tukey, J. W.
The Measurement of Power Spectra. Dover Publications, Inc., New York (1958).
5. Brown, R. G. and Nilsson, J. W.
Introduction to Linear Systems Analysis. John Wiley and Sons, Inc., New York, (1962).
6. Conn, C. E.
Determination of Reactor Kinetic Parameters by Pile Noise Analysis. Nucl. Sci. Engg., 5, pp. 331-5 (1959).
7. Crandall, S. H. and Mark, W. D.
Random Vibrations in Mechanical Systems. Academic Press, New York (1963).
8. Davenport, J. B. and Root, W. R.
An Introduction to the Theory of Random Signals and Noise. McGraw-Hill Book Company, Inc., New York (1958).
9. Fan, L. T., Schmitz, J. A., and Miller, E. N.
Dynamics of Liquid-Solid Fluidized Bed Expansion. A paper presented at the 47th National Meeting of A. I. Ch. E. (1962).
10. Homan, C. J. and Tierney, J. W.
Determination of Dynamic Characteristics of Processes in the Presence of Random Disturbances. Chem. Engg. Sci., 12, pp. 154-65 (1960).
11. Krause, Gary F.
Personal Communication, Department of Statistics, Kansas State University, Manhattan, Kansas.
12. Lee, Y. W.
Statistical Theory of Communication. John Wiley and Sons. Inc., New York (1960).

13. Mingle, J. O.
Personal Communication. Department of Nuclear Engineering, Kansas State University, Manhattan, Kansas.
14. Morris, J. B., Nicholls, C. M., and Feninng, F. W.
The Application of Fluidization Techniques to Nuclear Reactors: A Preliminary Assessment. Trans. Inst. Chem. Engg., 34, No. 2, pp. 168-94 (1956).
15. Piersol, A. G.
The Measurement and Interpretation of Ordinary Power Spectra for Vibration Problems. NASA CR-90.
16. Press, H. and Houbolt, J. C.
Some Applications of Generalized Harmonic Analysis to Gust Loads on Airplanes, J. Aero. Naut. Sci., 22, No. 1, pp. 17-26 (1955).
17. Schere, M. R.
Fluidized Bed Reactor Study. MND-FBR-1696.
18. Snedecor, George W.
Statistical Methods. The Collegiate Press, Inc., Ames, Iowa (1946).
19. Thie, J. A.
Reactor Noise: Monograph Series on Nuclear Science and Technology. Rowman and Littlefield, Inc., New York (1963).
20. Wax, Nelson
Selected Papers on Noise and Stochastic Processes. Dover Publications, Inc., New York (1954).

11.0 APPENDICES

APPENDIX A

Statistical Analysis of Continuous Random Functions

A random function is one whose future is not subject to precise prediction. Instead of being deterministic, a random function can only be specified to the extent that its probability density function, $p(x,t)$, is known. The probability density function is defined as that function which, when integrated between two limits, yields the probability that the random function, $x(t)$, will be within those two limits. Normalization of $p(x,t)$ requires that

$$\int_{-\infty}^{\infty} p(x,t) dx = 1.$$

The statistical average of a random function, commonly denoted by \bar{x} , is the first moment of the probability density function.

$$E\{x(t)\} = \int_{-\infty}^{\infty} x_1(t) p(x,t) dx. \quad (A-1)$$

The average so designated is computed over an infinite ensemble of records, $x_1(t)$, each of finite length. This average is also known as the mean, the mathematical expectation, the stochastic average, and the ensemble average.

A stationary random function is a random function whose probability density function is time independent. The statistical average of a stationary random function is thus independent of the time at which the average is computed. Stated mathematically

$$E\{x(t + \tau)\} = \int_{-\infty}^{\infty} x_1(t + \tau) p(x) dx = E\{x(t)\}$$

where τ is an arbitrary time displacement variable and $p(x)$ is the time independent probability density function.

The dependence of one continuous stationary random function, $x(t)$, upon another, $y(t)$, is expressed in terms of a joint probability density function, $p(x,y)$. The degree of correlation between the two random functions is given by the correlation function defined as

$$E\{x(t) y(t)\} = \int_{-\infty}^{\infty} \int_{-\infty}^{\infty} x_1(t) y_1(t) p(x,y) dx dy. \quad (A-2)$$

The joint probability density function is generally normalized so as to make $E\{x(t) y(t)\}$ equal to unity for perfect correlation, zero for no correlation, and minus one for anti-correlation.

The autocorrelation function of a stationary random function is a special case of Eq. (A-2). This function describes the statistical correlation between two values of the same random function displaced by an amount of time τ . Replacing $y_1(t)$ by $x_1(t + \tau)$ gives

$$E\{x(t) x(t + \tau)\} = \int_{-\infty}^{\infty} x_1(t) x_1(t + \tau) p(x) dx = R(\tau). \quad (A-3)$$

Equation (A-3) is the defining expression for the ensemble autocorrelation function, $R(\tau)$.

If the probability density function is unknown, it becomes more convenient to express the statistical behavior of a continuous stationary random function in terms of its time properties. The time average of the function $x(t)$ is defined as

$$\overline{x(t)} = \lim_{T \rightarrow \infty} \frac{1}{T} \int_{-\frac{T}{2}}^{\frac{T}{2}} x(t) dt$$

where T is the duration of the sample. This limit may or may not exist depending upon the behavior of $x(t)$. Also, the existence of $\overline{x(t)}$ does not guarantee that it will be equal to $E\{x(t)\}$. The equality of time and ensemble average holds only for ergodic random processes.

An ergodic random process is defined as one for which timewise sampling leads to the same statistical result as ensemble sampling. The ergodic hypothesis can seldom, if ever, be justified formally (5), however, in most physical problems a random function may be regarded as ergodic if it is time stationary. An important consequence of the ergodic hypothesis is that any function of an ergodic random function is itself ergodic. In particular, if the random process with sample function $x(t)$ is ergodic, then

$$\overline{x^n(t)} = E\{x^n(t)\}$$

i.e., the moments of the probability density function can be determined from timewise sampling of the random function.

The autocorrelation function stated as a time average is

$$\phi(\tau) = \lim_{T \rightarrow \infty} \frac{1}{T} \int_{-\frac{T}{2}}^{\frac{T}{2}} x(t) x(t + \tau) dt.$$

If $x(t)$ is the sample function of an ergodic random process, then

$$\phi(\tau) = R(\tau).$$

Thus, for an ergodic stationary random process, one can determine the auto-

correlation function without knowing the probability density function of the random function being correlated.

APPENDIX B

Input-Output Relationship of the Power Spectrum

The response, $y(t)$, of a linear, constant parameter system to general types on inputs, $x(t)$, may be described by its impulse response, $h(t)$, and the convolution integral (12).

$$y(t) = \int_{-\infty}^{\infty} h(\tau) x(t - \tau) d\tau \quad (B-1)$$

The function $h(t)$ is related to the system transfer function by the Fourier transform. To exhibit this relationship consider the transfer function, $Z(f)$, defined as

$$Z(f) = \frac{Y(f)}{X(f)} \quad (B-2)$$

where

$$Y(f) = \int_{-\infty}^{\infty} y(t) e^{-i\omega t} dt$$

and

$$X(f) = \int_{-\infty}^{\infty} x(t) e^{-i\omega t} dt.$$

Solving for $Y(f)$ in Eq. (B-2) and Fourier transforming to obtain $y(t)$ gives

$$y(t) = \int_{-\infty}^{\infty} \int_{-\infty}^{\infty} x(t') e^{-i\omega' t'} dt' Z(f) e^{i\omega t} df. \quad (B-3)$$

The impulse response, $h(t)$, is obtained by letting the input, $x(t')$, in Eq. (B-3) be the Dirac delta function $\delta(t')$. Making these substitutions gives

$$h(t) = \int_{-\infty}^{\infty} \int_{-\infty}^{\infty} \delta(t') e^{-i\omega' t'} dt' Z(f) e^{i\omega t} df. \quad (B-4)$$

By the properties of the delta function, the integral over t is unity, thus Eq. (B-4) reduces to

$$h(t) = \int_{-\infty}^{\infty} Z(f) e^{i\omega t} df \quad (B-5)$$

which is recognized as the Fourier transform of $Z(f)$. The inverse to Eq. (B-5) is given by

$$Z(f) = \int_{-\infty}^{\infty} h(t) e^{-i\omega t} dt. \quad (B-6)$$

According to Eq. (16) the power spectrum of the output of a linear system, $y(t)$, may be represented by

$$\phi_O(f) = \int_{-\infty}^{\infty} \phi_O(\tau) e^{-i\omega \tau} d\tau \quad (B-7)$$

where

$$\phi_O(\tau) = \lim_{T \rightarrow \infty} \frac{1}{T} \int_{-\frac{T}{2}}^{\frac{T}{2}} y(t) y(t + \tau) dt.$$

Substituting Eq. (B-1) for $y(t)$ and $y(t + \tau)$ in Eq. (B-7) yields

$$\begin{aligned} \phi_O(f) = \int_{-\infty}^{\infty} e^{-i\omega \tau} \lim_{T \rightarrow \infty} \frac{1}{T} \int_{-\frac{T}{2}}^{\frac{T}{2}} \int_{-\infty}^{\infty} h(z) x(t - z) dz \\ \int_{-\infty}^{\infty} h(\eta) x(t + \tau - \eta) d\eta dt d\tau. \end{aligned} \quad (B-8)$$

Rearranging the order of integration in (B-8) gives

$$\phi_0(f) = \int_{-\infty}^{\infty} e^{-1\omega\tau} \int_{-\infty}^{\infty} h(z) \int_{-\infty}^{\infty} h(\eta) \lim_{T \rightarrow \infty} \frac{1}{T} \int_{-\frac{T}{2}}^{\frac{T}{2}} x(t-z) \cdot x(t+\tau-\eta) dt d\eta dz d\tau. \quad (B-9)$$

Considering only the integration with respect to t , let $\sigma = t - z$ so that

$$\begin{aligned} \lim_{T \rightarrow \infty} \frac{1}{T} \int_{-\frac{T}{2}}^{\frac{T}{2}} x(t-z) x(t+\tau-\eta) dt \\ = \lim_{T \rightarrow \infty} \frac{1}{T} \int_{-\frac{T}{2}}^{\frac{T}{2}} x(\sigma) x(\sigma+z+\tau-\eta) d\sigma \\ = \phi_1(z+\tau-\eta). \end{aligned} \quad (B-10)$$

Substitution of Eq. (B-10) into Eq. (B-9) yields

$$\phi_0(f) = \int_{-\infty}^{\infty} e^{-1\omega\tau} \int_{-\infty}^{\infty} h(z) \int_{-\infty}^{\infty} h(\eta) \phi_1(z+\tau-\eta) d\eta dz d\tau. \quad (B-11)$$

Consider the integration with respect to τ in (B-11) and let $\xi = z + \tau - \eta$.

$$\phi_0(f) = \int_{-\infty}^{\infty} h(z) \int_{-\infty}^{\infty} h(\eta) \int_{-\infty}^{\infty} \phi_1(\xi) e^{-1\omega(\xi+\eta-z)} d\xi d\eta dz. \quad (B-12)$$

Rearranging terms of Eq. (B-12) gives

$$\phi_0(f) = \int_{-\infty}^{\infty} h(z) e^{1\omega z} dz \int_{-\infty}^{\infty} h(\eta) e^{-1\omega\eta} d\eta \int_{-\infty}^{\infty} \phi_1(\xi) e^{-1\omega\xi} d\xi. \quad (B-13)$$

By comparison with Eq. (B-6), the integrals with respect to z and ξ in Eq. (B-13) are recognized as $Z^*(f)$ and $Z(f)$ respectively, where the asterisk denotes complex conjugation. The integral with respect to ξ is $\phi_1(f)$. Making these substitutions yields

$$\phi_o(f) = Z^*(f) Z(f) \phi_1(f)$$

$$= |Z(f)|^2 \phi_1(f).$$

Thus it is noted that the power spectrum of the output is related to the power spectrum of the input by the square of the magnitude of the transfer function.

APPENDIX C

Description and Explanation of the IEM-1410
Computer Program Used for Calculation of the
Autocorrelation Function and Power Spectrum

This computer code was written to calculate the autocorrelation function and the power spectrum from the experimental data. The expressions employed in the program were discussed in the body of this thesis and are restated here for convenience. They are:

a) the autocorrelation function

$$\phi(\tau_n) = \frac{\frac{1}{N-n} \sum_{i=1}^{N-n} x_i x_{i+n}}{\frac{1}{N} \sum_{i=1}^n x_i^2}, \quad (40)$$

b) the power spectrum

$$\phi(\omega_n) = \Delta\tau \left\{ \phi(0) + 2 \sum_{i=1}^{M-1} \phi(\tau_i) \cos \omega_n \tau_i + \phi(\tau_M) \cos \omega_n \tau_M \right\}, \quad (42)$$

c) the prewhitening filter

$$x_i = x_{i+1} - \gamma x_i, \quad (35)$$

d) the transfer function of the prewhitening filter

$$\Gamma(\omega_n) = 1 + \gamma^2 - 2\gamma \cos \omega_n \Delta\tau. \quad (38)$$

These equations were programmed in FORTRAN IV language. The source program is listed and the logic diagram is shown in this Appendix. Table C-1 defines the various symbols used in the program.

Table C-1: Input data and variables required for the
IBM-1410 autocorrelation function and
power spectrum computer program

Symbol	Explanation
A	Raw spectral estimates
AVE	Average of input data
AZRO	Raw spectral estimate at zero frequency
COR	Correction factor for prewhitening
DELT	Time increment for input data
FREQ	Frequency at which power spectrum is evaluated
GAMMA	Prewhitening coefficient
KLAG	Maximum number of time lags to be employed
NPTS	Number of data points per sub-run
NPTST	Total number of data points per run
NRUN	Number of sub-runs per run
NUM	Run number
P	Power spectral estimates
PHI	Autocorrelation coefficients
PZRO	Power spectral estimate at zero frequency
RDT	Reciprocal time increment (film speed in frames per second)
SIGSQ	Variance for the entire run
VAR	Variance for each sub-run
X	Input data to be correlated

The input to the program was arranged as follows:

FIRST CARD: `FORMAT(2I5,2F10.4,I5)`

- 1) NUM: Run number, 2) KLAG: Number of power spectral estimates desired, 3) RDT: Film speed, 4) GAMMA: Prewhitening coefficient, and 5) NRUN: Number of sub-runs per run.

SECOND CARD: `FORMAT(I5)`

NPTS: Number of data points per sub-run

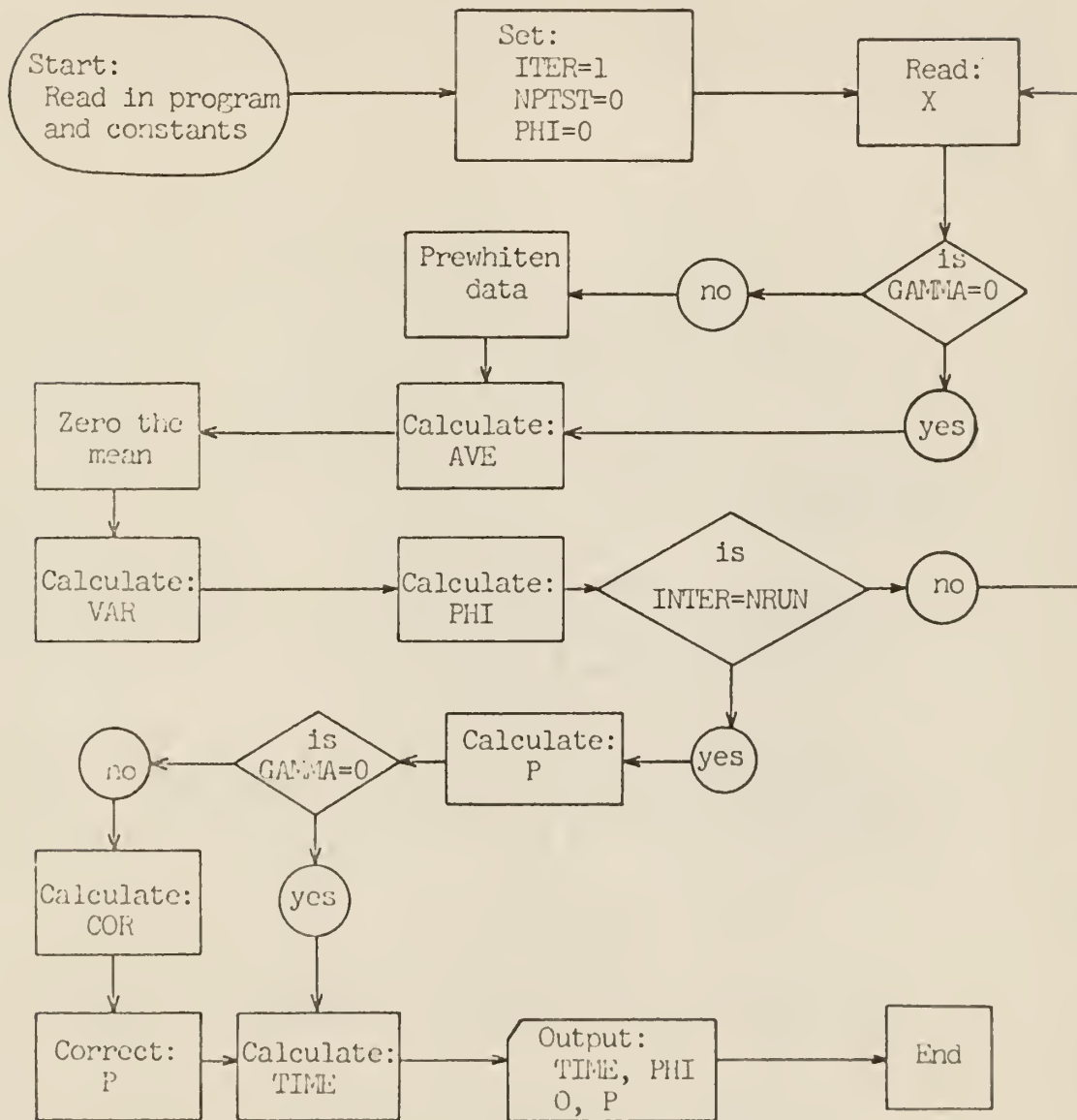
REMAINING CARDS: `FORMAT(7F10.4)`

X: Experimental data for a sub-run punched consecutively, seven to a card. (Multiple sub-runs were fed in order, each sub-run preceded by the appropriate second card described above.)

The output of the program is set up for both card and print-out form. The card output is to be used in the least squares analysis program in the same order as it comes from this program. The first card of the output contains NUM, NPTST, RDT, GAMMA, SIGSQ, and AVE, respectively. The following cards (KLAG of them) list TIME LAG, AUTO FXN, FREQ, and SPECTRUM, in that order, punched one set to a card. The on-line printer output is similar to the card output with the exception that the columns of output have headings telling what they are.

Prewhitening of the data was accomplished by entering a value of GAMMA different from zero in the initial parameter card. The program automatically computes the power spectrum of the prewhitening filter and corrects the experimental power spectrum. The program is written as a one pass code and accepts only one set of data at a time. The one run, however, may contain as many sub-runs as desired.

Fig. 25: Logic diagram for autocorrelation function and power spectrum computer program.



```

C      THIS PROGRAM COMPUTES THE AUTOCORRELATION FUNCTION AND POWER
C      SPECTRUM OF THE RAW DATA WITH OR WITHOUT PREWHITENING
      DIMENSION X(600),PHI(50),A(50),P(50),VAR(10)
101  FORMAT(2I5,2F10.4,I5)
102  FORMAT(I5)
103  FORMAT(7F10.4)
201  FORMAT(42H1RUN NUMBER   NO DATA PTS FILM SPEED   GAMMA,5X,8HVARIANCE
      1,7X,4HMEAN)
202  FORMAT(5X,12,9X,14,8X,F4.0,5X,F4.2,5X,E10.4,5X,F10.7)
203  FORMAT(/10X,8HTIME LAG,7X,8HAUTO FXN,10X,9HFREQUENCY,7X,8HSPECTRU
      1M)
204  FORMAT(10X,F8.5,5X,F11.8,10X,F8.4,5X,F11.9)
      ITER=1
      NPTST=0
      READ(1,101)NUM,KLAG,RDT,GAMMA,NRUN
      DO 1 I=1,50
1    PHI(I)=0.0
2    READ(1,102)NPTS
      READ(1,103)(X(I),I=1,NPTS)
      IF(GAMMA.EQ.0.0)GO TO 4
      DO 3 I=2,NPTS
        J=I-1
3      X(J)=X(I)-GAMMA*X(J)
        NPTS=NPTS-1
4      SUM=0.0
      DO 5 I=1,NPTS
5      SUM=SUM+X(I)
        AVE=SUM/FLCAT(NPTS)
      DO 6 I=1,NPTS
6      X(I)=X(I)-AVE
        SUM=0.0
      DO 7 I=1,NPTS
7      SUM=SUM+X(I)*X(I)
        VAR(ITER)=SUM/FLCAT(NPTS)
      DO 9 I=1,KLAG
        K=NPTS-I
        SUM=0.0
      DO 8 J=1,K
        L=I+J
8      SUM=SUM+X(J)*X(L)
9      PHI(I)=PHI(I)+SUM/(VAR(ITER)*FLCAT(NRUN*K))
        NPTST=NPTST+NPTS
        IF(NRUN.EQ.ITER)GO TO 10
        ITER=ITER+1
      GO TO 2
10  SIGSQ=0.0
      DO 20 I=1,NRUN
20  SIGSQ=SIGSQ+VAR(I)/FLCAT(NRUN)
      PI=3.14159265
21  ISUM=KLAG-1
      DELT=1./RDT
      SUM=0.0

```

```

      DO 11 I=1,ISUM
11  SUM=SUM+2.*PHI(I)
      AZRC=DELT*(1.+SUM+PHI(KLAG))
      DO 13 I=1,KLAG
      SUM=0.0
      DO 12 J=1,ISUM
      ARG=FLOAT(I*J)/FLOAT(KLAG)
12  SUM=SUM+COS(ARG*PI)*PHI(J)*2.
13  A(I)=DELT*(1.+SUM+COS(FLOAT(I)*PI)*PHI(KLAG))
      PZRC=0.5*AZRC+0.5*A(1)
      P(1)=0.25*AZRC+0.5*A(1)+0.25*A(2)
      L=KLAG-1
      P(KLAG)=0.5*A(L)+0.5*A(KLAG)
      DO 14 I=2,L
14  P(I)=0.25*A(I-1)+0.5*A(I)+0.25*A(I+1)
      IF(GAMMA.EQ.0.0)GO TO 16
      TERM=1.+GAMMA*GAMMA
      PZRC=PZRC/(TERM-2.*GAMMA)
      P(KLAG)=P(KLAG)/(TERM+2.*GAMMA)
      DO 15 I=1,ISUM
      COR=TERM-2.*GAMMA*COS(FLOAT(I)*PI/FLOAT(KLAG))
15  P(I)=P(I)/COR
16  WRITE(3,201)
      WRITE(2,202)NUM,NPTST,RDT,GAMMA,SIGSQ,AVE
      WRITE(3,202)NUM,NPTST,RDT,GAMMA,SIGSQ,AVE
      WRITE(3,203)
      DUM=0.0
      DUMM=1.0
      WRITE(3,204)DUM,DUMM,DUM,PZRC
      WRITE(2,204)DUM,DUMM,DUM,PZRC
      DO 17 I=1,KLAG
      TIME=FLOAT(I)/RDT
      FREQ=FLOAT(I)*RDT/FLOAT(2*KLAG)
      WRITE(3,204)TIME,PHI(I),FREQ,P(I)
17  WRITE(2,204)TIME,PHI(I),FREQ,P(I)
      STOP
      END

```

APPENDIX D

Description and Explanation of the IBM-1410
Computer Program Used for Calculation of the
Break Frequency and Damping Factor

This computer code was written to calculate the break frequency and damping factor by simultaneous solution of Eqs. (47) through (50). Equations (47) and (48) were solved for A and B in terms of α and β . Equations (49) and (50) were then solved for α and β by the Newton-Raphson iteration method. This code was written to accept the output of the program described in Appendix C directly.

Equations (49) and (50) were denoted by

$$\frac{\partial S}{\partial \alpha} = R_1(\alpha, \beta) = 0 \quad (D-1)$$

$$\frac{\partial S}{\partial \beta} = R_2(\alpha, \beta) = 0. \quad (D-2)$$

Although A and B were unknown quantities, they were considered as known values in the solution of Eqs. (D-1) and (D-2). Their values were calculated from the current values of α and β using Eqs. (47) and (48).

Expanding R_1 and R_2 in a Taylor series expansion about the initial guess (α_0, β_0) gives

$$R_1(\alpha, \beta) = 0 \pm R_1(\alpha_0, \beta_0) + \frac{\partial R_1}{\partial \alpha}(\alpha_0, \beta_0) \Delta \alpha + \frac{\partial R_1}{\partial \beta}(\alpha_0, \beta_0) \Delta \beta \quad (D-3)$$

$$R_2(\alpha, \beta) = 0 \pm R_2(\alpha_0, \beta_0) + \frac{\partial R_2}{\partial \alpha}(\alpha_0, \beta_0) \Delta \alpha + \frac{\partial R_2}{\partial \beta}(\alpha_0, \beta_0) \Delta \beta \quad (D-4)$$

Solving Eqs. (D-3) and (D-4) for $\Delta \alpha$ and $\Delta \beta$ yields

$$\Delta\alpha = \frac{1}{D} \begin{vmatrix} -R_1 & \frac{R_1}{\partial\beta} \\ -R_2 & \frac{\partial R_2}{\partial\beta} \end{vmatrix}, \quad \Delta\beta = \frac{1}{D} \begin{vmatrix} \frac{\partial R_1}{\partial\alpha} & -R_1 \\ \frac{\partial R_2}{\partial\alpha} & -R_2 \end{vmatrix}$$

where

$$D = \begin{vmatrix} \frac{\partial R_1}{\partial\alpha} & \frac{\partial R_1}{\partial\beta} \\ \frac{\partial R_2}{\partial\alpha} & \frac{\partial R_2}{\partial\beta} \end{vmatrix}$$

it being understood that the elements of the determinants are to be evaluated at (α_o, β_o) .

The derivatives, $\frac{\partial R_1}{\partial\alpha}$ and $\frac{\partial R_1}{\partial\beta}$, were determined using the following numerical approximations:

$$\frac{\partial R_1}{\partial\alpha} \doteq \frac{R_1(1.05\alpha_o, \beta_o) - R_1(\alpha_o, \beta_o)}{.05\alpha_o} \quad (D-6)$$

$$\frac{\partial R_1}{\partial\beta} \doteq \frac{R_1(\alpha_o, 1.05\beta_o) - R_1(\alpha_o, \beta_o)}{.05\beta_o} \quad (D-7)$$

The terms of the approximate derivatives were denoted by the matrix elements

$$G_{11} = R_1(\alpha_o, \beta_o) \quad G_{12} = R_2(\alpha_o, \beta_o)$$

$$G_{21} = R_1(\alpha_o, 1.05\beta_o) \quad G_{22} = R_2(\alpha_o, 1.05\beta_o)$$

$$G_{31} = R_1(1.05\alpha_o, \beta_o) \quad G_{32} = R_2(1.05\alpha_o, \beta_o).$$

Making these substitutions, Eqs. (D-6) and (D-7) become

$$\begin{aligned} G_{21}^* &= \frac{\partial R_2}{\partial\alpha} \doteq \frac{G_{21} - G_{11}}{.05\alpha_o} & G_{31}^* &= \frac{\partial R_1}{\partial\alpha} \doteq \frac{G_{31} - G_{11}}{.05\alpha_o} \\ G_{22}^* &= \frac{\partial R_2}{\partial\beta} \doteq \frac{G_{22} - G_{12}}{.05\beta_o} & G_{32}^* &= \frac{\partial R_1}{\partial\beta} \doteq \frac{G_{32} - G_{12}}{.05\beta_o} \end{aligned} \quad (D-8)$$

where the asterisk is used to denote the redefinition of the G_{1j} . The same symbol was used for G_{1j} and G_{1j}^* in the computer program.

Substitution of Eq. (D-8) into (D-5) yields

$$\Delta\alpha = \frac{1}{D} \begin{vmatrix} -G_{11} & G_{21}^* \\ -G_{12} & G_{22}^* \end{vmatrix}, \quad \Delta\beta = \frac{1}{D} \begin{vmatrix} G_{31}^* & -G_{11} \\ G_{32}^* & -G_{12} \end{vmatrix}$$

where

$$D = \begin{vmatrix} G_{31}^* & G_{21}^* \\ G_{32}^* & G_{22}^* \end{vmatrix}$$

The break frequency and damping factor were corrected by adding one half of the calculated correction factors. These values of α and β were then used to calculate new values of A and B. The process was continued until the iteration criterion was satisfied.

These equations were programmed in FORTRAN IV language. The sub-programs which perform the Newton-Raphson iteration were originally written by Mingle (13). Minor modifications were made by this author in order to apply the sub-programs to this particular problem. The source program is listed and the logic diagram is shown in this appendix. Table D-1 defines the symbols used in the program.

The input to this program consisted of the output of the program described in Appendix C. One additional card, the initial guesses for α and β , was read in as the last card in the FORMAT (2F10.4). The iteration accuracy criterion was included in the program itself and was not entered as a data parameter. The output of the program lists the iteration results through the on-

line printer. The first line of output lists NUM, NPTST, RDT, GAMMA, VAR, and AVE which identify the output with the experimental data. The second line of output gives the first estimates of the parameters A and B, followed by the first estimates of α and β in the third line. The estimates of the parameters are printed out after each iteration until the iteration criterion has been satisfied. The last few lines are the frequencies, the experimental power spectrum, and the corresponding calculated power spectrum in tabular form. The final line states the squared error associated with the least squares calculation.

The program took approximately forty seconds per iteration for a set of sixteen data points. The number of iterations depended upon the accuracy of the initial guess. In general it took on the order of forty iterations to converge. The slow convergence was due to the changes made in A and B during each iteration. The program tended to diverge if the initial guess was too far from the correct value. Appropriate upper and lower limits were chosen for α and β and the program was automatically terminated if these values were exceeded.

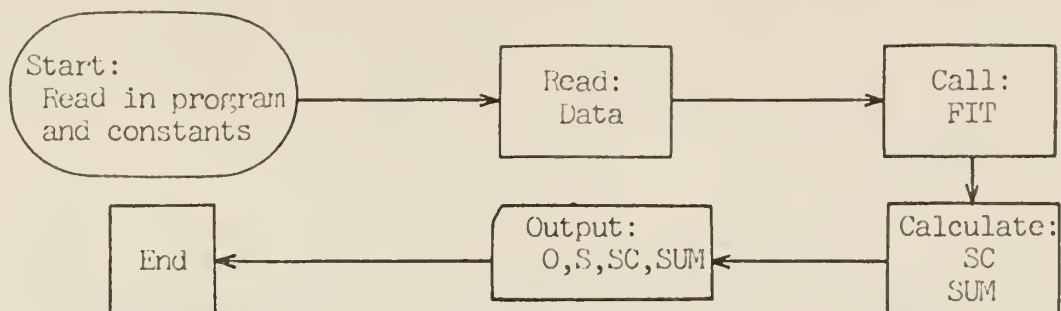
Table D-I: Input data and variables required for
the IBM-1410 break frequency and
damping factor computer program

Symbol	Explanation
A	Correlated noise constant of the power spectrum
AL	First guess of the break frequency
B	White noise constant of the power spectrum

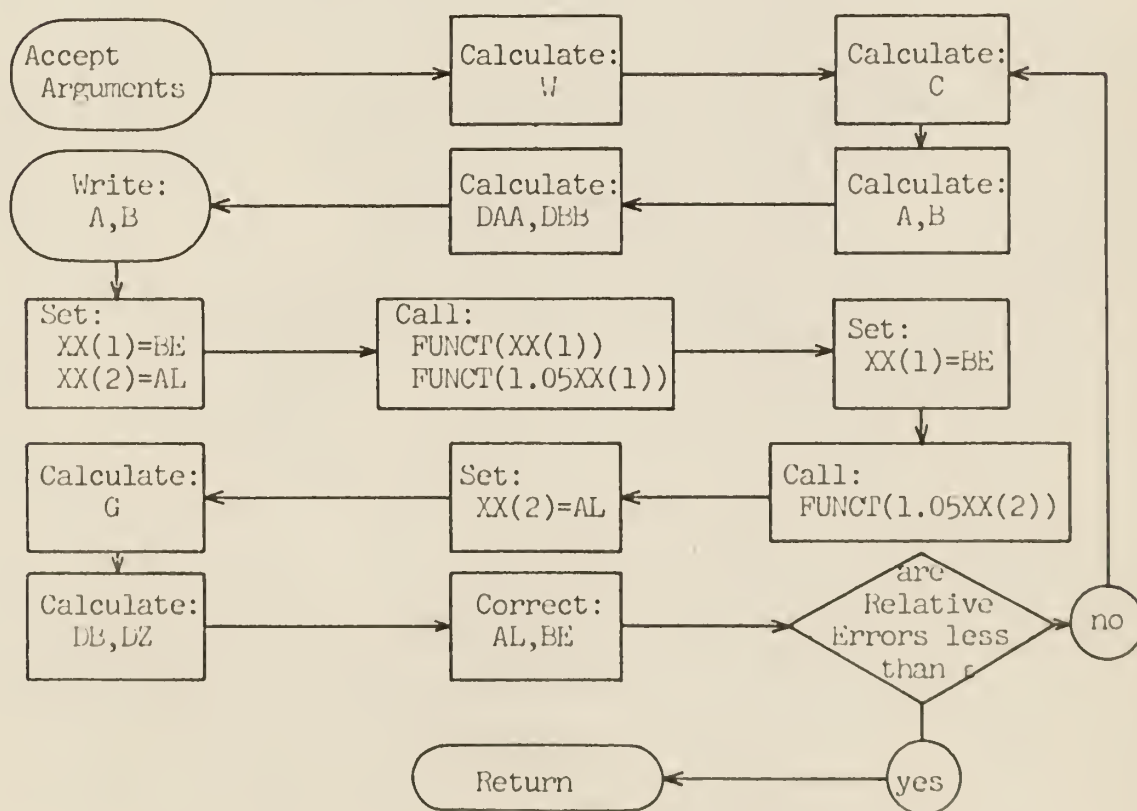
Table D-I (continued)

Symbol	Explanation
BE	First guess of the damping factor
NCDS	Number of data cards to be read
O	Frequencies at which the power spectrum has been computed
S	Input values of the power spectrum
SC	Calculated power spectrum using least squares value of A, B, α , and β
T	Statement function
XAL	Least squares value of the break frequency
XBE	Least squares value of the damping factor
<p>NUM, NPTS, RDT, GAMMA, VAR, AVE (These variables are not used directly in this program. They are computed in the power spectrum program and are used here as run indices only.)</p>	
SUBROUTINE FIT	
C	Matrix elements used in calculation of A and B
DAA	Iteration correction factor for A
DBB	Iteration correction factor for B
DB	Iteration correction factor for AL
DZ	Iteration correction factor for BE
G	Matrix elements used in calculating DB and DZ
W	Weighting factors used in the calculation of A and B

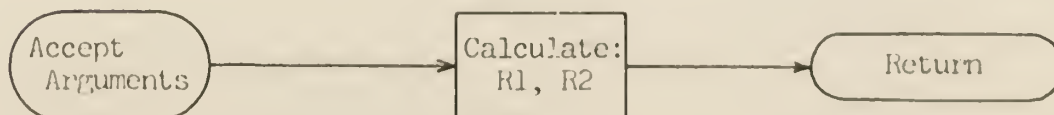
Fig. 26: Logic diagram for break frequency and damping factor computer program.



Logic diagram of subroutine FIT



Logic diagram for SUBROUTINE FUNCT



```

C      THIS PROGRAM SETS UP THE PROBLEM AND CALLS THE FIT SUBROUTINE
      DIMENSION S(25),C(25),SC(25)
      COMMON S,C,A,B,AL,BE,NCDS
101  FORMAT(44X,F8.4,5X,F11.9)
102  FORMAT(10X,2F10.4)
202  FORMAT(5X,12,9X,14,8X,F4.0,5X,F4.2,5X,F10.4,5X,F10.7)
203  FORMAT(11H1,5X,12,9X,14,8X,F4.0,5X,F4.2,5X,F10.4,5X,F10.7)
204  FORMAT(10H1FREQUENCY,4X,13HEXPERIMENTAL ,3X,10HCALCULATED)
205  FORMAT(2X,F6.2,7X,F11.9,3X,F11.9)
206  FORMAT(20X,F14.8)
      T(A,B,W)=A**4+2.*A*A*W*W*(2.*B*B-1.)+W**4
9  READ(1,202)NUM,NPTS,RTD,GAMMA,VAR,AVE
      WRITE(3,203)NUM,NPTS,RTD,GAMMA,VAR,AVE
      NCDS=25
      READ(1,101) ((C(I),S(I)),I=1,NCDS)
      READ(1,102)AL,BE
      NCDS=17
      CALL FIT(XAL,XBE)
      SUM=0.
      DO 1 I=1,NCDS
      SC(I)=B+A/T(XAL,XBE,C(I))
1  SUM=SUM+(S(I)-SC(I))**2
      WRITE(3,204)
      WRITE(3,205)((C(I),S(I),SC(I)),I=1,NCDS)
      WRITE(3,206)SUM
      GO TO 9
      STOP
      END

```

```

      SUBROUTINE FIT(XAL,XBE)
C      THIS SUBROUTINE COMPUTES THE NEWTON-RAPHSON CORRECTION FACTORS
C      FOR THE BREAK FREQUENCY AND DAMPING FACTOR
      DIMENSION S(25),C(25),G(3,2),XX(2),C(5),W(25)
      COMMON S,C,A,B,AL,BE,NCDS
201  FORMAT(10X,2E14.8)
202  FORMAT(15X,2E14.8)
      T(A,B,Z)=A**4+2.*A*A*Z*Z*(2.*B*B-1.)+Z**4
      A=C.
      B=.
      DO 10 I=2,NCDS
10  W(I)=1./S(I)
400  CONTINUE
      CLDA=A
      CLDB=B
      DO 1 I=1,5
1  C(I)=0.
      DO 2 I=2,NCDS
      TERM=1./T(AL,BE,C(I))
      C(1)=C(1)+TERM*W(I)
      C(2)=C(2)+TERM**2*W(I)
      C(3)=C(3)+S(I)*TERM*W(I)

```

```

      C(5)=C(5)+W(I)
2    C(4)=C(4)+S(I)*W(I)
      A=(C(1)*C(4)-C(3)*C(5))/(C(1)*C(1)-C(5)*C(2))
      B=(C(3)*C(1)-C(4)*C(2))/(C(1)*C(1)-C(5)*C(2))
      DAA=A-CLDA
      DBB=B-CLDB
      WRITE(3,201)A,B
411  XX(1)=BE
      XX(2)=AL
      DO 300 I=1,2
      CALL FUNCT(XX(2),XX(1),G(I,1),G(I,2))
300  XX(1)=XX(1)*1.05
      XX(1)=BE
      XX(2)=XX(2)*1.05
      CALL FUNCT(XX(2),XX(1),G(3,1),G(3,2))
      XX(2)=AL
      DO 301 J=2,3
      DO 301 I=1,2
301  G(J,I)=(G(J,I)-G(1,I))/(.05*XX(J-1))
      DZ=(-G(1,1)*G(3,2)+G(1,2)*G(3,1))/(G(2,1)*G(3,2)-G(2,2)*G(3,1))
      DB=(-G(1,1)-G(2,1)*DZ)/G(3,1)
      AL=AL+DB*0.5
      IF(ABS(AL).GT.5.)RETURN
      BE=BE+DZ*0.5
      IF(ABS(BE).GT.2.)RETURN
      WRITE(3,202)AL,BE
      IF(ABS(DB/AL).GT.1.E-3)GOTO499
      IF(ABS(DZ/BE).GT.1.E-3)GOTO499
      IF(ABS(DAA/A).GT.1.E-3)GOTO499
      IF(ABS(DBB/B).GT.1.E-3)GOTO499
      XAL=AL
      XBE=BE
      RETURN
      END

```

```

      SUBROUTINE FUNCT(AL,BE,R1,R2)
C    THIS PROGRAM COMPUTES THE VALUES OF THE NORMAL EQUATIONS
      DIMENSION S(25),C(25)
      COMMON S,C,A,B,X,Y,NCDS
      T(A,B,W)=A**4+2.*A*A*W*W*(2.*B*B-1.)+W**4
      U(A,B,W)=4.*A**3+4.*A*W*W*(2.*B*B-1.)
      V(A,B,W)=8.*B*A*A*W*W
      R1=0.
      R2=C.
      DO 1 I=2,NCDS
      R1=R1 +(S(I)-B-A/T(AL,BE,C(I)))*U(AL,BE,C(I))/(T(AL,BE,C(I)))**2
1    R2=R2 +(S(I)-B-A/T(AL,BE,C(I)))*V(AL,BE,C(I))/(T(AL,BE,C(I)))**2
      RETURN
      END

```

APPENDIX E

RESULTS OF AUTOCORRELATION FUNCTION
AND POWER SPECTRUM CALCULATIONS

RUN NUMBER A-7
 FILM SPEED = 24.
 NO. DATA POINTS = 1986
 PREWHITENING COEFF = 0.0
 AVERAGE BED HEIGHT = 6.346
 VARIANCE = .1497

TIME LAG	AUTO FXN	FREQUENCY	SPECTRUM
.00000	1.00000000	.0000	.231948840
.04166	.90106219	1.0000	.200811290
.08333	.72083944	2.0000	.118424960
.12500	.51274946	3.0000	.040045647
.16666	.31102967	4.0000	.010031101
.20833	.14385018	5.0000	.005036702
.25000	.02417163	6.0000	.002628733
.29166	-.05000729	7.0000	.001969492
.33333	-.07596604	8.0000	.001572291
.37500	-.06399005	9.0000	.001243723
.41666	-.02839590	10.0000	.000924842
.45833	.02127231	11.0000	.000893127
.50000	.06935995	12.0000	.000887264

APPENDIX E, CONTINUED

RUN NUMBER A-8
 FILM SPEED = 32.
 NO. DATA POINTS = 2020
 PREWHITENING COEFF = 0.0
 AVERAGE BED HEIGHT = 6.381
 VARIANCE = .1628

TIME LAG	AUTO FXN	FREQUENCY	SPECTRUM
.00000	1.000000000	.0000	.125815070
.03125	.84298746	1.0000	.115548200
.06250	.55256338	2.0000	.111778880
.09375	.25027385	3.0000	.105264380
.12500	.01394600	4.0000	.059169837
.15625	-.12175533	5.0000	.017805296
.18750	-.14894121	6.0000	.008420228
.21875	-.09048296	7.0000	.005805843
.25000	.01772836	8.0000	.003524270
.28125	.11886211	9.0000	.002274329
.31250	.16963701	10.0000	.001699633
.34375	.15925221	11.0000	.001459364
.37500	.09887175	12.0000	.001140298
.40625	.01577766	13.0000	.000926287
.43750	-.05423553	14.0000	.000885206
.46875	-.09633460	15.0000	.000916296
.50000	-.10895160	16.0000	.000948224

APPENDIX 5, CONTINUED

RUN NUMBER A-10
 FILM SPEED = 48.
 NO. DATA POINTS = 1990
 PREWHITENING COEFF = 0.0
 AVERAGE PED HEIGHT = 6.586
 VARIANCE = .1226

TIME LAG	AUTO FXN	FREQUENCY	SPECTRUM
.00000	1.00000000	.0000	.162079160
.02083	.93617291	1.0000	.153473460
.04166	.82872840	2.0000	.128335370
.06250	.68501018	3.0000	.078231507
.08333	.53148111	4.0000	.028597595
.10416	.37976181	5.0000	.009606935
.12500	.24269641	6.0000	.005428253
.14583	.12287975	7.0000	.003512119
.16666	.02850510	8.0000	.002147673
.18750	-.03868746	9.0000	.001375127
.20833	-.08028883	10.0000	.001082971
.22916	-.09637248	11.0000	.000808302
.25000	-.09118056	12.0000	.000654213
.27083	-.06854996	13.0000	.000551840
.29166	-.04052897	14.0000	.000563316
.31250	-.00785139	15.0000	.000574082
.33333	.02137368	16.0000	.000499331
.35416	.04670107	17.0000	.000426758
.37500	.06695139	18.0000	.000430470
.39583	.08299232	19.0000	.000434564
.41666	.09149825	20.0000	.000429514
.43750	.09180393	21.0000	.000480051
.45833	.08261237	22.0000	.000557161
.47916	.06935467	23.0000	.000525233
.50000	.05324193	24.0000	.000469041

APPENDIX E, CONTINUED

RUN NUMBER A-11
 FILM SPEED = 48.
 NO. DATA POINTS = 2007
 PREWHITENING COEFF = 0.0
 AVERAGE BED HEIGHT = 5.473
 VARIANCE = .0624

TIME LAG	AUTO FXN	FREQUENCY	SPECTRUM
.00000	1.000000000	.0000	.134356380
.02083	.88257535	1.0000	.128890900
.04166	.74453082	2.0000	.118477220
.06250	.58269833	3.0000	.086477674
.08333	.41632020	4.0000	.039560181
.10416	.26263229	5.0000	.014869063
.12500	.13111323	6.0000	.008029430
.14583	.02413762	7.0000	.005981229
.16666	-.05375740	8.0000	.005044259
.18750	-.09755578	9.0000	.003222917
.20833	-.11250285	10.0000	.002261517
.22916	-.09327403	11.0000	.002165960
.25000	-.06366697	12.0000	.001967379
.27083	-.03092280	13.0000	.001810653
.29166	.00238947	14.0000	.001624685
.31250	.02981361	15.0000	.001456877
.33333	.05826472	16.0000	.001543638
.35416	.08335522	17.0000	.001519272
.37500	.09966050	18.0000	.001298242
.39583	.09444705	19.0000	.001149999
.41666	.08535229	20.0000	.001179872
.43750	.06823623	21.0000	.001323238
.45833	.05392727	22.0000	.001267264
.47916	.03676763	23.0000	.001132204
.50000	.01725314	24.0000	.001136224

APPENDIX E, CONTINUED

RUN NUMBER A-12
 FILM SPEED = 48.
 NO. DATA POINTS = 1995
 PREWHITENING COEFF = 0.0
 AVERAGE REF HEIGHT = 7.738
 VARIANCE = .1604

TIME LAG	AUTO FXN	FREQUENCY	SPECTRUM
.00000	1.00000000	.0000	.218725760
.02083	.95260214	1.0000	.184619630
.04166	.88329897	2.0000	.120057850
.06250	.78825386	3.0000	.054797181
.08333	.67721231	4.0000	.012909701
.10416	.55923962	5.0000	.004358590
.12500	.43869145	6.0000	.002322656
.14583	.32752151	7.0000	.001707799
.16666	.22420703	8.0000	.001409885
.18750	.14013245	9.0000	.001006859
.20833	.07537402	10.0000	.000780414
.22916	.02974312	11.0000	.000666610
.25000	.00342143	12.0000	.000610889
.27083	-.00702268	13.0000	.000580676
.29166	-.00326367	14.0000	.000565903
.31250	.01150306	15.0000	.000509916
.33333	.03666175	16.0000	.000421011
.35416	.06727377	17.0000	.000391630
.37500	.10070658	18.0000	.000420968
.39583	.13319355	19.0000	.000489578
.41666	.16180561	20.0000	.000543919
.43750	.18272458	21.0000	.000521083
.45833	.19841290	22.0000	.000424529
.47916	.20792822	23.0000	.000350432
.50000	.20998410	24.0000	.000338753

APPENDIX E, CONTINUED

RUN NUMBER R-1
 FILM SPEED = 48.
 NO. DATA POINTS = 1991
 PREWHITENING COEFF = 0.0
 AVERAGE BED HEIGHT = 6.782
 VARIANCE = .0265

TIME LAG	AUTO FXN	FREQUENCY	SPECTRUM
.00000	1.00000000	.0000	.175870310
.02083	.89891686	1.0000	.141437690
.04166	.77911783	2.0000	.106494440
.06250	.63394203	3.0000	.079748284
.08333	.48198448	4.0000	.033984464
.10416	.34584076	5.0000	.011988531
.12500	.22658614	6.0000	.007950770
.14583	.12667270	7.0000	.005410273
.16666	.05777568	8.0000	.003585455
.18750	.01582368	9.0000	.002646984
.20833	-.00111315	10.0000	.002169852
.22916	.00896590	11.0000	.001699634
.25000	.04044887	12.0000	.001474675
.27083	.08010453	13.0000	.001291941
.29166	.13014352	14.0000	.001162533
.31250	.17279966	15.0000	.001230864
.33333	.20575190	16.0000	.001430585
.35416	.22457987	17.0000	.001386754
.37500	.23444710	18.0000	.001223664
.39583	.23226245	19.0000	.001093622
.41666	.22025802	20.0000	.001101756
.43750	.20495119	21.0000	.001058239
.45833	.17278218	22.0000	.000942618
.47916	.14087727	23.0000	.001007170
.50000	.11195771	24.0000	.001088036

APPENDIX E, CONTINUED

RUN NUMBER B-2
 FILM SPEED = 48.
 NO. DATA POINTS = 1983
 PREWHITENING COEFF = 0.0
 AVERAGE PED HEIGHT = 7.919
 VARIANCE = .0368

TIME LAG	AUTO FXN	FREQUENCY	SPECTRUM
.00000	1.00000000	.0000	.240046390
.02083	.91940244	1.0000	.169350500
.04166	.82253551	2.0000	.086123340
.06250	.71233182	3.0000	.056621629
.08333	.59647188	4.0000	.025448462
.10416	.49538281	5.0000	.010260240
.12500	.40442396	6.0000	.007191040
.14583	.33182515	7.0000	.004314886
.16666	.27625158	8.0000	.003057964
.18750	.23888499	9.0000	.002252792
.20833	.21616495	10.0000	.001748281
.22916	.20916504	11.0000	.001567869
.25000	.21827865	12.0000	.001372113
.27083	.23186834	13.0000	.001116717
.29166	.25152965	14.0000	.001012189
.31250	.27155871	15.0000	.001078610
.33333	.28813049	16.0000	.001108327
.35416	.29232681	17.0000	.001012453
.37500	.28539172	18.0000	.000969433
.39583	.26448367	19.0000	.000957216
.41666	.23460490	20.0000	.000947835
.43750	.20449785	21.0000	.000841799
.45833	.17225690	22.0000	.000670893
.47916	.14261680	23.0000	.000625258
.50000	.11902082	24.0000	.000653808

APPENDIX E, CONTINUED

RUN NUMBER B-3
 FILM SPEED = 48.
 NO. DATA POINTS = 1984
 PREWHITENING COEFF = 0.0
 AVERAGE BED HEIGHT = 9.096
 VARIANCE = .0581

TIME LAG	AUTO FXN	FREQUENCY	SPECTRUM
.00000	1.00000000	.0000	.203897860
.02083	.89834163	1.0000	.163518340
.04166	.80451764	2.0000	.103799630
.06250	.69560239	3.0000	.060774819
.08333	.57725250	4.0000	.023080472
.10416	.46384292	5.0000	.008225664
.12500	.35471477	6.0000	.006110788
.14583	.25752721	7.0000	.004220359
.16666	.18204503	8.0000	.003131932
.18750	.12730112	9.0000	.002665458
.20833	.08886573	10.0000	.002633468
.22916	.06694679	11.0000	.002250778
.25000	.06697204	12.0000	.001656465
.27083	.07969779	13.0000	.001489545
.29166	.10366097	14.0000	.001541648
.31250	.11888142	15.0000	.001544183
.33333	.13710367	16.0000	.001545741
.35416	.14655181	17.0000	.001538828
.37500	.14982124	18.0000	.001437685
.39583	.14069492	19.0000	.001309597
.41666	.12178577	20.0000	.001360221
.43750	.10221831	21.0000	.001305909
.45833	.08300623	22.0000	.001105277
.47916	.05797830	23.0000	.001156490
.50000	.03095679	24.0000	.001295436

APPENDIX E, CONTINUED

RUN NUMBER B-4
 FILM SPEED = 48.
 NO. DATA POINTS = 1966
 PREWHITENING COEFF = 0.0
 AVERAGE RED HEIGHT = 5.192
 VARIANCE = .0099

TIME LAG	AUTO FXN	FREQUENCY	SPECTRUM
.00000	1.00000000	.0000	.124966420
.02083	.86084095	1.0000	.118700120
.04166	.70524577	2.0000	.109841500
.06250	.52681439	3.0000	.085537468
.08333	.34658105	4.0000	.046245398
.10416	.19571251	5.0000	.022121647
.12500	.08134020	6.0000	.012158953
.14583	-.00631637	7.0000	.007156764
.16666	-.05357949	8.0000	.004877323
.18750	-.07427681	9.0000	.003823559
.20833	-.07721777	10.0000	.002999049
.22916	-.06143827	11.0000	.002371478
.25000	-.04000094	12.0000	.002118951
.27083	-.01649181	13.0000	.002014084
.29166	.01612253	14.0000	.001861827
.31250	.04232901	15.0000	.001873095
.33333	.06316820	16.0000	.002097971
.35416	.07664056	17.0000	.002063684
.37500	.08459669	18.0000	.001738223
.39583	.08509887	19.0000	.001443449
.41666	.08176645	20.0000	.001408460
.43750	.07892811	21.0000	.001428654
.45833	.06886620	22.0000	.001400544
.47916	.04995012	23.0000	.001465986
.50000	.02678155	24.0000	.001537146

APPENDIX E, CONTINUED

RUN NUMBER R-5
 FILM SPEED = 32.
 NO. DATA POINTS = 2027
 PREWHITENING COEFF = 0.0
 AVERAGE BED HEIGHT = 6.272
 VARIANCE = .0436

TIME LAG	AUTO FXN	FREQUENCY	SPECTRUM
.00000	1.00000000	.0000	.214457530
.03125	.87946292	1.0000	.172492240
.06250	.71687230	2.0000	.105259390
.09375	.54699361	3.0000	.055077043
.12500	.39343991	4.0000	.021580063
.15625	.26407762	5.0000	.010305236
.18750	.16543217	6.0000	.006361125
.21875	.10691922	7.0000	.004666722
.25000	.07837673	8.0000	.003696520
.28125	.07196643	9.0000	.002644039
.31250	.07754425	10.0000	.002010750
.34375	.09801685	11.0000	.001806813
.37500	.12095030	12.0000	.001626639
.40625	.13716529	13.0000	.001576614
.43750	.14939586	14.0000	.001571644
.46875	.15791032	15.0000	.001431291
.50000	.15166118	16.0000	.001330199

APPENDIX E, CONTINUED

RUN NUMBER C-1
 FILM SPEED = 48.
 NO. DATA POINTS = 1978
 PREWHITENING COEFF = 0.0
 AVERAGE BFD HEIGHT = 5.669
 VARIANCE = .0370

TIME LAG	AUTO FXN	FREQUENCY	SPECTRUM
.00000	1.000000000	.0000	.141416110
.02083	.92991089	1.0000	.140809650
.04166	.81015229	2.0000	.132512380
.06250	.65474702	3.0000	.089797529
.08333	.48387914	4.0000	.033729232
.10416	.31520323	5.0000	.010363286
.12500	.16461789	6.0000	.005779744
.14583	.03677646	7.0000	.003182099
.16666	-.05707506	8.0000	.002182841
.18750	-.11792428	9.0000	.001469301
.20833	-.15024374	10.0000	.001242401
.22916	-.15200011	11.0000	.001082352
.25000	-.12881170	12.0000	.000883831
.27083	-.09143911	13.0000	.000664090
.29166	-.04556423	14.0000	.000613566
.31250	.00267188	15.0000	.000663485
.33333	.04555103	16.0000	.000717838
.35416	.08031584	17.0000	.000611210
.37500	.10062993	18.0000	.000478865
.39583	.10571303	19.0000	.000423604
.41666	.09581901	20.0000	.000430322
.43750	.07480752	21.0000	.000435364
.45833	.04117206	22.0000	.000474491
.47916	-.00146686	23.0000	.000498007
.50000	-.03735137	24.0000	.000492816

APPENDIX E, CONTINUED

RUN NUMBER C-2
 FILM SPEED = 48.
 NO. DATA POINTS = 1985
 PREWHITENING COEFF = 0.0
 AVERAGE BED HEIGHT = 6.556
 VARIANCE = .1366

TIME LAG	AUTO FXN	FREQUENCY	SPECTRUM
.00000	1.00000000	.0000	.170286580
.02083	.94812779	1.0000	.162035830
.04166	.85029046	2.0000	.133311480
.06250	.72042544	3.0000	.073915408
.08333	.57481385	4.0000	.021932241
.10416	.42788686	5.0000	.007773081
.12500	.28904537	6.0000	.004792393
.14583	.16498366	7.0000	.002433823
.16666	.06017877	8.0000	.001572545
.18750	-.01960189	9.0000	.001131297
.20833	-.07646816	10.0000	.000896976
.22916	-.11100705	11.0000	.000659970
.25000	-.11960208	12.0000	.000498391
.27083	-.10935182	13.0000	.000425175
.29166	-.08157044	14.0000	.000434024
.31250	-.04302687	15.0000	.000448404
.33333	-.00040129	16.0000	.000420777
.35416	.04130599	17.0000	.000306996
.37500	.07714757	18.0000	.000264928
.39583	.10249287	19.0000	.000310856
.41666	.11701291	20.0000	.000342534
.43750	.12188229	21.0000	.000299158
.45833	.11502798	22.0000	.000250441
.47916	.09983006	23.0000	.000259987
.50000	.07867914	24.0000	.000279911

APPENDIX E, CONTINUED

RUN NUMBER C-3
 FILM SPEED = 48.
 NO. DATA POINTS = 1973
 PREWHITENING COEFF = 0.0
 AVERAGE BED HEIGHT = 7.330
 VARIANCE = .2358

TIME LAG	AUTO FXN	FREQUENCY	SPECTRUM
.00000	1.000000000	.0000	.242553320
.02083	.94967074	1.0000	.185902900
.04166	.87325515	2.0000	.101911160
.06250	.77873437	3.0000	.050103338
.08333	.67341256	4.0000	.016816079
.10416	.56660009	5.0000	.006587507
.12500	.46683115	6.0000	.003909440
.14583	.37663151	7.0000	.002336521
.16666	.29600304	8.0000	.001863263
.18750	.23235071	9.0000	.001409158
.20833	.18568884	10.0000	.000854139
.22916	.15446641	11.0000	.000698390
.25000	.13460744	12.0000	.000788422
.27083	.12515395	13.0000	.000741877
.29166	.12509288	14.0000	.000691112
.31250	.12498036	15.0000	.000622846
.33333	.12491438	16.0000	.000513682
.35416	.12487137	17.0000	.000429848
.37500	.12482859	18.0000	.000407084
.39583	.12478583	19.0000	.000400110
.41666	.12474397	20.0000	.000401382
.43750	.12470224	21.0000	.000411947
.45833	.12466159	22.0000	.000401145
.47916	.12462190	23.0000	.000355510
.50000	.12458357	24.0000	.000332762

APPENDIX E, CONTINUED

RUN NUMBER D-1
 FILM SPEED = 48.
 NO. DATA POINTS = 2074
 PREWHITENING COEFF = 0.0
 AVERAGE BED HEIGHT = 8.236
 VARIANCE = .0491

TIME LAG	AUTO FXN	FREQUENCY	SPECTRUM
.00000	1.00000000	.0000	.205496330
.02083	.94111165	1.0000	.162367470
.04166	.83507594	2.0000	.106652920
.06250	.70498429	3.0000	.068475306
.08333	.56893305	4.0000	.028053541
.10416	.44019811	5.0000	.010340945
.12500	.32496865	6.0000	.005919274
.14583	.22903111	7.0000	.003844248
.16666	.15719094	8.0000	.002442703
.18750	.10712258	9.0000	.001462286
.20833	.07702486	10.0000	.001265954
.22916	.06939048	11.0000	.001092988
.25000	.08003091	12.0000	.000807471
.27083	.10074724	13.0000	.000550864
.29166	.12480649	14.0000	.000459759
.31250	.14772051	15.0000	.000459497
.33333	.16889458	16.0000	.000480860
.35416	.18620364	17.0000	.000447790
.37500	.19934555	18.0000	.000392917
.39583	.20425294	19.0000	.000341998
.41666	.20202880	20.0000	.000319482
.43750	.19105959	21.0000	.000324661
.45833	.17349232	22.0000	.000305313
.47916	.15398887	23.0000	.000291933
.50000	.13382857	24.0000	.000303261

APPENDIX E, CONTINUED

RUN NUMBER F-1
 FILM SPEED = 48.
 NO. DATA POINTS = 1988
 PREWHITENING COEFF = 0.0
 AVERAGE PED HEIGHT = 10.937
 VARIANCE = .0517

TIME LAG	AUTO FXN	FREQUENCY	SPECTRUM
.00000	1.00000000	.0000	.252015390
.02083	.95109774	1.0000	.176176300
.04166	.87043467	2.0000	.093446826
.06250	.76835741	3.0000	.061565092
.08333	.65236046	4.0000	.021132733
.10416	.53824138	5.0000	.005585339
.12500	.43523666	6.0000	.004021728
.14583	.34296695	7.0000	.002308439
.16666	.26954763	8.0000	.001702735
.18750	.22151888	9.0000	.001165651
.20833	.19390578	10.0000	.000791363
.22916	.18866029	11.0000	.000652180
.25000	.20450422	12.0000	.000587770
.27083	.23095003	13.0000	.000489721
.29166	.26507911	14.0000	.000540654
.31250	.30414068	15.0000	.000653968
.33333	.33739869	16.0000	.000658421
.35416	.36130084	17.0000	.000458661
.37500	.37110104	18.0000	.000324691
.39583	.36574207	19.0000	.000329287
.41666	.34992891	20.0000	.000330484
.43750	.32651981	21.0000	.000313443
.45833	.29503550	22.0000	.000311712
.47916	.26684460	23.0000	.000301892
.50000	.24235140	24.0000	.000286346

APPENDIX E, CONTINUED

RUN NUMBER A-10-R
 FILM SPEED = 48.
 NO. DATA POINTS = 1987
 PREWHITENING COEFF = 0.0
 AVERAGE BED HEIGHT = 6.461
 VARIANCE = .1453

TIME LAG	AUTO FXN	FREQUENCY	SPECTRUM
.00000	1.00000000	.0000	.194418960
.02083	.92594445	1.0000	.166139080
.04166	.82217585	2.0000	.113465500
.06250	.70320785	3.0000	.062388525
.08333	.58109976	4.0000	.023223737
.10416	.46072551	5.0000	.008370066
.12500	.34639267	6.0000	.005547935
.14583	.24368361	7.0000	.004704718
.16666	.15441976	8.0000	.003548422
.18750	.08804333	9.0000	.002375362
.20833	.04152210	10.0000	.001812077
.22916	.02004466	11.0000	.001545485
.25000	.01571293	12.0000	.001308950
.27083	.02220691	13.0000	.001063812
.29166	.03095549	14.0000	.000915109
.31250	.04371305	15.0000	.000884415
.33333	.05503687	16.0000	.000808838
.35416	.06518827	17.0000	.000678137
.37500	.07463563	18.0000	.000622977
.39583	.07994730	19.0000	.000621921
.41666	.08200350	20.0000	.000625028
.43750	.07982060	21.0000	.000675774
.45833	.07707245	22.0000	.000672275
.47916	.07414934	23.0000	.000552688
.50000	.07259227	24.0000	.000479305

APPENDIX E, CONTINUED

RUN NUMBER R-1-R
 FILM SPEED = 48.
 NO. DATA POINTS = 1989
 PREWHITENING COEFF = 0.0
 AVERAGE PED HEIGHT = 6.767
 VARIANCE = .0317

TIME LAG	AUTO FXN	FREQUENCY	SPECTRUM
.00000	1.000000000	.0000	.130466020
.02083	.91464240	1.0000	.129020450
.04166	.78233480	2.0000	.129344810
.06250	.61210643	3.0000	.096116061
.08333	.43082718	4.0000	.038210632
.10416	.26028352	5.0000	.012657379
.12500	.11219224	6.0000	.007542533
.14583	-.01077200	7.0000	.004507150
.16666	-.09911279	8.0000	.003014030
.18750	-.15279307	9.0000	.001964505
.20833	-.16995727	10.0000	.001554822
.22916	-.16228250	11.0000	.001170965
.25000	-.12602553	12.0000	.000906158
.27083	-.07258031	13.0000	.000815041
.29166	-.01597424	14.0000	.000903852
.31250	.04308704	15.0000	.000952895
.33333	.09342829	16.0000	.000844592
.35416	.13131687	17.0000	.000689716
.37500	.15743525	18.0000	.000771380
.39583	.16316701	19.0000	.000805982
.41666	.15377730	20.0000	.000654381
.43750	.13031951	21.0000	.000581812
.45833	.09385657	22.0000	.000635771
.47916	.05209735	23.0000	.000718021
.50000	.00862744	24.0000	.000768014

APPENDIX E, CONTINUED

RUN NUMBER C-2-R
 FILM SPEED = 48.
 NO. DATA POINTS = 1990
 PREWHITENING COEFF = 0.0
 AVERAGE BED HEIGHT = 6.618
 VARIANCE = .1670

TIME LAG	AUTO FXN	FREQUENCY	SPECTRUM
.00000	1.00000000	.0000	.170751920
.02083	.93264920	1.0000	.156231000
.04166	.82983190	2.0000	.125227890
.06250	.69472834	3.0000	.075791564
.08333	.54832641	4.0000	.026885750
.10416	.40417730	5.0000	.008333803
.12500	.26704779	6.0000	.004758808
.14583	.14778225	7.0000	.003329700
.16666	.05290020	8.0000	.002306406
.18750	-.01535609	9.0000	.001686078
.20833	-.05563374	10.0000	.001354905
.22916	-.07068705	11.0000	.000997902
.25000	-.06545547	12.0000	.000810012
.27083	-.04399218	13.0000	.000684352
.29166	-.01437944	14.0000	.000629196
.31250	.01681533	15.0000	.000582746
.33333	.04608173	16.0000	.000579399
.35416	.06983401	17.0000	.000620113
.37500	.08910532	18.0000	.000650301
.39583	.10272703	19.0000	.000624279
.41666	.11074633	20.0000	.000589683
.43750	.10940901	21.0000	.000580496
.45833	.10003676	22.0000	.000560823
.47916	.08310980	23.0000	.000537960
.50000	.05938738	24.0000	.000541696

APPENDIX F

RESULTS OF LEAST SQUARES FIT
TO POWER SPECTRUM

RUN NUMBER A-7

BREAK FREQUENCY = 1.968

DAMPING FACTOR = .6232

ERROR SQUARED = .00002169

FREQUENCY	EXPERIMENTAL	CALCULATED
1.0000	.200811290	.200547520
2.0000	.118424960	.119168330
3.0000	.040045647	.036157585
4.0000	.010031101	.012400452
5.0000	.005036702	.005452313
6.0000	.002628733	.002954765
7.0000	.001969492	.001893249
8.0000	.001572291	.001382346
9.0000	.001243723	.001112292
10.0000	.000924842	.000958790
11.0000	.000893127	.000866344
12.0000	.000887264	.000807984

RUN NUMBER A-8

BREAK FREQUENCY = 3.235

DAMPING FACTOR = .5184

ERROR SQUARED = .00031437

FREQUENCY	EXPERIMENTAL	CALCULATED
1.0000	.115548200	.105345940
2.0000	.111778880	.122285850
3.0000	.105264380	.102756460
4.0000	.059169837	.050746909
5.0000	.017805296	.022037774
6.0000	.008420228	.010578804
7.0000	.005805843	.005771003
8.0000	.003524270	.003527850
9.0000	.002274329	.002376079
10.0000	.001699633	.001736170
11.0000	.001459364	.001358948
12.0000	.001140298	.001123983
13.0000	.000926287	.000971582
14.0000	.000885206	.000869189
15.0000	.000916296	.000798307
16.0000	.000948224	.000747962

APPENDIX F, CONTINUED

RUN NUMBER A-10

BREAK FREQUENCY = 2.666

DAMPING FACTOR = .6284

ERROR SQUARED = .00011606

FREQUENCY	EXPERIMENTAL	CALCULATED
1.0000	.153473460	.150636840
2.0000	.128335370	.134023860
3.0000	.078231507	.070051189
4.0000	.028597595	.028514364
5.0000	.009606935	.012455075
6.0000	.005428253	.006200226
7.0000	.003512119	.003476474
8.0000	.002147673	.002155951
9.0000	.001375127	.001456802
10.0000	.001082971	.001059527
11.0000	.000808302	.000820501
12.0000	.000654213	.000669779
13.0000	.000551840	.000570951
14.0000	.000563316	.000503974
15.0000	.000574082	.000457283
16.0000	.000499331	.000423929

RUN NUMBER A-11

BREAK FREQUENCY = 3.005

DAMPING FACTOR = .6084

ERROR SQUARED = .00007918

FREQUENCY	EXPERIMENTAL	CALCULATED
1.0000	.128890900	.125436160
2.0000	.118477220	.123984830
3.0000	.086477674	.081670601
4.0000	.039560181	.038199782
5.0000	.014869063	.017793665
6.0000	.008029430	.009393515
7.0000	.005981229	.005689805
8.0000	.005044259	.003893177
9.0000	.003222917	.002944361
10.0000	.002261517	.002406869
11.0000	.002165960	.002084405
12.0000	.001967379	.001881575
13.0000	.001810653	.001748858
14.0000	.001624685	.001659072
15.0000	.001456877	.001596573
16.0000	.001543638	.001551982

APPENDIX F, CONTINUED

RUN NUMBER A-12
 BREAK FREQUENCY = 2.139
 DAMPING FACTOR = .6274
 ERROR SQUARED = .00015907

FREQUENCY	EXPERIMENTAL	CALCULATED
1.0000	.184619630	.183565230
2.0000	.120057850	.123524240
3.0000	.054797181	.043175273
4.0000	.012909701	.015198375
5.0000	.004358590	.006493905
6.0000	.002322656	.003302666
7.0000	.001707799	.001935989
8.0000	.001409885	.001275970
9.0000	.001006859	.000926496
10.0000	.000780414	.000727663
11.0000	.000666610	.000607848
12.0000	.000610889	.000532186
13.0000	.000580676	.000482508
14.0000	.000565903	.000448802
15.0000	.000509916	.000425282
16.0000	.000421011	.000408466

RUN NUMBER B-1
 BREAK FREQUENCY = 2.928
 DAMPING FACTOR = .6925
 ERROR SQUARED = .00026379

FREQUENCY	EXPERIMENTAL	CALCULATED
1.0000	.141437690	.136792490
2.0000	.106494440	.116588880
3.0000	.079748284	.068629542
4.0000	.033984464	.032495934
5.0000	.011988531	.015727685
6.0000	.007950770	.008466453
7.0000	.005410273	.005118311
8.0000	.003585455	.003440998
9.0000	.002646984	.002534834
10.0000	.002169852	.002013058
11.0000	.001699634	.001696238
12.0000	.001474675	.001495141
13.0000	.001291941	.001362634
14.0000	.001162533	.001272495
15.0000	.001230864	.001209473
16.0000	.001430585	.001164347

APPENDIX F, CONTINUED

RUN NUMBER B-2
 BREAK FREQUENCY = 2.824
 DAMPING FACTOR = 1.0197
 ERROR SQUARED = .00016310

FREQUENCY	EXPERIMENTAL	CALCULATED
1.0000	.169350500	.167973660
2.0000	.086123340	.092882498
3.0000	.056621629	.046386576
4.0000	.025448462	.023693398
5.0000	.010260240	.012921703
6.0000	.007191040	.007603603
7.0000	.004314886	.004825163
8.0000	.003057964	.003288630
9.0000	.002252792	.002393657
10.0000	.001748281	.001847975
11.0000	.001567869	.001501733
12.0000	.001372113	.001274283
13.0000	.001116717	.001120279
14.0000	.001012189	.001013202
15.0000	.001078610	.000936994
16.0000	.001108327	.000881622

RUN NUMBER B-3
 BREAK FREQUENCY = 2.552
 DAMPING FACTOR = .7748
 ERROR SQUARED = .00012011

FREQUENCY	EXPERIMENTAL	CALCULATED
1.0000	.163518340	.162052730
2.0000	.103799630	.108775690
3.0000	.060774819	.051721199
4.0000	.023080472	.023120714
5.0000	.008225664	.011473161
6.0000	.006110788	.006541276
7.0000	.004220359	.004253729
8.0000	.003131932	.003094913
9.0000	.002665458	.002462207
10.0000	.002633468	.002094643
11.0000	.002250778	.001869848
12.0000	.001656465	.001726335
13.0000	.001489545	.001631327
14.0000	.001541648	.001566449
15.0000	.001544183	.001520247
16.0000	.001546741	.001488280

APPENDIX F, CONTINUED

RUN NUMBER B-4

BREAK FREQUENCY = 3.353

DAMPING FACTOR = .6466

ERROR SQUARED = .00002195

FREQUENCY	EXPERIMENTAL	CALCULATED
1.0000	.118700120	.116689030
2.0000	.109841500	.113120260
3.0000	.085537468	.083269513
4.0000	.046245398	.045545290
5.0000	.022121647	.023111043
6.0000	.012158953	.012550352
7.0000	.007156764	.007576237
8.0000	.004877323	.005080069
9.0000	.003823559	.003736697
10.0000	.002999049	.002967032
11.0000	.002371478	.002501927
12.0000	.002118951	.002207947
13.0000	.002014084	.002014929
14.0000	.001861827	.001884023
15.0000	.001873095	.001792730
16.0000	.002097971	.001727501

RUN NUMBER B-5

BREAK FREQUENCY = 2.550

DAMPING FACTOR = .8265

ERROR SQUARED = .00002940

FREQUENCY	EXPERIMENTAL	CALCULATED
1.0000	.172492240	.171927320
2.0000	.105259390	.107298610
3.0000	.055077043	.050628216
4.0000	.021580063	.023178447
5.0000	.010305236	.011713617
6.0000	.006361125	.006719022
7.0000	.004666722	.004352124
8.0000	.003696520	.003134681
9.0000	.002644039	.002462678
10.0000	.002010750	.002069167
11.0000	.001806813	.001827069
12.0000	.001626639	.001671805
13.0000	.001576614	.001568654
14.0000	.001571644	.001498018
15.0000	.001431291	.001448363
16.0000	.001330199	.001412651

APPENDIX F, CONTINUED

RUN NUMBER C-1

BREAK FREQUENCY = 2.759

DAMPING FACTOR = .5643

ERROR SQUARED = .00016278

FREQUENCY	EXPERIMENTAL	CALCULATED
1.0000	.140809650	.135808600
2.0000	.132512380	.139951850
3.0000	.089797529	.081517003
4.0000	.033729233	.032498836
5.0000	.010363286	.013698786
6.0000	.005779744	.006682771
7.0000	.003182099	.003725341
8.0000	.002182841	.002322848
9.0000	.001469301	.001591469
10.0000	.001242401	.001180310
11.0000	.001082352	.000934858
12.0000	.000883831	.000780990
13.0000	.000664090	.000680553
14.0000	.000613566	.000612726
15.0000	.000663485	.000565576
16.0000	.000717838	.000531972

RUN NUMBER C-2

BREAK FREQUENCY = 2.491

DAMPING FACTOR = .6106

ERROR SQUARED = .00014516

FREQUENCY	EXPERIMENTAL	CALCULATED
1.0000	.162035830	.159574390
2.0000	.133311480	.138545480
3.0000	.073915408	.063831311
4.0000	.021932241	.023980520
5.0000	.007773081	.010146598
6.0000	.004792393	.004981327
7.0000	.002433823	.002771417
8.0000	.001572545	.001708950
9.0000	.001131297	.001148919
10.0000	.000896976	.000831511
11.0000	.000659970	.000640842
12.0000	.000498391	.000520738
13.0000	.000425175	.000442043
14.0000	.000434024	.000388738
15.0000	.000448404	.000351592
16.0000	.000420777	.000325066

APPENDIX F, CONTINUED

RUN NUMBER C-3
 BREAK FREQUENCY = 2.286
 DAMPING FACTOR = .8044
 ERROR SQUARED = .00006256

FREQUENCY	EXPERIMENTAL	CALCULATED
1.0000	.185902900	.185258350
2.0000	.101911160	.104742670
3.0000	.050103338	.043080219
4.0000	.016816079	.017864767
5.0000	.006587507	.008373454
6.0000	.003909440	.004463098
7.0000	.002336521	.002667067
8.0000	.001863263	.001760498
9.0000	.001409158	.001266122
10.0000	.000854139	.000979000
11.0000	.000698390	.000803386
12.0000	.000788422	.000691244
13.0000	.000741877	.000616982
14.0000	.000691112	.000566258
15.0000	.000622846	.000530672
16.0000	.000513682	.000505119

RUN NUMBER D-1
 BREAK FREQUENCY = 2.745
 DAMPING FACTOR = .7818
 ERROR SQUARED = .00016406

FREQUENCY	EXPERIMENTAL	CALCULATED
1.0000	.162367470	.160132770
2.0000	.106652920	.113655940
3.0000	.068475306	.058447384
4.0000	.028053541	.026923139
5.0000	.010340945	.013013794
6.0000	.005919274	.006879875
7.0000	.003844248	.003973884
8.0000	.002442703	.002484111
9.0000	.001462286	.001664781
10.0000	.001265954	.001186556
11.0000	.001092988	.000893143
12.0000	.000807471	.000705392
13.0000	.000550864	.000580888
14.0000	.000459759	.000495760
15.0000	.000459497	.000435994
16.0000	.000480860	.000393055

APPENDIX F, CONTINUED

RUN NUMBER E-1
 BREAK FREQUENCY = 2.397
 DAMPING FACTOR = .8198
 ERROR SQUARED = .00039070

FREQUENCY	EXPERIMENTAL	CALCULATED
1.0000	.176176300	.174257760
2.0000	.093446826	.102137000
3.0000	.061565092	.044405686
4.0000	.021132733	.019011632
5.0000	.005585339	.008993197
6.0000	.004021728	.004757374
7.0000	.002308439	.002782796
8.0000	.001702735	.001777002
9.0000	.001165651	.001225253
10.0000	.000791363	.000903503
11.0000	.000652180	.000706134
12.0000	.000587770	.000579826
13.0000	.000489721	.000496047
14.0000	.000540654	.000438748
15.0000	.000653968	.000398509
16.0000	.000658421	.000369591

RUN NUMBER A-10-R
 BREAK FREQUENCY = 2.552
 DAMPING FACTOR = .7370
 ERROR SQUARED = .00007221

FREQUENCY	EXPERIMENTAL	CALCULATED
1.0000	.166139080	.164948800
2.0000	.113465500	.117047270
3.0000	.062388525	.055612244
4.0000	.023223737	.023971784
5.0000	.008370066	.011376313
6.0000	.005547935	.006166417
7.0000	.004704718	.003790209
8.0000	.003548422	.002600341
9.0000	.002375362	.001955926
10.0000	.001812077	.001583736
11.0000	.001545485	.001357092
12.0000	.001308950	.001212870
13.0000	.001063812	.001117635
14.0000	.000915109	.001052732
15.0000	.000884415	.001007285
16.0000	.000808838	.000974701

APPENDIX F. CONTINUED

RUN NUMBER P-1-R

BREAK FREQUENCY = 2.904

DAMPING FACTOR = .5432

ERROR SQUARED = .00011540

FREQUENCY	EXPERIMENTAL	CALCULATED
1.0000	.129020450	.124031800
2.0000	.129344810	.135950190
3.0000	.096116061	.090178471
4.0000	.038210632	.037820799
5.0000	.012657379	.016013841
6.0000	.007542533	.007824402
7.0000	.004507150	.004396856
8.0000	.003014030	.002783738
9.0000	.001964505	.001947676
10.0000	.001554822	.001479887
11.0000	.001170965	.001201642
12.0000	.000906158	.001027708
13.0000	.000815041	.000914425
14.0000	.000903852	.000838058
15.0000	.000952895	.000785048
16.0000	.000844593	.000747312

RUN NUMBER C-2-R

BREAK FREQUENCY = 2.607

DAMPING FACTOR = .6375

ERROR SQUARED = .00016108

FREQUENCY	EXPERIMENTAL	CALCULATED
1.0000	.156231000	.153244690
2.0000	.125227890	.131601250
3.0000	.075791564	.065846382
4.0000	.026885750	.026525598
5.0000	.008333803	.011666587
6.0000	.004758808	.005894865
7.0000	.003329700	.003377861
8.0000	.002306406	.002155224
9.0000	.001686078	.001506817
10.0000	.001354905	.001137879
11.0000	.000997902	.000915668
12.0000	.000810012	.000775432
13.0000	.000684252	.000683417
14.0000	.000629196	.000621025
15.0000	.000582746	.000577510
16.0000	.000579399	.000546414

NOISE ANALYSIS APPLIED TO
A LIQUID-SOLID FLUIDIZED BED

by

DARROL HOLT TIMMONS

B. S., Kansas State University, 1963

AN ABSTRACT OF
A MASTER'S THESIS

submitted in partial fulfillment of the
requirements for the degree

MASTER OF SCIENCE

Department of Nuclear Engineering

KANSAS STATE UNIVERSITY

Manhattan, Kansas

1966

ABSTRACT

A study was made of the application of noise analysis to the determination of the dynamic behavior of a copper-water fluidized bed system. The fluctuations of the upper fluid-bed interface were recorded as a function of time during steady state operation of the fluidized bed. The input to the system was assumed to be Gaussian white noise and the system was assumed to be an ergodic random process. Under these conditions the significant time constants were available from the power spectrum of the system.

The theory of noise analysis was summarized with particular emphasis on the analysis of digital data spaced at equal time increments. A computer program was developed to calculate the autocorrelation function and the power spectrum from the experimentally observed bed height data. It was found that the power spectrum of the fluidized bed system could be described in terms of a second order transfer function. Using this model, the break frequency and damping factor associated with the transfer function were determined from the experimental power spectrum by the method of least squares.

The break frequencies and damping factors were observed to vary as a function of particle diameter and bed expansion ratio. Plots of the results indicated that the break frequency decreased as a function of bed expansion ratio while the damping factor increased as a function of bed expansion ratio. No such trends were apparent in the dependence upon the particle diameter, however, statistical analysis showed that both the particle diameter and the bed expansion ratio had a significant effect on the break frequency and damping factor.

Step input responses were recorded and the experimental results were compared with those calculated from the second order transfer function. It was found that the results compared quite well for both positive and negative small perturbations. For large step inputs the transfer function predicted more overshoot than was observed experimentally. The results, however, indicated that noise analysis should not be overlooked as a method of determining the significant time constants of a fluidized bed system.

